Optimisation des techniques avancées en IRM cérébrale dans la détection des lésions développementales épileptogènes

Charles Mellerio

Université Paris Descartes

Ecole Doctorale Cerveau, Cognition, Comportement (ED n°158)

Laboratoire INSERM U894

Optimisation des techniques avancées en IRM cérébrale dans la détection des lésions développementales épileptogènes

Par Charles MELLERIO

Thèse de doctorat de Neurosciences

Dirigée par Catherine Oppenheim

Présentée et soutenue publiquement le 29 Septembre 2014

Devant un jury composé de :

Catherine OPPENHEIM (PU-PH), directrice de thèse

François COTTON (PU-PH), rapporteur

Alexandre KRAINIK (PU-PH), rapporteur

Nathalie BODDAERT (PU-PH), examinatrice

Francine CHASSOUX (PH), examinatrice

Didier DORMONT (PU-PH), examinateur

Résumé (français) :

Les dysplasies corticales focales de type 2 (DCF2) sont une cause fréquente d'épilepsie partielle pharmacorésistante pouvant bénéficier d'un traitement chirurgical. Leur détection en IRM est un facteur indépendant de bon pronostic. Leur diagnostic reste difficile avec jusqu'à 40% d'IRM négatives.

Le travail de cette thèse a pour principal objectif d'améliorer la détection des DCF2 à partir des séquences conventionnelles, d'évaluer la pertinence d'une augmentation de champ magnétique, et de valider de nouveaux outils de détection, en particulier par l'identification d'anomalies des sillons associées aux DCF2 de manière automatique puis visuelles. Cette étude a été réalisée à partir d'une des plus importante cohorte de patients (>80 patients) porteurs de DCF2 prouvée histologiquement.

L'évaluation de la fréquence de chacun des signes en IRM nous a permis de démontrer que, bien qu'aucune anomalie ne soit visible dans 41% des cas, les différents signes chez les patients avec une IRM positive n'étaient jamais isolés et que la combinaison des 3 signes les plus évocateurs de DCF2 (épaississement cortical, flou de l'interface blanc-gris et « transmantle sign »), était retrouvée chez 27 patients (64%) suggérant que l'IRM puisse être un examen très caractéristique.

En augmentant le champ magnétique de 1,5 à 3T en IRM le taux de détection n'est que peu modifié mais la caractérisation des DCF2 est améliorée en raison d'une meilleure visualisation du « transmantle sign », considéré comme une signature en IRM des DCF2.

L'analyse automatisée des sillons basés sur le calcul d'un nouveau paramètre appelé « énergie sulcale » permet d'identifier des motifs sulcaux anormaux chez les patients porteurs de DCF2 dans la région centrale en comparaison aux sujets sains. Ce résultat souligne l'importance d'une étude des sillons et pourrait fournir un critère supplémentaire pour détecter et localiser la lésion chez des patients à IRM négative.

Enfin, l'analyse visuelle des sillons par un reformatage 3D du cortex nous a permis de décrire un nouveau marqueur des DCF2 de la région centrale : un motif sulcal dénommé le "Power Button Sign". Compte tenu de son excellente reproductibilité et de sa spécificité, il pourrait être utilisé comme un nouveau critère diagnostic majeur de DCF2 de la région centrale.

L'ensemble de ces résultat participe à la meilleure compréhension des phénomènes développementaux impliqués dans la physiopathologie des DCF2 et offre de nombreuses perspectives pour l'amélioration de leur détection en imagerie.

Title : Optimization of advanced MRI tools in the detection and characterization of epileptogenic developmental lesions

Abstract :
Focal cortical dysplasia type 2 (FCD2) is a common cause of intractable partial epilepsy surgically treatable. Their detection by MRI is an independent factor of good prognosis. The MR imaging diagnosis remains difficult with up to 40% negative MRI.

Our main objective is to improve the detection of FCD2from conventional sequences, to assess the relevance of increased magnetic field and validate new tools for detection, in particular by identifying sulcal abnormalities associated with FCD2 automatically and visually. This study was carried out from one of the largest cohort of patients (> 80 patients) with histologically proven FCD2.

The evaluation of the frequency of each MR signs showed that, although no abnormality is seen in 41% of cases, the different signs in patients with a positive MRI were never isolated and the combination of the 3 most suggestive signs of FCD2 (cortical thickening, bluring of the gray-white matter interface and "transmantle sign") was found in 27 patients (64%), indicating that MRI can be very suggestive.

By increasing the magnetic field from 1.5 to 3T MRI detection rate is only slightly changed but characterization of FCD2 is improved thanks to a better visualization of the " transmantle sign " considered as a MR signature of FCD2.

The automated sulcus analysis based on the calculation of a new parameter called "sulcal energy" identifies abnormal sulcal patterns in patients with FCD2 in the central region in comparison to healthy subjects. This result underlines the importance of the identification of sulci and could provide an additional criterion for detecting and locating the lesion in patients with negative MRI.

Finally, the visual analysis of sulci by 3D reformatting of the cortex allowed us to describe a new MR sign of FCD2 in the central region: a sulcal pattern called the "Power Button Sign". Given its excellent reproducibility and specificity, it could be used as a new major diagnostic criterion of FCD2 in the central region.

All these results contribute to the better understanding of the developmental processes involved in the pathophysiology of FCD2 and offers many opportunities for improving their MR detection.

Mots clés (français) :
Epilepsie partielle pharmacorésistante, IRM, dysplasie corticale focale, transmantle sign, anatomie sulcale, sillon central

Keywords :
Intractable epilepsy, MR imaging, focal cortical dysplasia, transmantle sign, sulcal anatomy, central Sulcus

Remerciements

Au Professeur Catherine Oppenheim pour son enthousiasme, sa compétence et sa grande disponibilité. Qu'elle trouve ici le témoignage de mon admiration et de ma reconnaissance pour ces trois années de soutien et d'accompagnement.

Au Professeur Jean-François Meder pour son accueil dans le service d'imagerie, pour m'avoir fait partager sa passion de l'enseignement et de la transmission de savoir aux plus jeunes, pour m'avoir guidé et conseillé avec bienveillance depuis mes débuts en neuroradiologie.

Au Docteur Francine Chassoux, pour sa compétence et son dévouement au service des patients, pour m'avoir permis d'accéder à des données exceptionnelles sans lesquelles cette thèse n'aurait pas vu le jour, et en souhaitant que se prolonge dans l'avenir notre fructueuse collaboration.

Au Professeur François Cotton, pour m'avoir chaleureusement accueilli comme interne dans son service et pour m'avoir donné goût à l'anatomie et à l'imagerie cérébrale. Qu'il trouve dans ce travail le témoignage de mon amitié et de ma gratitude.

Au Professeur Alexandre Krainik, qui me fait l'honneur de porter son regard d'expert en neuroradiologie sur cette thèse et d'en être rapporteur.

Au Professeur Nathalie Boddaert, qui me fait l'honneur d'accepter de juger ce travail. Qu'elle trouve ici l'expression de mon respect le plus sincère.

Au Professeur Didier Dormont, qui me fait l'immense honneur de participer au jury de cette thèse.

A tous mes collègues du service d'imagerie de Sainte-Anne, en souhaitant que se perpétue cette ambiance de travail unique et inégalable.

A ma famille et ma belle famille, ainsi qu'à mes amis pour leur soutien inaltérable pendant ces années de thèse.

A mes trois enfants Camille, Garance et Colombe pour leur joie de vivre dès le matin au réveil.

Enfin à Hélène, pour ton amour inoxydable, pour ton appui, pour ton humour solaire. Ce travail t'est dédié.

Table des matières

Articles originaux de l'auteur correspondant au travail présenté dans la thèse :

1. **Mellerio C**, Labeyrie M-A, Chassoux F, Daumas-Duport C, Landre E, Turak B, et al. Optimizing MR Imaging Detection of Type 2 Focal Cortical Dysplasia: Best Criteria for Clinical Practice. American Journal of Neuroradiology. 2012;33(10):1932-8.

2. **Mellerio C**, Labeyrie M-A, Chassoux F, Roca P, Alami O, Plat M, et al. 3T MRI improves the detection of transmantle sign in type 2 focal cortical dysplasia. Epilepsia. janv 2014;55(1):117-122.

3. **Mellerio C**, Roca P, Chassoux F, Danière F, Cachia A, Lion S, Naggara O, Devaux B, Meder JF, Oppenheim C. The "power button sign": a new sulcal magnetic resonance pattern of type 2 focal cortical dysplasia of the central region. Radiology – Accepted in July 2014

4. Roca P, **Mellerio C**, Chassoux F, Rivière D, Cachia A, Mangin JF, Devaux B, Meder JF, Oppenheim C. Sulcus-based MR analysis of focal cortical dysplasia located in the central region. Epilepsia – submitted July 2014.

Autres articles de l'auteur illustrant ou en rapport avec le travail présenté dans la thèse.

1. Canale S, Rodrigo S, Tourdias T, **Mellerio C**, Perrin M, Souillard R, et al. Évaluation du degré de malignité des tumeurs gliales primitives de l'adulte en IRM de perfusion par marquage des spins. Journal of Neuroradiology. 2011;38(4):207-13.

2. Chassoux F, Rodrigo S, Semah F, Beuvon F, Landre E, Devaux B, **Mellerio C**, et al. FDG-PET improves surgical outcome in negative MRI Taylor-type focal cortical dysplasias. Neurology. 2010;75(24):2168-75.

3. Chassoux F, Landré E, **Mellerio C**, Turak B, Mann MW, Daumas-Duport C, et al. Type II focal cortical dysplasia: electroclinical phenotype and surgical outcome related to imaging. Epilepsia. 2012;53(2):349-58.

4. Chassoux F, Rodrigo S, **Mellerio C**, Landré E, Miquel C, Turak B, et al. Dysembryoplastic neuroepithelial tumors An MRI-based scheme for epilepsy surgery. Neurology. 2012;79(16):1699-707.

5. Kuchcinski G, **Mellerio** C, Pallud J, Dezamis E, Turc G, Rigaux-Viodé O, et al. Glioma-related Perfusion Modifications Alter Functional Magnetic Resonance Language Mapping. Neurology. In press.

6. **Mellerio C**, Farhat WH, Calvet D, Oppenheim C, Lefaucheur JP, Bartolucci P. Cerebral reorganization of language and motor control secondary to chronic hemispheric vasculopathy in a patient with homozygous sickle-cell disease. Am J Hematol. 25 mars 2014;

7. Naggara O, Letourneau-Guillon L, **Mellerio C**, Belair M, Pruvo JP, Leclerc X, et al. Diffusion-weighted MR imaging of the brain]. Journal de radiologie. 2010;91(3 Pt 2):329.

Introduction

L'épilepsie représente la deuxième affection neurologique du sujet jeune après la migraine et touche près de 1 % de la population (1). Les formes graves sont rares mais responsables d'une altération de la qualité de vie et des capacités intellectuelles, et d'une augmentation de morbi-mortalité accidentelle, iatrogénique, ou par décompensation de la maladie épileptique. Certaines formes d'épilepsie, appelées pharmaco-résistantes, échappent au traitement médical. On estime à 10000 le nombre de ces patients qui pourraient bénéficier d'un traitement chirurgical curatif (2).

Appartenant au spectre des malformations du développement cortical, les dysplasies corticales focales (DCF) représentent la première cause d'épilepsie partielle pharmaco résistante (EPPR) opérée de l'enfant et la troisième de l'adulte après la sclérose de l'hippocampe et les tumeurs développementales (2,3).

L'imagerie par résonnance magnétique (IRM) cérébrale a changé le diagnostic de cette maladie, en permettant une exploration morphologique et tissulaire non invasive du cerveau avec une résolution millimétrique. Elle a participé à l'augmentation du nombre de candidats à la chirurgie et à l'amélioration des résultats de celle-ci avec un taux de guérison de l'épilepsie aux environ de 60 % quand l'IRM est négative, contre plus de 80 % quand elle est positive (3–7). Cependant, le diagnostic des DCF2 à l'IRM est difficile y compris dans les centres spécialisés utilisant des protocoles adaptés, expliquant que près de 40 % de ces lésions soient méconnues et/ou caractérisées tardivement, privant les patients d'un traitement efficace pendant de nombreuses années (3). Le délai moyen entre le début des symptômes et la chirurgie reste en moyenne de 14 ans dans la plupart des séries (8–11).

Dans ce contexte, une amélioration de la détection des DCF2 en IRM est un défi pour améliorer la prise en charge de ces patients. Cette problématique a motivé ce travail de thèse dont quatre études répondent aux principaux objectifs : Améliorer la détection des DCF2 à partir des séquences conventionnelles, évaluer la pertinence d'une augmentation de champ magnétique, identifier les anomalies des sillons associées aux DCF2 et développer un outil de détection automatique de ces anomalies sulcales.

- **Etude n°1 : Optimiser la détection des DFC2 en IRM. Définition des critères les plus pertinents pour la pratique clinique.**

L'objectif de cette étude a été premièrement d'évaluer la fréquence de chacune des anomalies IRM. En effet, même si la sémiologie des DCF2 en IRM est bien décrite, les études les plus récentes portant sur de larges séries de patients ne fournissent pas une analyse exhaustive de tous ces signes en IRM et la prévalence de chaque signe varie considérablement entre les études. En outre, la proportion d'IRM négatives varie largement, probablement en raison de différences dans les protocoles d'acquisition et de biais de sélection. L'objectif secondaire a été d'évaluer la proportion d'IRM négative et les facteurs qui lui sont associés, afin de rechercher des outils permettant d'en améliorer la performance diagnostique. Les résultats de cette première étude, en particulier le taux important d'IRM négative à 1,5 Tesla dans notre population de patients opérés, nous a conduit à évaluer l'intérêt d'utiliser un champ magnétique plus élevé pour améliorer le taux de détection.

- **Etude n°2 : IRM 3 Tesla vs. IRM 1,5 Tesla dans la détection et la caractérisation des DCF2.**

Le choix du champ magnétique n'est pas trivial pour l'imagerie du cortex, avec une balance entre une amélioration du rapport signal sur bruit et de la résolution d'une part et le risque d'artéfacts d'autre part. Les résultats de cette seconde étude, tout en confirmant la supériorité de champ magnétique plus élevé en particulier pour la caractérisation de signes subtils associés aux DCF, montrent que le taux d'IRM négative reste élevé à 3 Tesla. Nous nous sommes donc attachés à rechercher, toujours à partir des données de l'IRM conventionnelle, de nouveaux critères diagnostiques et de nouveaux outils de détection.

- **Etude n°3 : Analyse automatique des anomalies sulco-gyrales associées aux DCF2 de la région centrale.**

Les anomalies sulcales font partie des critères de détection des DCF2 en IRM bien que leur description soit souvent équivoque : sillons élargis, plus profond avec une angulation « inhabituelle ». Encouragés par l'observation peropératoire de sillons « aberrants » à proximité des DCF2, nous avons testé l'hypothèse selon laquelle la morphologie des sillons pourrait être un outil de détection des DCF2, en particulier dans la région centrale, connue pour sa faible variabilité interindividuelle. Nous avons dans un premier temps adapté une méthode automatique de labellisation des sillons (Morphologist – Brainvisa) à la détection de sillons aberrants. Cet outil, initialement développé pour identifier les sillons à partir d'une base d'apprentissage de 60 sujets

sains, génère une carte d' « énergie » pour chaque sillon détecté. Cette énergie est d'autant plus élevée pour un sillon que ses critères de description (largeur, profondeur, angulation et surtout rapport avec les sillons voisins) s'éloignent de ceux de la base d'apprentissage. Un sillon aberrant associé à une DCF2 sera plus difficilement identifié, et donc associé à une « énergie » plus élevée. Notre objectif était de tester si cette méthode d'analyse sulcale automatique pourrait aider à la détection et à la localisation des DCF2 non visibles en IRM. Forts des résultats de l'analyse automatique et quantitative, nous nous sommes interrogés sur la possibilité d'une détection à l'œil nu de sillons aberrants chez les patients porteurs d'une DCF2 de la région centrale.

- **Etude n°4 : Détection visuelle des anomalies sulcales associées aux DCF2 de la région centrale.**

Pour ce faire, nous avons analysé les variantes anatomiques du sillon central chez des patients porteurs de DCF2 localisée dans la région centrale, en comparaison avec les témoins. L'analyse des sillons de cette région nous a permis de mettre en évidence un motif proche du symbole du bouton « marche-arrêt » des appareils électroniques : le « Power Button Sign » (PBS) dont nous rapportons la sensibilité et la spécificité pour le diagnostic de DCF2.

Ce document débutera par une introduction sur le bilan préopératoire de l'épilepsie pharmacorésistante et la nature des dysplasies corticales focales (hormis les données d'imagerie et d'embryologie qui seront traitées dans la dernière partie de synthèse). Chacun des quatre articles originaux composant ce travail de thèse sera ensuite inséré, précédé d'une brève introduction. La discussion fera la synthèse de ces travaux et les perspectives seront présentées dans le dernier chapitre.

Première partie : Contexte et revue de la littérature

1 L'épilepsie partielle pharmaco résistante (EPPR)

La décharge épileptique

La décharge épileptique est définie par une décharge rythmique, hyper synchrone et auto entretenue d'un groupe de neurones du cortex. L'enregistrement électro encéphalographique (EEG) retrouve des anomalies paroxystiques s'organisant en décharges synchrones sur un territoire plus ou moins étendu. Sur le plan moléculaire, cette décharge est liée à un déséquilibre entre l'activité des neurones excitateurs (glutaminergiques) et inhibiteurs (GABAergiques). Des situations métaboliques et/ou génétiques impliquant notamment les boucles de régulation thalamo-corticales peuvent expliquer une hypersensibilité de l'ensemble des neurones du cortex. Les crises sont alors d'emblée généralisées. Une décharge localisée initialement à un groupe de neurone définit les crises partielles dont la physiopathologie diffère radicalement de la crise d'emblée généralisée. La crise partielle peut se propager dans un second temps à l'ensemble du cortex (crise secondairement généralisée) via des voies de conductions préférentielles appelées *réseau épileptogène*. La topographie initiale de la décharge et sa propagation rendent compte de la grande diversité clinique des crises d'épilepsies partielles dont les symptômes peuvent facilement être méconnus ou mal interprétés. Les crises partielles sont dans la grande majorité des cas secondaires à une lésion du cortex (crises symptomatiques ou cryptogéniques).

L'épidémiologie de l'EPPR

L'épilepsie est une affection fréquente que représente la deuxième affection neurologique du sujet jeune après la migraine. Avec une incidence de 0.7 à 1 %, elle compte plus de 500 000 patients en France. On considère que 60 % des épilepsies sont classées parmi les épilepsies partielles et que 20 à 50 % d'entre elles sont pharmaco résistantes. C'est donc 60 000 patients qui sont atteints de EPPR. Parmi ces patients, près de 10 000 seraient éligibles pour une

opération soit en termes d'incidence 500 nouveaux patients par an (2). La répartition des différentes causes d'EPPR opérées est résumée dans la figure 1. La chirurgie s'adresse à des épilepsies partielles médicalement intraitables et graves. Elle constitue le seul traitement curatif reconnu. Son objectif est de supprimer les crises par l'exérèse des structures corticales primitivement affectées par les décharges épileptiques. La technique chirurgicale varie d'une cortectomie très localisée à une lobectomie plus élargie selon la nature et la topographie de la lésion. (Conférence de Consensus - ANAES 2004)

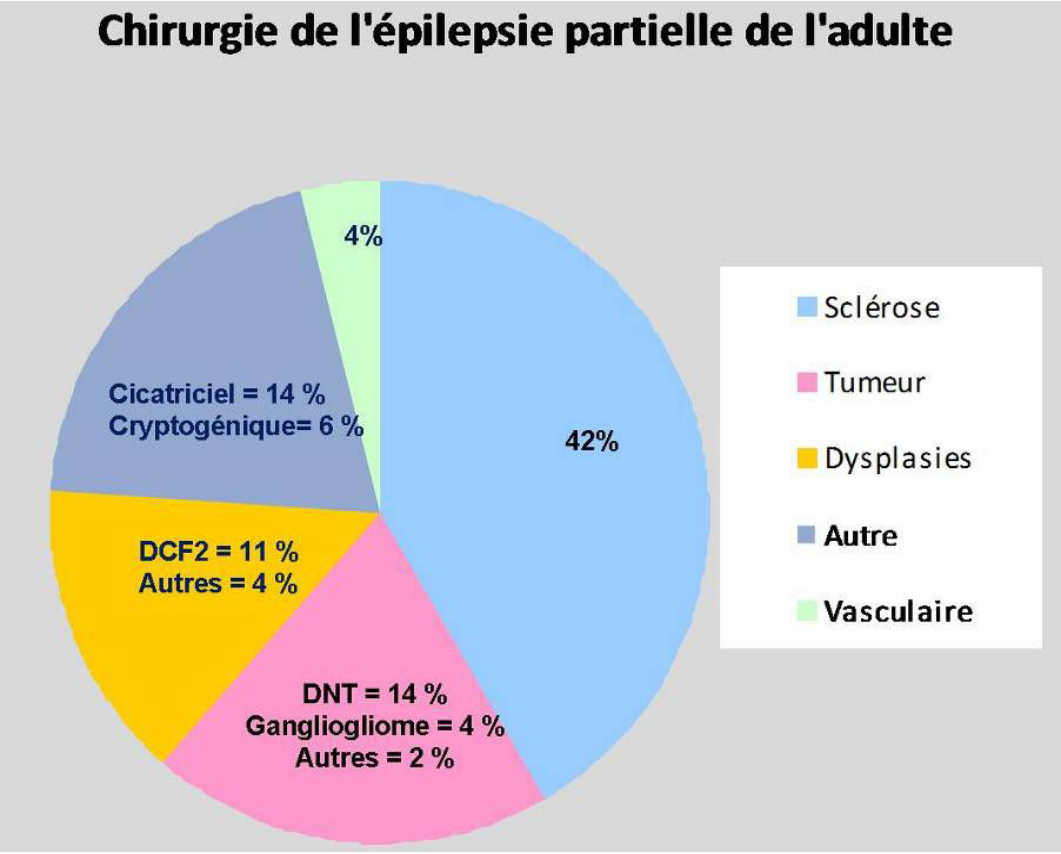

Fig. 1 : Chirurgie de l'épilepsie en France d'après B. Devaux Neurochirurgie 2008

1.1 Les principes du bilan pré chirurgical de l'EPPR

La chirurgie suppose que la preuve a été faite de l'origine univoque des crises, que leur localisation corticale a été précisément identifiée, que la nature et la délimitation de la lésion sous-jacente ont été déterminées, et que la résection envisagée ne crée pas un déficit neurologique ou cognitif inacceptable (Conférence de consensus – ANAES 2004) (12). Le bilan pré chirurgical implique une démarche multi modale et multi disciplinaire intégrant de

nombreux examens cliniques et paracliniques avec des sensibilités, spécificités et cibles très différentes dont la concordance maximale est nécessaire pour décider de la chirurgie. L'accessibilité, le coût et le caractère invasif de chaque examen sont à prendre en compte dans ce bilan qui doit respecter une certaine gradation.

1.1.1 Zones épileptogènes, lésionnelles et fonctionnelles

- La zone épileptogène (ZE) est la région de cortex nécessaire et suffisante pour déclencher les crises d'épilepsie. La décharge épileptogène se propage à d'autres régions du cortex via des voies de conductions formant le réseau épileptogène (RE).
- La zone lésionnelle (ZL) est le substratum pathologique dont une partie ou l'ensemble contient la zone épileptogène. Il peut s'agir d'une lésion dysplasique, tumorale, cicatricielle ou vasculaire. La zone épileptogène et la zone lésionnelle ne sont pas nécessairement identiques.
- Les zones fonctionnelles (ZF) sont les zones cérébrales ayant une fonction bien définie comme la motricité ou la sensibilité dont l'exérèse serait préjudiciable pour le patient. La topographie des aires fonctionnelles primaires est relativement bien conservée d'un individu à l'autre. Leur délimitation précise est en revanche beaucoup plus variable et ne peut être prédite sur les seules données anatomiques. Par ailleurs, de nombreuses lésions épileptogènes situées sur les zones anatomiques habituellement fonctionnelles déplacent les aires fonctionnelles (généralement autour de la lésion) ; on parle de réorganisation fonctionnelle. Elle est liée à la plasticité cérébrale.

Cette distinction est fondamentale car elle détermine les exigences et les contraintes du chirurgien en termes de résection. Ceci est particulièrement vrai pour les lésions situées dans des régions éloquentes où la résection doit être la plus limitée possible.

1.1.2 Les antécédents et la sémiologie des crises

La description des crises est le premier temps du bilan pré chirurgical :

- les antécédents familiaux et personnels (souffrance périnatale, traumatisme crânien, crises convulsives hyperthermique, retard mental) orientent sur la nature de la lésion sous-jacente.

- la sémiologie des crises a une valeur localisatrice (Tableau 1), oriente vers le type de lésion, et permet de déterminer la sévérité de la maladie épileptique.

1.1.3 Les explorations morphologiques

Le scanner cérébral n'a aucune place dans la recherche de lésion corticale epileptigène tant le contraste entre cortex et substance blanche est limité.
L'IRM cérébrale conventionnelle est l'exploration non invasive de première intention d'une EPPR. Elle est susceptible de détecter la zone lésionnelle, d'en apprécier sa taille, éventuellement sa nature et ses rapports anatomiques. Elle peut être limitée par son manque de sensibilité, toutes les lésions n'étant pas visibles à l'IRM, ou par son manque de spécificité, une anomalie IRM corticale n'étant pas nécessairement à l'origine d'une épilepsie partielle.

Manifestations initiales de la crise	Région cérébrale probablement impliquée
Aura épigastrique	Hippocampe
Aura olfactive	Uncus
Anxiété	Amygdales ou cortex frontomédian
Automatismes oro-alimentaires	Lobe temporal mésial
Aura auditives	Circonvolution temporale supérieure (postérieure)
Clonies focales unilatérales	Circonvolution précentrale
Phénomènes somato-sensibles focaux unilatéraux	Circonvolution postcentrale
Pseudo-hallucinations visuelles élémentaires	Cortex visuel occipital
Rires	Hypothalamus
Vertiges, sensation de lift	Cortex pariétal inférieur
Hyper motricité teintée d'affectivité	Cortex cingulaire

Tab. 1 : Exemples d'éléments localisateurs dans la sémiologie des crises (Kurthen et al.)

1.1.4 Les explorations électrophysiologiques (EEG)

Elles permettent d'enregistrer l'activité électrique de différentes régions du cerveau et donc de localiser avec plus ou moins de précision la zone épileptogène.

- L'EEG inter critique réalisé entre 2 crises peut être très localisateur. Il décèle la zone irritative et permet d'interpréter les tracés critiques.
- Le Vidéo EEG, réalisé avec enregistrement vidéo (VEEG), associe les informations cliniques et EEG inter et per critiques pour localiser la zone épileptogène avec une très grande sensibilité. Il est systématiquement réalisé dans le bilan d'une épilepsie partielle pharmaco résistante
- L'EEG intracrânien (ou stéréo EEG) est la méthode de référence pour délimiter la zone épileptogène. Il s'agit d'une technique invasive nécessitant l'implantation d'électrodes intra cérébrales, dont les indications sont actuellement limitées en fonction du rapport bénéfice risque.
- La magnéto encéphalographie (MEG), disponible uniquement dans certains centres, localiserait avec une plus grande précision que le vidéo EEG la zone épileptogène.

1.1.5 Les explorations métaboliques et de perfusion

- La TEP (tomographie par émission de positons) au 18- fluoro-déoxy-glucose (FDG) mesure le métabolisme cérébral du glucose et détecte en période inter-ictale un hypo métabolisme focal qui affecte la zone épileptogène, mais sans superposition stricte entre l'étendue de l'hypo métabolisme et celle des anomalies IRM morphologiques ou celle de la zone épileptogène identifiée en stéréo-électroencéphalographie. Cette technique d'exploration, dont l'intérêt dans la détection et la localisation des DCF2 est considérable (8,11,13,14), fait l'objet d'un chapitre particulier dans la dernière partie de cette thèse (3ème partie, 3.3).
- Le TEMP (tomographie d'émission mono photonique) au technétium marqué permet de détecter une hyper vascularisation de la zone épileptogène pendant une crise. La complexité de sa mise en œuvre limite actuellement ses indications.

1.1.6 Les explorations fonctionnelles

Elles permettent de préciser le rapport de la lésion avec les zones fonctionnelles. Elles sont utiles quand la lésion est située dans une aire anatomique habituellement éloquente.

- Les tests neuropsychologiques permettent de latéraliser le langage et la mémoire. Ils aident à localiser la zone épileptogène et à prédire les risques fonctionnels post opératoires (Figure 10 dans la 3ème partie).
- L'IRM fonctionnelle a fait ses preuves en pratique clinique pour localiser les aires sensorimotrices primaires et latéraliser le langage (15). La latéralisation de la mémoire est prometteuse (16) et pourrait supplanter le *test de Wada*.
- Le test de Wada explore de manière invasive la latéralisation du langage et de la mémoire par l'injection intra carotidienne de barbiturique d'action rapide. Il reste exceptionnellement indiqué depuis l'avènement de l'IRM fonctionnelle.

1.1.7 L'exploration per opératoire

Outre l'aspect macroscopique et la consistance de la lésion qui diffèrent du cerveau normal et qui permettent au chirurgien de localiser la lésion, les stimulations électriques per opératoires permettent d'apprécier avec le plus de précision les zones fonctionnelles à proximité de la lésion (Figure 2).

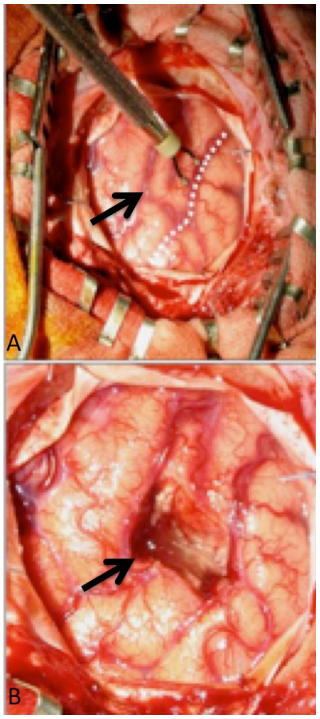

Figure 2 : Stimulation électrique corticale peropératoire à proximité d'une DCF2 précentrale (flèche) sur une vue avant (A) et après (B) exérèse de la lésion. Les stimulations le long du sillon central (pointillés blancs) sont réalisées jusqu'à obtention d'une réponse motrice, permettant un cortectomie épargnant les zones fonctionnelles de la motricité. (Remerciements B. Devaux)

1.2 Démarche diagnostique

Au total, le bilan pré chirurgical se déroule en trois temps. En première intention sont analysés les antécédents, l'anamnèse des crises, l'EEG inter critique et l'IRM cérébrale morphologique qui confirment le plus souvent la nature partielle de l'épilepsie et permettent

de formuler une hypothèse sur la topographie de la zone épileptogène et la nature de la lésion sous-jacente. En seconde intention, quand la chirurgie est évoquée, le VEEG et les tests neuropsychologiques corroborent cette hypothèse topographique. Pour certains, un PET, SPECT ou MEG sera réalisé systématiquement en plus du VEEG. En troisième intention, en cas de doute sur la topographie, la délimitation exacte, ou de discordance entre les tests précédemment évoqués, un EEG invasif (stéréo EEG) sera réalisé et constituera la technique de référence pour localiser et délimiter précisément la zone épileptogène. (Tableau 2).

Techniques	Cible(s)	Principes
IRM morphologique	ZL	Visualisation non invasive de la lésion sous-jacente
Vidéo EEG	ZE	Détection des décharges per critique de la ZE
TEP au FDG	ZE + RE?	Hypo métabolisme inter critique de la ZE
TEMP au Tc	ZE + RE?	Hyper débit per critique de la ZE
MEG	ZE, ZF	Détection et stimulation non invasive de la ZE et des ZF
SEEG	ZE, ZF	Détection et stimulation invasive de la ZE et des ZF
IRM fonctionnelle	ZF	Détection des aires primaires et latéralisation du langage
Test de Wada	ZF	Latéralisation du langage et de la mémoire
Per opératoire	ZL, ZF	Stimulation des AF, visualisation directe de la lésion
Histologie	ZL	Caractérisation microscopique de la lésion et de ses berges

Tab. 2 : Principales modalités d'exploration pré chirurgicale d'une EPPR (ZL = zone lésionnelle, ZE = zone épileptogène, RE = réseau épileptogène, ZF = zone fonctionnelle)

2 Les dysplasies corticales focales

Les dysplasies corticales focales sont définies par une désorganisation focale de la cytoarchitecture du cortex. Elles sont la principale cause d'épilepsie chirurgicalement curable chez l'enfant (3). Elles regroupent sous le même nom plusieurs pathologies très différentes qui ont en commun leur caractère focal et cortical et donc par nature une accessibilité potentielle à un traitement chirurgical curatif. En dehors des DCF2 qui a fait l'objet de ce travail de thèse, les autres DCF sont encore imparfaitement caractérisées, et ne constituent pas

des entités homogènes (17), expliquant le nombre de classifications différentes dont elles ont fait l'objet.

DCF de type 1 (isolé)

- 1a : DCF avec une lamination corticale radiale anormale
- 1b : DCF avec une lamination corticale tangentielle anormale
- 1c : DCF avec des laminations corticales radiale et tangentielle anormales

DCF de type 2 (isolée)

- 2a : DCF avec des neurones dysmorphiques
- 2b : DCF avec des neurones dysmorphiques et des cellules ballonisées

DCF de type 3 (associé à une lésion principale)

- 3a : Anomalies de la lamination corticale dans le lobe temporal associé à une sclérose hippocampique
- 3b : Anomalies de la lamination corticale adjacentes à une tumeur gliale ou neurogliale
- 3c : Anomalies de la lamination corticale adjacentes à une malformation vasculaire
- 3d : Anomalies de la lamination corticale adjacentes à tout autre lésion acquise précocement dans la vie (traumatique, ischémique, encéphalite)

Tab. 3 : Nouvelle classification des DCF (Blümcke et al. Lancet 2011)

Les DCF résultent d'un désordre intervenant précocement dans la gestation, pendant la période de la prolifération des cellules neuronales et gliales, ayant pour conséquence un trouble de l'organisation corticale. Cette désorganisation focale de la cytoarchitecture du cortex (18) est associée ou non à des cellules anormales est à l'origine des classifications les plus récentes (19,20). Celle décrite par Blümcke et al., issue d'un consensus de l'ILAE en 2011 (tableau 3) est la plus répandue a l'heure actuelle et semble présenter l'avantage d'une bonne concordance inter- et intra-observateur (21).

Les dysplasies corticales focales de type 2 (DCF2) se distinguent des autres dysplasies corticales focales opérées car elles constituent une entité nosologique homogène et bien définie histologiquement (4,17,22). Elles ont été décrites pour la première fois en 1971 par Taylor et al. à partir de pièces de lobectomie dans le cadre de chirurgie de l'épilepsie (23) et ont, pour cette raison, longtemps été appelées « dysplasie de Taylor ». Elles sont définies

histologiquement par l'association d'une désorganisation focale de la cytoarchitecture du cortex, de neurones géants et de cellules ballonisées caractéristiques (Figure 3). Leur cause n'est pas connue mais des études génétiques récentes ont mis en évidence dans les DCF2 des anomalies sur un des gènes (TSC1) impliqué dans la sclérose tubéreuse de Bourneville, constituant un argument en faveur d'un continuum nosologique entre ces deux maladies (23). Le mécanisme physiopathologique supposé serait une perturbation in utero du développement cortical lors de la phase de prolifération des neuroblastes avec des répercussions sur les phases de migration et d'organisation laminaire du cortex (24,25).

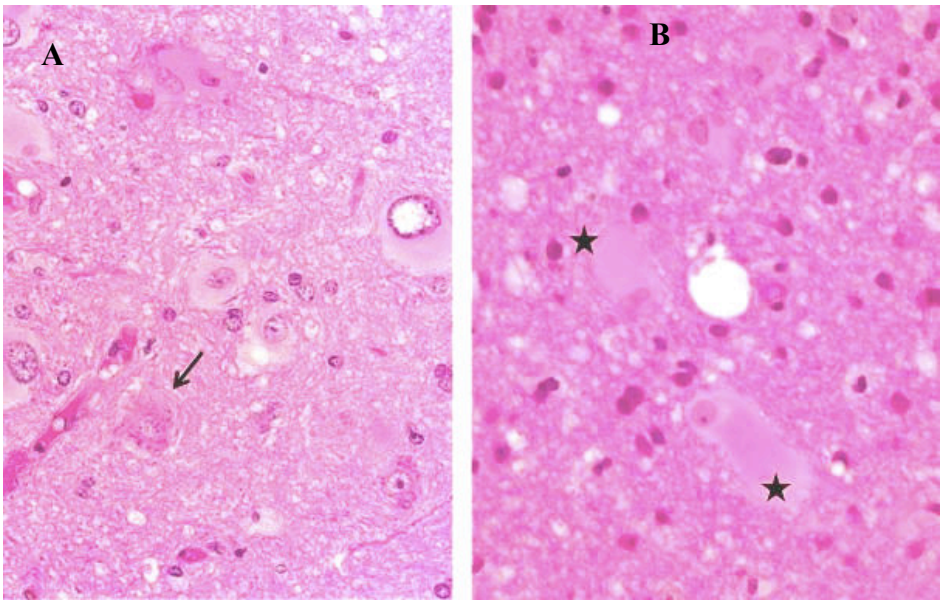

Figure 3 : Caractéristiques histologiques des DCF2 : a) coloration HPS (Hémalin, Phloxyn, Safran) grossissement x 200 mettant en évidence des neurones géants dont le corps cellulaire a un aspect tigré caractéristique (flèches), ainsi que des cellules gliales anormales à cytoplasme éosinophile ballonisé (étoiles) ; b) Même préparation à un grossissement supérieur x 400, centré sur des cellules ballonisées (étoiles). (remerciement : C Daumas Duport)

Leur présentation clinique correspond typiquement à une épilepsie partielle extra temporale, de début précoce, chez des patients jeunes sans antécédent en dehors de spasmes infantiles. L'âge moyen de début de l'épilepsie est de 5 à 7 ans. L'épilepsie est le plus souvent pharmaco résistante avec des crises pluri quotidiennes, avec recrudescence nocturne, se généralisant peu mais donnant volontiers des états de mal partiels . Les DCF2 sont ainsi connues comme étant des lésions hautement épileptogènes avec une activité électrique intrinsèque élevée (26,27).

Cependant, la relation de cause à effet entre la lésion structurelle causée par la dysplasie corticale et la genèse des crises reste débattue. Trois différents modèles animaux ont été étudiés afin de rendre compte de cette relation :

- Le modèle de la sclérose tubéreuse par le rat Eker, dans lequel une mutation génétique du gène TSC donne lieu à une désorganisation corticale avec des éléments cellulaires anormaux (28,29)
- La souris knock-out du gène p35, dans laquelle l'inhibition de l'expression du gène p35 donne lieu à un trouble d'organisation et de lamination corticale, mais dans laquelle les éléments cellulaires restent normaux (30)
- le rat exposé au méthylazoxyméthanol, un agent alkylant, dans lequel l'ADN est soumis à une perturbation chimique à un temps précis, conduisant des amas de neurones hétérotopiques (31).

L'intégration de données provenant de l'étude de ces différents modèles animaux avec des observations cliniques connexes montre que les caractéristiques neuropathologiques des lésions dysplasiques corticales en soi ne sont insuffisantes pour initier le processus de crise comitiale . En revanche, une interaction avec les cellules corticales avoisinantes, en dehors de la région de désorganisation architecturale, serait à l'origine de l'activité épileptiforme (32).

De manière contradictoire, de nombreuses données indiquent que les neurones dysmorphiques sont strictement liés à cette « épileptogénèse ». Tout d'abord, les données de stéréo-EEG ont montré que les décharges per-critiques ainsi que l'activité rythmique inter-critiques proviennent toutes deux de la zone dysplasique où les neurones dysmorphiques se situent (26). Deuxièmement, les enregistrements électriques directs du cortex en per opératoire ont démontré l'apparition de crises au sein de régions corticales caractérisées par la présence de neurones dysmorphiques et non de cellules ballonisées (33). Troisièmement, Des analyses électro-physiologiques post opératoires ont été réalisées sur des tranches de cortectomie sièges d'une dysplasie corticale. Celles-ci suggèrent que ces échantillons de tissus sont dotés d'hyperexcitabilité et peuvent générer des décharges épileptiformes spontanés (34–36).

Enfin, et de manière plus concrète, de nombreuses études suggèrent que la guérison dépend du caractère complet de l'exérèse de la dysplasie (5,6,26) et que son exérèse incomplète est associée à la persistance de survenue de crises (37). Cette constatation clinique primordiale a, pour partie, justifié et motivé notre travail d'optimisation de la détection en imagerie des DCF2.

Deuxième partie : Optimisation des techniques avancées en IRM cérébrale dans la détection des dysplasies corticales focales

Chapitre 1 : Définition des critères de détection des DCF2 les plus pertinents en IRM pour la pratique clinique

Cette première étude a fait l'objet d'une publication dans l' ***American Journal of NeuroRadiology*** **publié en 2012 dont le manuscrit est inséré ci-après (la version au format de la revue est également disponible en Annexe 1) est également et dont les principaux résultats sont ici résumés :**

Introduction

L'objectif de cette étude introductive a été de réaliser un état des lieux de l'aspect en IRM des DCF2. Celles-ci bénéficient d'une sémiologie riche, amplement détaillée dans la littérature récente associant six principaux critères : 1- épaississement du cortex, 2- anomalies de signal du cortex, 3- anomalies de signal de la substance blanche sous-corticale, 4- flou de l'interface blanc-gris, 5- « transmantle sign », et 6- anomalies sulco-gyrales. Nous nous sommes intéressés à la prévalence de chacun de ces signes, à la fréquence de leur association ainsi qu'à l'identification des facteurs associés à leur absence (IRM négatives).
Pour cela, nous avons revu rétrospectivement les IRM réalisées à 1,5 Tesla (1,5T) de 71 patients consécutifs porteurs d'une DCF2 prouvée histologiquement. Le protocole d'exploration comprenait des séquences 3D T1 millimétriques, et des séquences 2D coronales et/ou axiales T2 et FLAIR. Deux neuroradiologues expérimentés ont recherché les 6 critères de DCF2 précités. La fréquence de chaque signe et leur combinaison a été évaluée. Nous avons également comparé le délai âge d'apparition de l'épilepsie – âge à la chirurgie avec le délai de détection des DCF2 en IRM.

Résumé des principaux résultats

- Parmi les 71 patients étudiés, seuls 42 patients (59%) avaient une IRM positive, c'est-à-dire qu'au moins un des 6 critères était visualisé et ce malgré un protocole conforme aux recommandations les plus récentes.
- Cependant, un critère n'était jamais isolé : au moins 3 des 6 critères étaient systématiquement associés. Par ailleurs, chez 12 patients (29%), les 6 critères étaient

présents. Enfin, si l'on considère les 3 signes les plus évocateurs de DCF2 (épaississement cortical, flou de l'interface blanc-gris et « transmantle sign »), ceux-ci étaient associés chez 27 patients (64%) suggérant que l'IRM peut être caractéristique.

- Une « anomalie » sulcale était présente chez près de la moitié des patients à IRM positive. Chez les patients à IRM négative, des anomalies sulcales étaient notées dans une proportion similaire. Ces dernières étaient alors considérées comme mineure en raison de l'absence de description sémiologique précise.
- 40% des patients avec une IRM positive au moment de l'étude disposaient d'au moins une IRM précédente qui avait été considérée comme normale, entrainant un retard d'environ 5 ans de la prise charge chirurgicale. Il est intéressant de noter que la lésion était rétrospectivement visible dans tous les cas.

Conclusion

Cette étude souligne que près de 60% des DCF2 peuvent être diagnostiqués en IRM. L'association de 3 signes caractéristiques (épaississement cortical, flou de l'interface blanc-gris et un « transmantle sign »), est très évocatrice de ce sous-type de DCF. L'identification précoce de cette lésion est essentielle pour guider ces patients vers la chirurgie.

Optimizing MRI detection of type2 focal cortical dysplasia: best criteria for clinical practice

ABSTRACT

Background and purpose: type2-FCD is one of the main causes of drug-resistant partial epilepsy. Its detection by MRI has greatly improved the surgical outcome but it often remains overlooked. Our objective was to determine the prevalence of typical MRI criteria for type2-FCD, in order to provide a precise MRI pattern and optimize its detection.

Materials and Methods: 1.5T MRI of 71 consecutive patients with histologically proven type2-FCD were retrospectively reviewed. The MRI protocol included millimetric 3D T1-weighted, 2D coronal and axial T2-weighted, and 2D or 3D FLAIR images. Two experienced neuroradiologists looked for six criteria: cortex thickening, cortical and subcortical signal changes, blurring of the GWM interface, transmantle sign and gyral abnormalities. The frequency of each sign and their combination was assessed. We compared the delay between epilepsy-onset and surgery taking into account the time of type2-FCD detection by MRI.

Results: Only 42 patients (59%) had a positive-MRI. In this group, a combination of at least 3 criteria was always found. Subcortical signal changes were constant. Three characteristic signs (cortical thickening, GWM blurring and transmantle sign) were combined in 64% of patients, indicating that MRI can be highly suggestive. However, typical features of type2-FCD were overlooked on initial imaging in 40% of cases, contributing to a delay in referral for surgical consideration (17 versus 11.5 years when initial MRI was positive).

Conclusion: Combination of 3 major MRI signs allows type2-FCD to be recognized in clinical practice, thereby enabling early identification of candidates for surgery.

Abbreviations: Type2-FCD = type 2 focal cortical dysplasia; GWM = gray-white matter; ^{18}FDG = Fluorodeoxyglucose; EEG = electroencephalography; FOV = field of view.

Introduction

Type2-FCD is one of the main causes of extra-temporal drug-resistant partial epilepsy that is surgically curable. It corresponds to Taylor type focal cortical dysplasia, according to recent classifications,1,2 a more homogeneous pathological entity than other subtypes of cortical dysplasia, especially type1-FCD. The major predictor of a favorable surgical outcome is complete removal of the dysplastic cortex3-7 and accurate presurgical assessment of the lesion extent is crucial to improve surgical results. During the past decade, the development of MRI protocols specifically designed for type2-FCD detection has contributed to the steady increase of candidates for surgery and to a favorable outcome, with a remission rate of up to 90% when MRI is positive compared to 40-60% when MRI is negative.3,6-9 The MR diagnosis remains difficult, however, even in specialized centers using appropriate protocols, with up to 50% of type2-FCD cases remaining undetected or being diagnosed late, thereby depriving patients of effective treatment for years.3 Despite severe and intractable epilepsy, the average time from onset of seizures to surgery is around 14 years in most reported series.3,10-12

Typical MRI features have previously been described.3,6,7,13-21 They include abnormalities of the cortex (thickening, T2 signal increase, gyral abnormalities) and of subcortical white matter (blurring of the GWM interface, T2 signal increase, transmantle sign). Initial MRI descriptions relied on a limited sample of patients.7,15 However, more recent, larger series do not provide a comprehensive analysis of all reported MR signs and the prevalence of each sign varies considerably between studies (table 1). In addition, the proportion of negative-MRI in type2-FCD differs widely, likely because of differences in imaging protocols and selection bias.

We carried out a retrospective study on a large cohort of surgically treated type2-FCD patients investigated with high resolution MRI during the past decade. Our goal was to

determine the prevalence of each previously described MRI criterion for type2-FCD and define a precise MRI pattern so as to optimize its detection in clinical practice. Our second goal was to determine the influence of MRI positivity on delay to surgical referral.

Table 1 Frequency of typical MR signs of histologically proven type2-FCD reported in the literature

	Urbach et al. 2002	Colombo et al. 2003	Widdess-Walsh et al. 2005	Besson et al. 2008	Widjaja et al. 2008	Kim et al. 2009	Krsek et al. 2009	Lerner et al. 2009	This study
Period of study	1996-2000	1996-2000	1990-2002	NA	1991-2005	1995-2005	2002-2005	2000-2007	2000-2011
No. of patients	22	15	48	26	13	28	16	64	71
Negative MRI	0	5 (33%)	10 (21%)	0	2 (15%)	6 (21%)	0	1	29 (41%)
Cortical thickening	18 (81%)	10(67%)	NA	NA	8 (61%)	NA	8 (50%)	43 (67%)	30 (71%)
Blurring of GWM junction	8 (36%)	13 (87%)	NA	NA	11 (84%)	NA	11 (69%)	47 (73%)	38 (90%)
Cortical signal changes	NA	6 (40%)	NA	NA	2 (15%)	NA	10 (62%)	22 (35%)	21 (50%)
Subcortical signal changes	22 (100%)	13 (87%)	27 (56%)	NA	11 (84%)	NA	14 (87%)	64 (100%)	42 (100%)
Transmantle sign	18 (81%)	3 (20%)	NA	5 (19%)	8 (72%)	NA	6 (37%)	NA	35 (83%)
Sulcal abnormalities	NA	NA	NA	NA	3 (23%)	NA	11 (69%)	NA	22 (52%)
Atrophy	NA	3 (20%)	NA	NA	2 (15%)	NA	7 (44%)	11 (17%)	0

GWM = gray-white matter; NA = not available

Patients and Methods

Patients. We retrospectively reviewed the MR data of 71 consecutive patients (40 males, 24 children) with a histological diagnosis of type2-FCD who underwent surgery for intractable epilepsy between May 2000 and May 2011. Presurgical evaluation included ictal video-EEG,

high-resolution MRI, functional MRI and 18FDG–PET scans for all patients, and stereo-EEG for 43 of them (60%). Median age was 6 years (range: 1-20) at epilepsy onset and 20 years (range: 8-52) at surgery. No patient had clinical criteria for tuberous sclerosis. The study was approved by the Ethics Committee of Ile de France III and was found to conform to generally accept scientific principles and ethical standards.

MRI acquisition. Brain MRIs were performed on a 1.5 Tesla MRI (Signa Excite, General Electric Healthcare, Milwaukee, WI) and included the following sequences: volumetric gradient-echo T1-weighted inversion recovery acquisition (slice thickness = 1.2 mm, FOV = 240 × 240 mm, 256 × 192 matrix, 1 nex), coronal and axial 2D fast spin-echo T2-weighted acquisition (thickness 4 mm, no gap, FOV = 240 · 240 mm, 512 × 256 matrix, 2 nex), FLAIR using 2D contiguous slices (thickness 5 mm, FOV = 240 × 240 mm, matrix 256 × 192, 1 nex) or 3D acquisition (slice thickness = 1.2 mm, FOV = 240 × 240 mm, matrix 256 × 226, 1 nex). A 3D T1 fast gradient-echo acquisition after injection of gadolinium was also performed; this was not part of the epilepsy presurgical standard protocol but was needed for accurate identification of vascular landmarks with neuronavigational guidance during intracranial recordings or surgery.

Data analysis. Two neuroradiologists (7 and 9 years of experience), aware of the final localization of the operated lesion, retrospectively reviewed all MRIs in consensus to look for structural abnormalities. Six criteria were analyzed: (1) abnormal cortical thickness, defined as a thickening (or thinning) of at least 50% of the normal cortex, visible on T1WI and T2WI sequences, on at least two orthogonal plans, to rule out partial volume effects; when visible on one sequence only, it was defined as a “pseudo-thickening”; (2) abnormal cortical signal intensity on T1WI, T2WI and/or FLAIR, defined as signal changes involving the entire thickness of the cortex; (3) blurring of the GWM junction, visible on at least one sequence and in 2 orthogonal plans; (4) abnormal signal intensity of subcortical white matter, relative to

normal cortex. This latter abnormality was further classified as either "marked", when the subcortical white matter signal was at least identical to that of the normal cortex, or "subtle", otherwise (figure 1); (5) abnormal signal intensity of deep white matter, the so-called transmantle sign, defined as a subcortical white matter signal intensity change, tapering towards the ventricle on T1WI and/or T2WI (figure 1);22 (6) a major abnormality of sulcal morphology, defined as an abnormality of the depth, angulation or shape of a sulcus, as compared to the contralateral side, on reformatted 3D T1WI or on T2WI sequences. The presence of calcifications, cysts, contrast enhancement, atrophy or mass effect, and vascular abnormalities was also recorded. MRI was considered negative for the diagnosis of type2-FCD when none of the above abnormalities was present, and positive when at least one of the 6 MR criteria was present. In addition, we looked for minor sulcal abnormalities in patients with negative-MRI, i.e. unusual sulci patterns not discernible enough to be classified as major. As these findings were regarded as non-specific or doubtful, MRI was still considered negative.

In order to determine the influence of MRI positivity on referring the patient for a presurgical work-up, we compared the time from epilepsy onset to surgery between the positive-MRI and negative-MRI groups using a Wilcoxon test. In addition, in the subgroup of positive-MRI patients, we reviewed all previous negative-MRIs available in the medical records in order to retrospectively detect the lesion and compared the time from epilepsy onset to surgery with that of patients whose first MRI was considered positive, using a Wilcoxon test.

Figure 1 Typical MR signs of type2-FCD. (A) coronal 3D T1WI, (B) coronal FLAIR, (C) coronal T2WI in a 45-year-old male with left motor seizures, epilepsy onset at 6 years, several previous MRI considered as normal. Unusually deep and straight sulcus in the pre-central region (asterisk), with minimal cortical thickening at the bottom of the sulcus, and cortical signal increase in T2WI and FLAIR. Abnormal subcortical signal, "marked" at the bottom (arrow) surrounded by an area of "subtle" signal increase (arrowheads), responsible

for a gradient of signal abnormalities from the periphery to the center of the dysplasia. Barely perceptible transmantle sign (C, double arrows). (D) Coronal FLAIR, (E) magnification of the left central region in a 19-year-old female with right motor seizure, epilepsy onset at 16 years. This MRI shows a marked increased signal, tapering gradually from the gray-white matter interface to the supero-lateral edge of the lateral ventricle (triple arrows), typical of a transmantle sign.

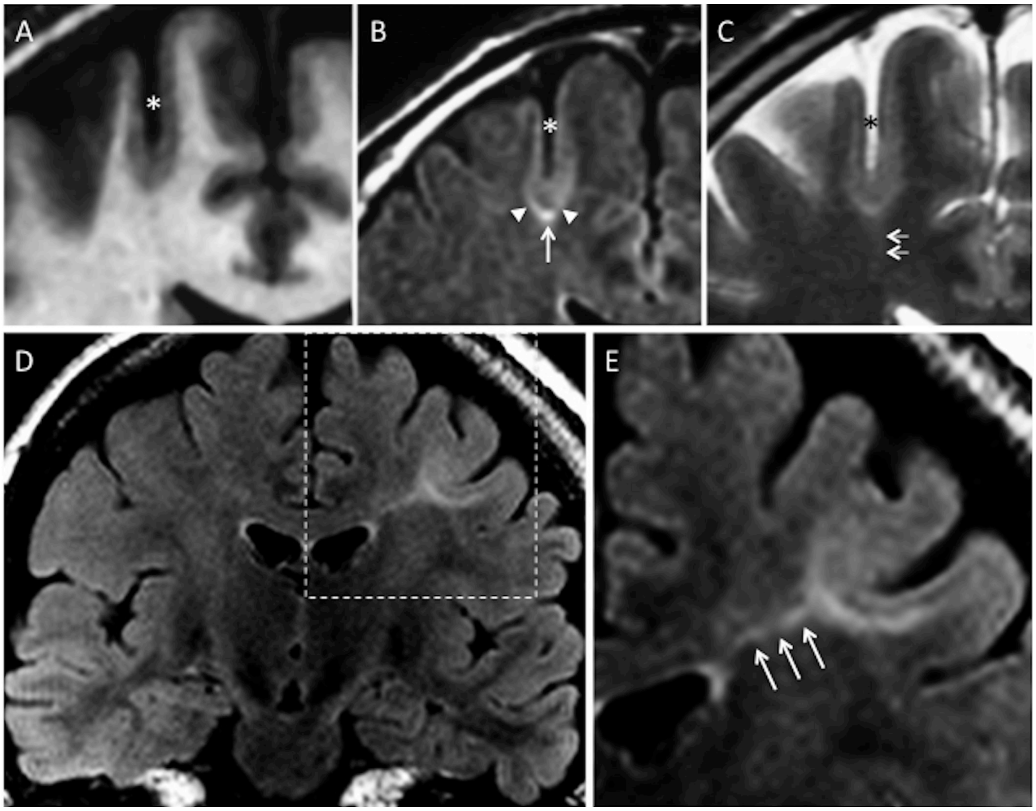

Results

Among the 71 patients, type2-FCD was located in the frontal lobe (n=60, including 28 in the central region limited by pre- and post-central sulcus, and 3 in the insula), parietal lobe (n=7), occipital lobe (n=2), or temporal (n=2) lobe. All lesions were limited to a single lobe and unilateral, with a right/left hemisphere ratio of 1.3. Histological confirmation of type2-FCD was based on a focal disorganization of the cortical cytoarchitecture with giant dysmorphic neurons. Balloon cells were present in 63 patients (type2b-FCD) and were not found in the cortical specimen in the remaining patients (type2a-FCD).

Table 2 Clinical and histological data of positive-MRI and negative-MRI patients

	Negative-MRI	**Positive-MRI**	**Total**
No. of patients	29	42	71
Sex ratio (M/F)	0.8	1.8	1.3
Age at onset (in years): median (range)	6 (1-20)	5.8 (1-20)	6 (1-20)
Age at surgery (in years): median (range)	17 (8-41)	22.5 (8-52)	20 (8-52)
Location of FCD			
Left/right ratio	1.4	1.25	1.35
Frontal lobe	23	37	60
Parietal lobe	4	3	7
Temporal lobe	1	1	2
Occipital lobe	1	1	2
Type2-FCD subtypes			
Type 2a (no balloon cells)	6	2	8
Type 2b (balloon cells)	23	40	63

Positive-MRI. Forty-two patients (59%) had positive-MRI. Twelve patients (29%) had all 6 criteria. All patients had at least 3 of the 6 criteria. All patients had either cortical thickening, blurring of GWM interface or transmantle sign, and 27 patients (64%) had all 3 of these signs. *Cortical thickening* was present in 30 patients (71% of positive-MRI), did not exceed twice the normal cortex and was limited to a small cortical area. Seven other patients (17%) had "pseudo-thickening", visible on only one of the sequences. This "pseudo-thickening" was related to signal changes of the subcortical white matter (figure 2).

Figure 2 Cortical pseudo-thickening. (A, B) Axial T1WI and (C) coronal T2WI in a 29-year-old male with left motor seizures, onset at 3 years. These images show cortical thickening (arrow) and blurring (asterisk) of the gray-white matter interface of the right central sulcus. (D) Coronal FLAIR allowing cortical to be distinguished from subcortical signal increase (arrowheads).

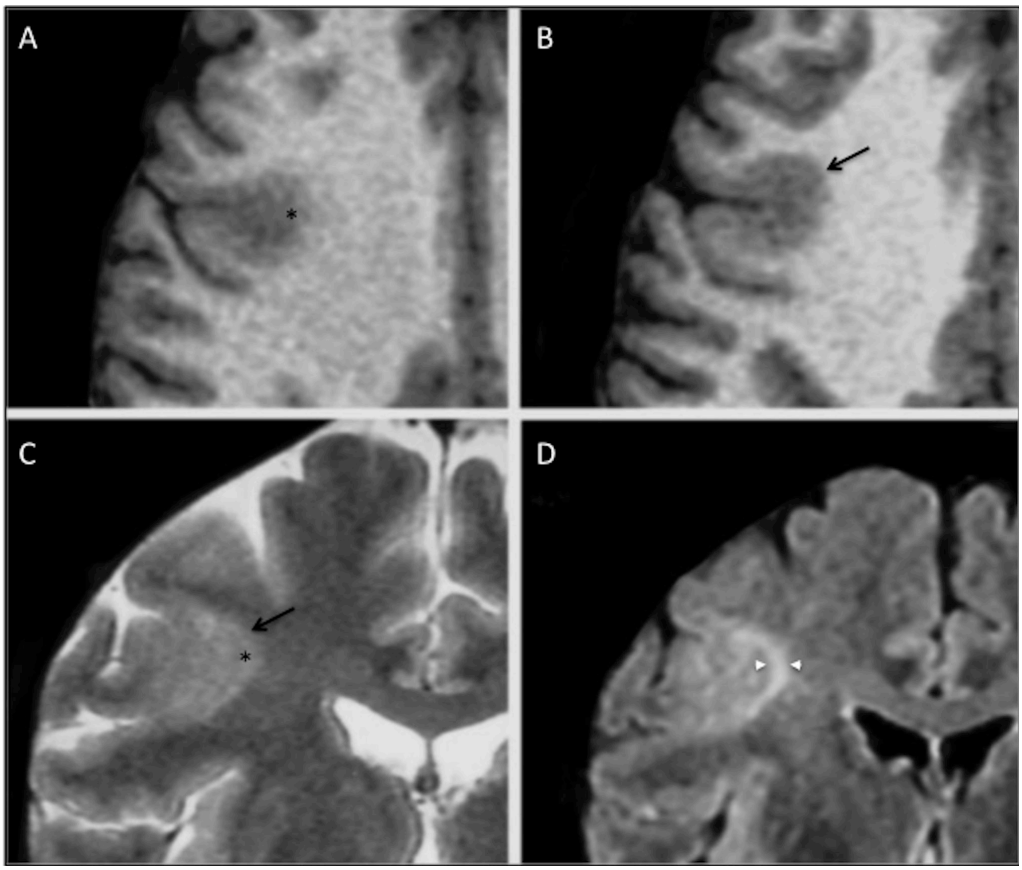

Cortical signal changes were present in 21 patients (50% of positive-MRI). They consisted in hyperintensity on T2WI in 15 patients (best seen on FLAIR sequence), hyperintensity on T1WI in 2 patients and in increased signal on both sequences in the remaining 4 patients. They were located at the bottom of the dysplastic sulcus, variably spreading to the surrounding gyri.

Blurring of the GWM interface was present in 38 patients (90% of positive-MRI). It was co-located with cortical thickening, when present, in all patients except one. As with cortical thickening, this sign could be obvious on one sequence and barely visible on others (figure 2).

Abnormal signal intensity of subcortical white matter was seen in all patients with positive-MRI. It was "marked" in 31 patients (73%). "Subtle" changes were not visible on T1WI. Interestingly, in 13 of the 31 patients with marked subcortical increased signal, this abnormality extended from the depth of the sulcus to the surrounding white matter, with a symmetrical gradual centrifugal signal decrease (figure 1).

Transmantle sign was present in 35 patients (83% of positive-MRI), and was typically mildly hyperintense on T2WI and FLAIR and hypointense in T1WI. It spread along the axis of the abnormal sulcus, running perpendicular towards the wall of the lateral ventricle (figure 1). Its thickness was proportional to the width of subcortical abnormalities.

Major sulcal abnormalities were present in 22 patients (52% of positive-MRI). They consisted in sulci that were unusually deep (n=15), wide (n=5) and/or with unusual angulation (n=11) (figure 1). Such sulcal abnormalities were never isolated but were associated with other typical type2-FCD features.

Micro-calcifications were observed in the peri-ventricular region in a patient with a large dysplasia in the temporal lobe. A developmental venous abnormality adjacent to a frontal dysplasia was seen in another patient. A small (< 10 mm) cystic component was present in 3

patients. Parenchymal contrast enhancement, focal atrophy or mass effect, complete disappearance of the GWM interface or marked thinning of the cortex was never observed.

Worthy of note, among the 42 patients with positive-MRI, 16 had at least one brain MRI that had been considered normal during the course of epilepsy. In all 16 cases, the lesion was retrospectively visible. The delay from epilepsy onset to surgery was more than 5 years longer in patients with negative initial MRI (median: 17 years; range: 6-42) than in those whose first MRI was positive (11.5 years; range: 1-29), although not reaching significance due to the small number of patients ($p = 0.06$).

Negative-MRI. Twenty-nine patients (41%) had a negative-MRI (figure 3) despite histological confirmation of type2-FCD (table 2). For these patients, FDG-PET was positive in 25 (86%) cases, showing a focal or regional hypometabolism, contributing to the detection of the lesion. In addition, intracranial recording using depth electrodes (Stereo-EEG) was used to determine the epileptogenic zone and the extent of the cortical resection. In 4 patients, intracranial recording was deemed not necessary because PET demonstrated a focal hypo-metabolism corresponding to a single gyrus, highly suggestive of a focal lesion.

Moreover, in 13 cases of negative MRI, minor sulcal abnormalities were observed in the vicinity of type2-FCD (figure 4), sometimes not strictly colocalized with the dysplastic lesion. As with major sulcal abnormalities, minor features corresponded to unusual depth, width or shape of the sulcus, but were not clear enough to be considered abnormal. In addition, none of the other criteria suggestive of type2-FCD was found in these cases, in contrast to the major sulcal abnormalities described in positive-MRI cases, which were never isolated findings (figure 1).

Balloon cells were present in 79% of the negative-MRI cases and were similarly found in cases with minor sulcal abnormalities (10 out of 13) than in strictly normal MRI (13 out of 16).

Worthy of note, the delay from epilepsy onset to surgery was shorter in the negative-MRI (median: 11.5 years; range: 1-31) than in the positive-MRI group (16 years; range: 1-42), (p = 0.03). This apparently surprising finding is related to a bias of recruitment, with a high proportion of children with negative-MRI and short epilepsy duration due to special collaboration with pediatric teams and systematic use of FDG-PET in this population.

Figure 3 Negative-MRI. (A, C) axial and coronal 3D T1WI, (B, D) axial and coronal 3D FLAIR in a 15-year-old male with right frontal lobe epilepsy, nocturnal seizure predominance, onset at 12 years. Absence of the 6 criteria, no minor sulcal abnormality found. (E) ^{18}FDG-PET coregistered on MRI (axial slice) allows recognition of a gyral hypometabolism corresponding to the anterior part of the right cingulate cortex (arrow). (F,G) Histology slides (Klüver-Barrera; original magnification ×40) showing typical features of type2b-FCD with giant dysmorphic neurons in the cortex (double arrow) and balloon cells in the underlying white matter (arrow head).

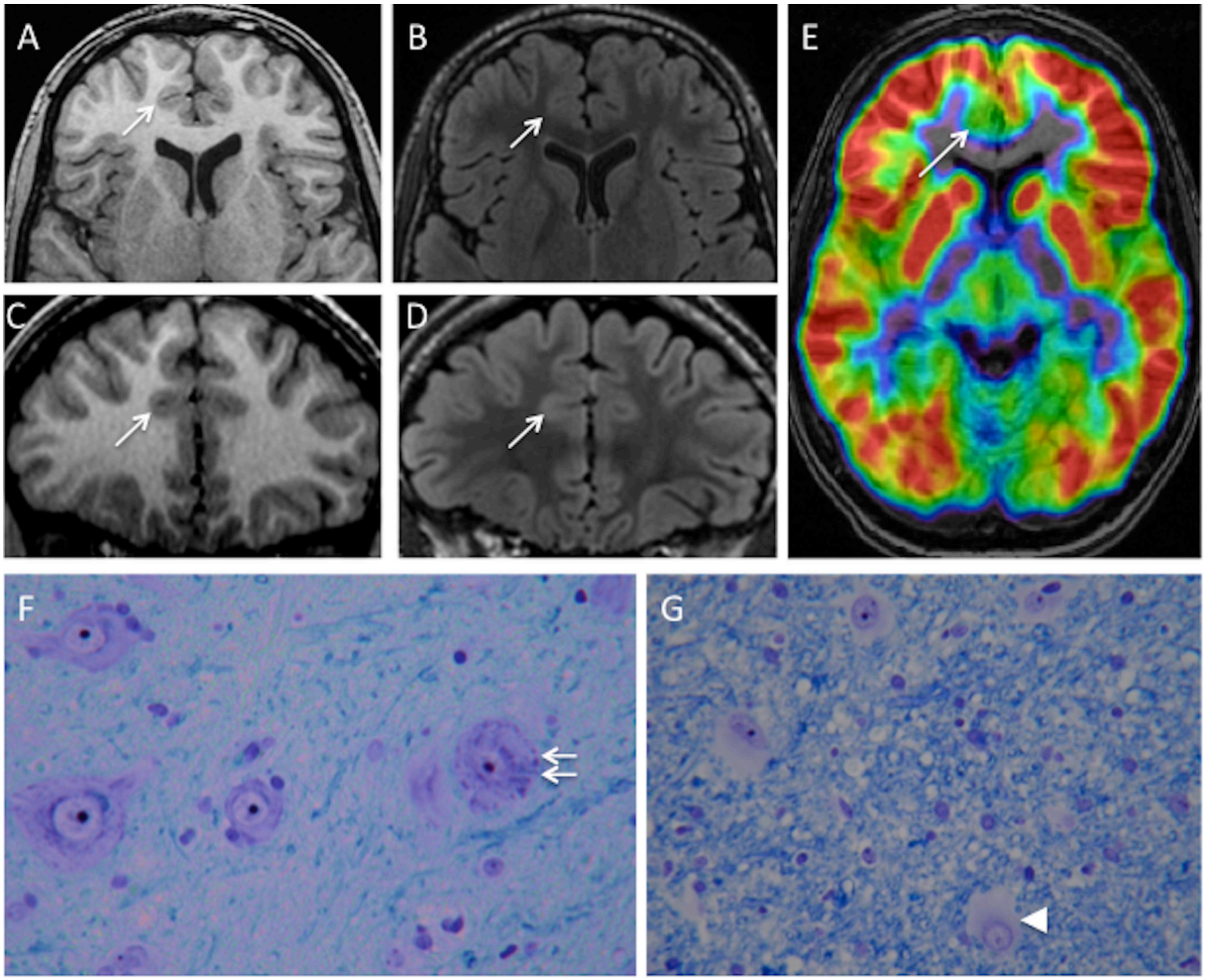

Figure 4 Negative-MRI with minor sulcal abnormality. (A) coronal T2WI, (B) FLAIR and (C) T1WI in an 36 year-old male with right nocturnal frontal lobe epilepsy, onset at 20 years. None of the 6 criteria is found. A minor sulcal abnormality is perceptible in the right superior frontal area, with an unusually large and deep sulcus (arrow). (D,E) Cortical specimen (Klüver-Barrera; original magnification D: ×5; E: ×15). Deep part of the pathological sulcus with typical type2a-FCD features: cortical disorganization and presence of giant neurons (arrowhead) without balloon cells. Note the good delineation of the gray-white matter interface (double arrow) correlated with absence of blurring on MRI.

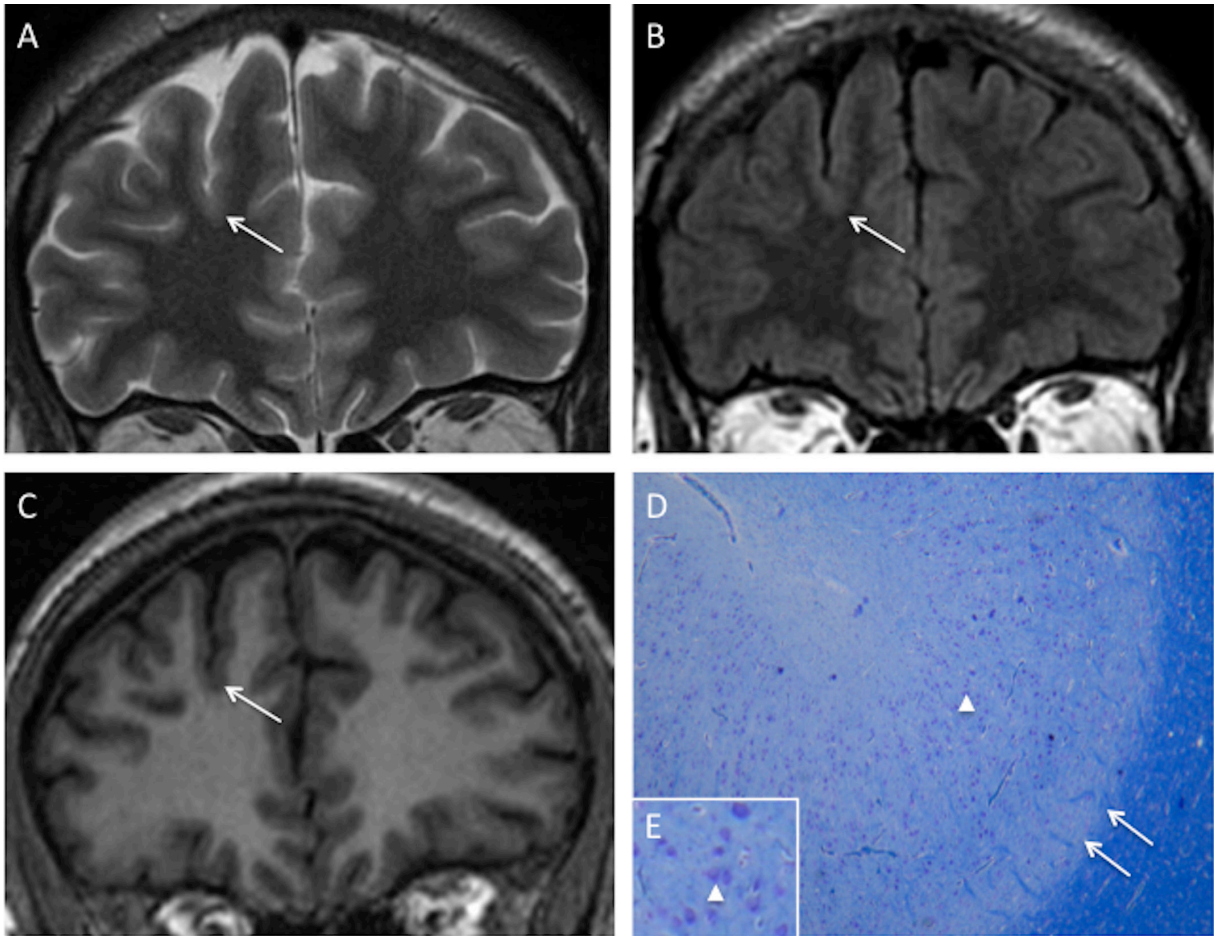
A
B
C
D
E

Discussion

The main findings of this systematic qualitative MRI analysis, in a series of 71 consecutive patients with histologically confirmed type2-FCD, are as follows: (1) only 59% had a positive-MRI despite optimal MRI techniques according to recommended guidelines;23 (2) all patients with positive-MRI presented at least 3 of the 6 recognized MR criteria for type2-FCD, with combined cortical thickening, blurring of GWM interface and transmantle sign in 64% of patients; (3) MRI features suggestive of type2-FCD were overlooked on initial imaging in 40% of the cases, leading to late referral for surgical consideration.

Cortical thickening and blurring of the GWM demarcation are considered to be major signs, corresponding to the presence of dysmorphic neurons and balloon cells in the cortex and the GWM junction, ectopic neurons or axonal loss in white matter.7,8,14,15 We additionally found subtle pseudo-thickening, i.e. a subtle subcortical signal increase similar to that of the cortex, in a few patients, contrasting with the extensive thickening reported in previous studies.3,7,11,15 The subtlety of this sign is in line with histological data showing that cortical thickening is more focal and less obvious than previously described.24,25 To avoid being confounded with pseudo-thickening, cortical thickening has been the focus of an expert consensus, stipulating that it must be seen in two adjacent sections and with two different pulse weightings.25 We did not observe any sign of lobar, gyral or focal cortical atrophy, in contrast with others who reported atrophy in 15 to 44% of cases (table 1). This subtle and subjective sign, more common in type 1 focal cortical dysplasia,6 may have been underestimated in our analysis. It is also possible that what we considered as deep dysplastic sulcus was interpreted by others as pseudo focal atrophy.26 Worthy of note, we never observed any major cortical thinning as encountered in ischemic or traumatic sequelae.

The third major sign consisted of subcortical white matter abnormalities, which were found in all patients with positive-MRI. This is likely due to the clear-cut signal changes on T2WI or FLAIR. Contrary to previous reports16, we found no correlation between the presence of balloon cells and subcortical signal abnormalities (table 2).

The signal increase of the cortex is a well-known sign of type2-FCD, although rarely emphasized.3,14 It was found in 48% of patients with positive-MRI, within the 15-62% range of previous reports3,6,13,15 (see also table 1). It was often moderate and was more clearly seen on FLAIR sequences. This abnormality could be related to a high density of balloon cells in the cortex.14 With the increased use of 3D FLAIR and high-field MRI, this sign may in future be easier to detect and become more reliable.

The transmantle sign is reported to be a specific feature for malformations of cortical development.22 This typical pattern overlaps the path of migrating neuroblasts, consistent with a disruption of early corticogenesis. It has been related to the presence of balloon cells and hypomyelination in the white matter underlying the dysplastic lesion.7,22 This sign may also occur in other developmental abnormalities, such as venous or arterio-venous malformations,27 and, when isolated, is not specific for type2-FCD. However, its association with cortical thickening and GWM blurring provides the most reliable pattern for the diagnosis of type2-FCD. We observed the transmantle sign in more than 80% of patients with positive-MRI, which is a higher proportion than that reported in even the most recent studies. In two recent studies, the frequency of the transmantle sign reached 60%,7,28 whereas its frequency did not exceed 30% in other studies, suggesting that it may have been underestimated in earlier reports.6,7,13,15,26

Abnormalities of sulcal morphology were present in nearly one half of the positive-MRI cases. Such features are difficult to assess and are likely underestimated. We stress that isolated minor sulcal abnormalities may also retrospectively be found in cortical areas

containing a small type2-FCD, as observed in nearly half of the negative-MRI cases (figure 4). Sulcal abnormalities have already been described29 but have received little attention and their prevalence has never been evaluated. Only one study26 confirmed by quantitative analysis that small type2-FCD were preferentially located at the bottom of an abnormally deep sulcus. Their physiological mechanisms have not been elucidated to date. Nevertheless, the majority of malformations of cortical development are associated with abnormal gyral/sulcal morphology, suggesting that the organization of sulci is intimately linked to the early stages of cortical development.30

Another striking finding in this study is that abnormalities were arranged symmetrically relative to an axis perpendicular to the cortex. Of note, the axis of symmetry overlapped the trajectory of the transmantle sign. In addition, we highlighted that, in half of the cases, a gradient of decreasing abnormal signal intensity from the bottom of the dysplastic sulcus to the surrounding gyri was found (figure 1). This finding confirms that, irrespective of the size of the lesion, maximum cellular abnormalities are located deep in the sulcus.

The proportion of type2-FCD patients with negative-MRI (41%) was higher than that in most reported series3,6-8,13-15,26 but similar to the rate reported when using stereo-EEG as a diagnostic tool.31 This is likely explained by the fact that, in our patients with negative-MRI, surgery was based on a combination of FDG-PET and stereo-EEG. Noteworthy, balloon cells were found in the cortical specimen of 79% of our negative-MRI patients (table 2), in contrast with previous reports suggesting that balloon cell FCDs (type2b) are generally characterized by signal changes in the white matter.16

Finally, the localization of type2-FCD was overwhelmingly frontal and rarely temporal in our series, as in others,8,14,15 whereas other epileptogenic lesions are predominantly located in the temporal lobe. This suggests that frontal drug-resistant partial epilepsy with normal MRI should raise the suspicion of type2-FCD, and this is supported by surgical series of

cryptogenic partial epilepsy, in which up to 40% of the resected cortical specimens (especially in the frontal lobe) corresponded to type2-FCD at histology.9,31,32 Moreover, a recent report of the International League against Epilepsy noted that none of the epileptic children diagnosed with tumor or ischemia had normal MRI.

Our study has some limitations. It was retrospective and was based solely on patients who underwent surgery and thus does not represent the entire spectrum of type2-FCD. Nevertheless, the study of unoperated patients is limited by the lack of histological confirmation. Furthermore, due to the lack of a control group, we cannot assess the specificity of the MRI abnormalities, especially the transmantle sign. In addition, positive-MRI (59% of our patients) was based on conventional visual analysis. Voxel-based post-processing methods proved a significant benefit in comparison with visual analysis alone33,34 and would possibly decrease our negative-MRI rate. However, these techniques apply algorithms not applicable in routine practice. Furthermore, the feature maps direct the attention to suspicious regions but the interpretation still requires an experienced reader to confirm, with conventional MRI, the presence of a type2-FCD. Finally, the use of a 3T magnetic field could have increased the number of positive MRIs as reported in recent studies.35

Conclusion

We emphasize that nearly 60% of type2-FCD may be recognized on 1.5T MRI and propose that a combination of features (found in 2/3 of the cases), comprising focal cortical thickening, GWM blurring and transmantle sign, are highly suggestive of this FCD subtype. Early identification of this lesion is crucial to minimize the delay in referring patients for surgical consideration.

References

1. Blumcke I, Thom M, Aronica E, et al. The clinicopathologic spectrum of focal cortical dysplasias: a consensus classification proposed by an ad hoc Task Force of the ILAE Diagnostic Methods Commission. Epilepsia 2011;52:158-174.

2. Palmini A, Najm I, Avanzini G, et al. Terminology and classification of the cortical dysplasias. Neurology 2004;62(suppl 3):S2-8.

3. Lerner JT, Salamon N, Hauptman JS, et al. Assessment and surgical outcomes for mild type I and severe type II cortical dysplasia: a critical review and the UCLA experience. Epilepsia 2009;50:1310-1335.

4. Kim DW, Lee SK, Chu K, et al. Predictors of surgical outcome and pathologic considerations in focal cortical dysplasia. Neurology 2009;72:211-216.

5. Chassoux F, Devaux B, Landre E, et al. Stereoelectroencephalography in focal cortical dysplasia: a 3D approach to delineating the dysplastic cortex. Brain 2000;123:1733-1751.

6. Krsek P, Maton B, Jayakar P, et al. Incomplete resection of focal cortical dysplasia is the main predictor of poor postsurgical outcome. Neurology 2009;72:217-223.

7. Urbach H, Scheffler B, Heinrichsmeier T, et al. Focal cortical dysplasia of Taylor's balloon cell type: a clinicopathological entity with characteristic neuroimaging and histopathological features, and favorable postsurgical outcome. Epilepsia 2002;43:33-40.

8. Tassi L, Colombo N, Garbelli R, et al. Focal cortical dysplasia: neuropathological subtypes, EEG, neuroimaging and surgical outcome. Brain 2002;125:1719-1732.

9. Jeha LE, Najm I, Bingaman W, Dinner D, Widdess-Walsh P, Luders H. Surgical outcome and prognostic factors of frontal lobe epilepsy surgery. Brain 2007;130:574-584.

10. Salamon N, Kung J, Shaw SJ, et al. FDG-PET/MRI coregistration improves detection of cortical dysplasia in patients with epilepsy. Neurology 2008;71:1594-1601.

11. Widdess-Walsh P, Diehl B, Najm I. Neuroimaging of focal cortical dysplasia. J Neuroimaging 2006;16:185-196.

12. Chassoux F, Rodrigo S, Semah F, et al. FDG-PET improves surgical outcome in negative MRI Taylor-type focal cortical dysplasias. Neurology 2010;75:2168-2175.

13. Widjaja E, Nilsson D, Blaser S, Raybaud C. White matter abnormalities in children with idiopathic developmental delay. Acta Radiol 2008;49:589-595.

14. Widdess-Walsh P, Kellinghaus C, Jeha L, et al. Electro-clinical and imaging characteristics of focal cortical dysplasia: correlation with pathological subtypes. Epilepsy research 2005;67:25-33.

15. Colombo N, Citterio A, Galli C, et al. Neuroimaging of focal cortical dysplasia: neuropathological correlations. Epileptic Disord 2003;5(suppl 2):S67-72.

16. Chan S, Chin SS, Nordli DR, Goodman RR, DeLaPaz RL, Pedley TA. Prospective magnetic resonance imaging identification of focal cortical dysplasia, including the non-balloon cell subtype. Annals of neurology 1998;44:749-757.

17. Kuzniecky R, Morawetz R, Faught E, Black L. Frontal and central lobe focal dysplasia: clinical, EEG and imaging features. Developmental medicine and child neurology 1995;37:159-166.

18. Lee SK, Choe G, Hong KS, et al. Neuroimaging findings of cortical dyslamination with cytomegaly. Epilepsia 2001;42:850-856.

19. Mackay MT, Becker LE, Chuang SH, et al. Malformations of cortical development with balloon cells: clinical and radiologic correlates. Neurology 2003;60:580-587.

20. Bernasconi A, Antel SB, Collins DL, et al. Texture analysis and morphological processing of magnetic resonance imaging assist detection of focal cortical dysplasia in extra-temporal partial epilepsy. Ann Neurol 2001;49:770-775.

21. Colombo N, Tassi L, Galli C, et al. Focal cortical dysplasias: MR imaging, histopathologic, and clinical correlations in surgically treated patients with epilepsy. AJNR Am J Neuroradiol 2003;24:724-733.

22. Barkovich AJ, Kuzniecky RI, Bollen AW, Grant PE. Focal transmantle dysplasia: a specific malformation of cortical development. Neurology 1997;49:1148-1152.

23. Duncan JS. Imaging in the surgical treatment of epilepsy. Nat Rev Neurol 2010;6:537-550.

24. Chamberlain WA, Cohen ML, Gyure KA, et al. Interobserver and intraobserver reproducibility in focal cortical dysplasia (malformations of cortical development). Epilepsia 2009;50:2593-2598.

25. Colombo N, Salamon N, Raybaud C, Ozkara C, Barkovich AJ. Imaging of malformations of cortical development. Epileptic Disord 2009;11:194-205.

26. Besson P, Andermann F, Dubeau F, Bernasconi A. Small focal cortical dysplasia lesions are located at the bottom of a deep sulcus. Brain 2008;131:3246-3255.

27. Lasjaunias P, Manelfe C, Terbrugge K, Lopez Ibor L. Endovascular treatment of cerebral arteriovenous malformations. Neurosurg Rev 1986;9:265-275.

28. Widjaja E, Otsubo H, Raybaud C, et al. Characteristics of MEG and MRI between Taylor's focal cortical dysplasia (type II) and other cortical dysplasia: surgical outcome after complete resection of MEG spike source and MR lesion in pediatric cortical dysplasia. Epilepsy research 2008;82:147-155.

29. Bronen RA, Spencer DD, Fulbright RK. Cerebrospinal fluid cleft with cortical dimple: MR imaging marker for focal cortical dysgenesis. Radiology 2000;214:657-663.

30. Regis J, Tamura M, Park MC, et al. Subclinical abnormal gyration pattern, a potential anatomic marker of epileptogenic zone in patients with magnetic resonance imaging-negative frontal lobe epilepsy. Neurosurgery 2011;69:80-93.

31. McGonigal A, Bartolomei F, Regis J, et al. Stereoelectroencephalography in presurgical assessment of MRI-negative epilepsy. Brain 2007;130:3169-3183.

32. Chapman K, Wyllie E, Najm I, et al. Seizure outcome after epilepsy surgery in patients with normal preoperative MRI. J Neurol Neurosurg Psychiatry 2005;76:710-713.

33. Bernasconi A, Bernasconi N, Bernhardt BC, Schrader D. Advances in MRI for 'cryptogenic' epilepsies. Nat Rev Neurol 2011;7:99-108.

34. Wagner J, Weber B, Urbach H, Elger CE, Huppertz HJ. Morphometric MRI analysis improves detection of focal cortical dysplasia type II. Brain 2011;134:2844-2854.

35. Knake S, Triantafyllou C, Wald LL, et al. 3T phased array MRI improves the presurgical evaluation in focal epilepsies: a prospective study. Neurology 2005;65:1026-1031.

Chapitre 2 : Apport de l'IRM 3 Tesla en comparaison avec l'IRM 1,5 Tesla dans la détection et caractérisation des DCF2

Cette étude a fait l'objet d'une publication dans *Epilepsia* en 2013 dont le manuscrit est inséré ci-après (la version au format de la revue est également disponible en Annexe 2) et dont les principaux résultats sont ici résumés :

Introduction

Parmi les facteurs d'amélioration de la détection des DCF2 en IRM, nous nous sommes ici intéressés à l'apport d'une augmentation du champ magnétique principal (B0). Peu d'études (26–28) avaient comparé la détection des lésions épileptogène à 1,5T et à 3T. Ces études portaient par ailleurs sur des populations hétérogènes de patients épileptiques avec peu de DCF2 et les acquisitions réalisées à l'aide d'antenne différente pouvant induire un facteur confondant. Nous nous sommes donc basés sur une population homogène de 25 patients, tous porteurs d'une DCF2 prouvée histologiquement et scannés respectivement à 1,5T et à 3T avec des antennes et des temps d'acquisition comparables. L'analyse d'image consistait dans un premier temps en la détection d'une lésion par deux radiologues indépendants à partir des deux sets d'images et dans un ordre aléatoire. Chaque critère typique des DCF2 en IRM, décrit dans la précédente étude, était ensuite recherché et noté selon une échelle de visualisation (de 0 à 3) de même que la présence d'artéfacts

Résumé des principaux résultats

- Le taux de détection n'était que peu modifié par l'élévation du champ magnétique avec 17/25 (68%) DCF2 détectées à 3T contre 15/25 (60%) à 1,5T.
- En revanche, le passage à 3T permettait une meilleure visualisation et une caractérisation des lésions détectées comme en témoignait un meilleur score de visualisation des principaux critères de détection
- Cette meilleure visualisation concernait en particulier le « transmantle sign » dont le score de visualisation à 3T environ 3 fois supérieur à celui obtenu à 1,5T (1,72 vs. 0,56 ; p=0,002)

- De même, une meilleure concordance inter-observateur pour la détection des lésions était obtenue à 3T.
- Le taux d'artéfact était en revanche un peu plus élevé à 3T (incluant des artéfacts de mouvement, de susceptibilité et de repliement).

Conclusion

Le passage de 1,5 à 3T en IRM chez les patients suspects de DCF2 améliore la caractérisation des lésions en raison d'une meilleure visualisation du « transmantle sign ». Ce résultat est d'autant plus intéressant que ce signe est considéré comme une signature en IRM des DCF2.

3T MRI improves the detection of transmantle sign in type 2 focal cortical dysplasia

ABSTRACT

OBJECTIVE: Type 2 focal cortical dysplasia (FCD2) is one of the main causes of refractory partial epilepsy, but often remains overlooked by MRI. This study aimed to elucidate whether 3T MRI offers better detection and characterization of FCD2 than 1.5T, using similar coils and acquisition time.

METHODS: Two independent readers reviewed the 1.5T and 3T MR images of 25 patients with histologically proven FCD2. For both magnetic fields, the ability to detect a lesion was analyzed. We compared the identification of each of the 5 criteria typical of FCD2 (cortical thickening, blurring, cortical and subcortical signal changes, "transmantle" sign) and artifacts, using a 4-point scale (0 to 3). Inter-observer reliability for lesion detection was calculated.

RESULTS: Seventeen lesions (68%) were detected at 3T, two of which were overlooked at 1.5T. Inter-observer reliability was better at 3T (κ=1) than at 1.5T (κ =0.83). The transmantle sign was more clearly identified at 3T than 1.5T (mean visualization score: 1.72 vs. 0.56; P = 0.002).

SIGNIFICANCE: The use of 3T MRI in patients suspected of type2 FCD improves the detection rate and the lesion characterization owing to the transmantle sign being more clearly seen at 3T. This point is of interest since this feature is considered as an MR signature of FCD2.

KEYWORDS: Intractable Epilepsy, MR imaging, Focal Cortical Dysplasia, transmantle sign

Introduction

Type 2 focal cortical dysplasia (FCD2) is one of the main causes of extra-temporal drug-resistant partial epilepsy that is surgically curable. MRI has contributed to the steady increase of candidates for surgery. According to large surgical series, the majority of patients with extra-temporal cryptogenic epilepsy suffer from focal cortical dysplasia (FCD) that can be not recognized on MRI.1-6 Indeed, even with dedicated protocols, MR diagnosis remains difficult, with up to 40% of FCD2 cases either undetected or diagnosed late.7-9 Consequently, detection and delineation of FCD2 with MRI in patients with medically refractory extra-temporal epilepsy has become one of the most challenging goals for improving surgical outcome.10, 11

Owing to its higher signal-to-noise ratio and smaller voxel size for a given acquisition time, 3 Tesla (3T) may be better than 1.5 Tesla (1.5T) MRI for the detection of FCDs. Two studies suggested that MRI at 3T using phased array coils performed better than 1.5T MRI using a standard quadrature head coil for the detection and characterization of epileptogenic lesions.12, 13 Yet, this improvement might not solely be due to the increase in field strength but rather to the use of phased array coils.13-15 The benefit of 3T MRI, if any, is likely not identical for all types of epileptic lesions. Hippocampal sclerosis and tissue loss are reported to be best seen at 1.5T14, 16 whereas cortical development lesions, including FCDs, would be best seen at 3T.12-14, 17 However, these studies relied on heterogeneous series of epileptogenic lesions with only a few cases of histologically proven FCD2. The most recent studies dealing with epilepsy and FCD imaging used 3T MR.18-23 One would not therefore expect its superiority over 1.5T for detecting subtle lesions such as FCD to be in doubt, though a comparison of these two magnetic fields focusing on FCD has never been carried out.

Based on a population of proven FCD2, we compared the yield of 1.5T and 3T MRI both using an 8-channel phased-array head coil and similar acquisition time for the detection and characterization of FCD2. To further elucidate the expected superiority of 3T over 1.5T MRI, we also analyzed separately each MR sign of FCD2 at both magnetic fields.

Methods

Patients

We retrospectively identified all consecutive epileptic patients who underwent both 1.5 and 3T MRI between January 2010 and May 2013 and who had a final diagnosis of FCD2.

Twenty-five patients fulfilled these criteria. The reasons for re-scanning patients at 3T MRI (3T MR unit installed at the start of the study period) included previously normal or equivocal 1.5T MRI findings or referral for fMRI tasks or neuronavigation in the case of visible 1.5T lesion. In such cases, additional morphological sequences were obtained during the same imaging session. Presurgical evaluation included ictal video-EEG, and 18 Fluorodeoxyglucose Positron Emission Tomography scans for all patients, and stereo-EEG for 10 of them. The diagnosis of FCD2 was based on histologic confirmation (focal disorganization of the cortical cytoarchitecture and presence of giant dysmorphic neurons) in all patients. Balloon cells were found in all specimens (type IIb), except in three (type IIa). The study was approved by the Ethics Committee of Ile de France III and was found to conform to generally accept scientific principles and ethical standards.

Data Acquisition

Patients were scanned using a 1.5T (Signa Excite, General Electric Healthcare, Milwaukee, WI) and a 3T (Discovery MR750, General Electric Healthcare, Milwaukee, WI) clinical MRI with similar 8-channel phased-array head coils. The epilepsy imaging protocol included

volumetric gradient-echo T1-weighted inversion recovery acquisition, coronal and/or axial 2D fast spin-echo T2-weighted acquisition, FLAIR using 2D contiguous slices and/or 3D acquisition (Table 1).

Table 1. MRI protocol at 1.5T and at 3T

	Slice thickness (mm)	FOV (mm)	Acquisition matrix	TE (ms) / TR (ms) / TI (ms) / Flip angle	Scan time (min:sec)	No. of patients
1.5T						
Axial and/or coronal FLAIR	5	240×240	256×192	140/9202/90°	3:41	25
3D FLAIR	1.2	240×240	256×226	162/6000/90°	5:39	4
Axial and/or coronal T2 FSE	4	240×240	512×256	102/4200/90°	5:11	25
3D T1 SPGR IR	1.4	240×240	256×192	2.1/10/15°	5:57	25
3T						
Axial FLAIR	3.5	220×220	356×256	143/8000/90°	3:13	5
3D FLAIR	1	256×230	256×224	127/5000/90°	5:23	25
Axial and/or coronal T2 FSE	3.5	220×165	512×320	102/9757/90°	3:25	25
3D T1 SPGR IR	1.2	250×175	512×256	4.3/10/15°	5:29	25

FLAIR, Fluid attenuated inversion recovery; SPGR IR, spoiled gradient-echo inversion recovery; FSE, Fast spin echo; FOV, Field of view; TE, Echo time; TR, Repetition time; TI, Inversion time.

Data Analysis

Both 1.5T and 3T MR images were reviewed on a dedicated workstation (Advantage Windows Workstation, General Electric Medical Systems, Buc, France) for each patient, first independently and then in consensus, by 2 neuroradiologists (7 and 9 years of experience), one of whom was specialized in epilepsy imaging. Readers were aware of electro-clinical data and that all patients had one histology confirmed FCD2. Each MR exam (3T or 1.5T) was

analyzed in a random order, with availability of the complete MR image set at a given magnetic field. Each reader was asked to state if the lesion was visible, based on 5 imaging criteria: (1) cortical thickness, (2) cortical signal intensity (3) blurring of the gray-white matter junction (4) signal intensity of subcortical white matter and (5) transmantle sign, defined as a subcortical white matter signal intensity change, tapering towards the ventricle. Each feature was rated on a 4-point visualization scale from 0 (normal) to 3 (marked). Imaging artifacts (susceptibility, motion or aliasing artifacts) were also quoted using a similar scale from 0 (none) to 3 (marked).

We compared the findings (number of lesions detected, visualization scores) between readers at a given magnetic field, and the consensus reading at 1.5 and 3T using a Wilcoxon test. Interobserver agreements were measured at 1.5T and 3T, using Cohen's kappa test. All data were analyzed using the SAS® v9.1 statistical package (SAS Institute Inc., Cary, NC).

Results

The 25 patients (15 males) had a median age of 21 years (range: 13-50) at surgery. The median (interquartile range) delay from 1.5T to 3T MRI was 13.1 (1-20) months. FCD2 was located in the frontal lobe in 22 cases (including 9 in the central region and 1 in the insula), 2 lesions were parietal and 1 in the temporal lobe, with 12 lesions in the right hemisphere and 13 in the left hemisphere. Interobserver reliability for the detection of the lesion (detected vs. not detected) was perfect at 3T (κ=1) and almost perfect at 1.5T (κ=0.83). No lesion was detected elsewhere than in the area corresponding to the site of FCD2, as determined by histology. After consensus, 15 of the 25 FCD2s (60%) were detected at both magnetic field strengths and 2 lesions were only detected at 3T (Fig. 1 and 2) reaching thus 68% of detected lesions. Visualization scores for each individual sign of FCD2 were higher at 3T than at 1.5T (table 2) and reached significance for the transmantle sign (P = 0.002) (Fig. 3). Of note, in our

study, 4 patients had 3D FLAIR at both magnetic field strength, among which 2 were negative. For the 2 other patients, transmantle sign was not or barely visible at 1.5T due to a low signal-to-noise ratio, while being conspicuous at 3T (fig. 3, case 1). Artifacts were less recorded at 1.5T than at 3T with slight to moderate artifacts in both cases involving 5 patients at 3T (motion, n=2; aliasing, n=2; susceptibility artifact, n=1) and 2 patients at 1.5T (motion). No marked artifacts were recorded.

Table 2. Comparison of visualization scores for each criterion between 3T and 1.5T.

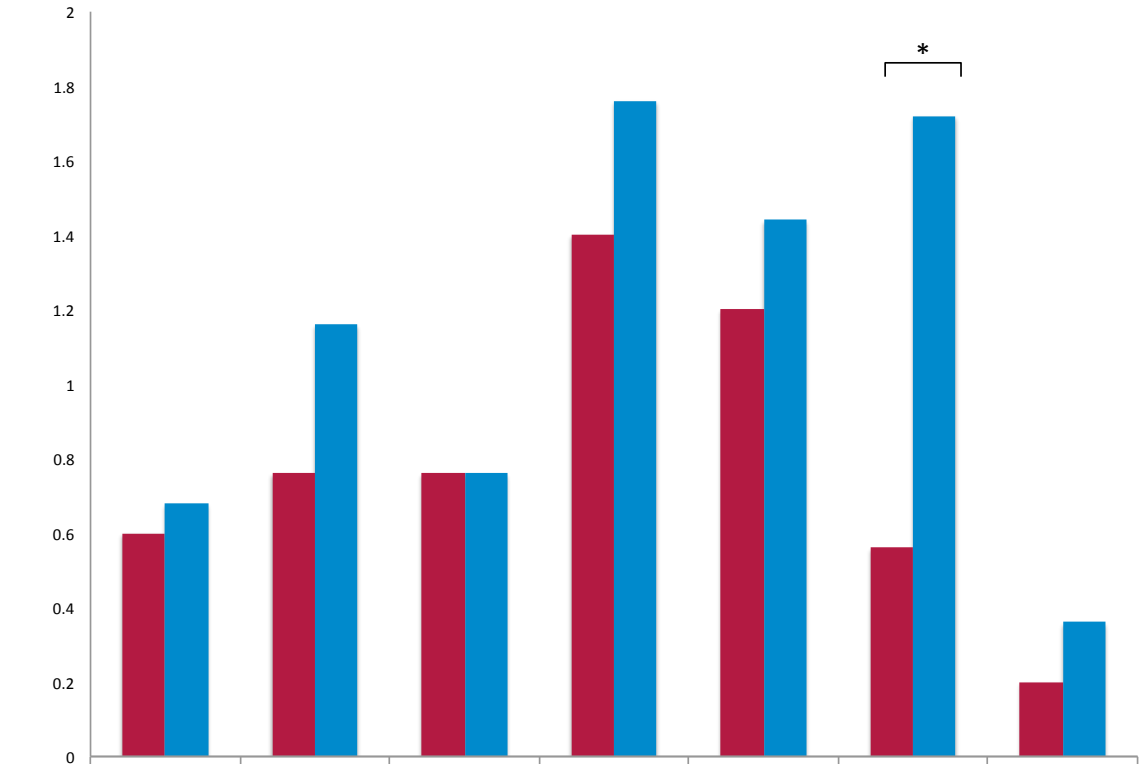

	detection score	cortical thickening	cortical signal change	subcortical signal change	Blurring	Transmantle sign	Artifact
1.5 Tesla	0.6	0.76	0.76	1.4	1.2	0.56	0.2
3 Tesla	0.68	1.16	0.76	1.76	1.44	1.72	0.36

Numbers correspond to the mean of the scores calculated for each of the 25 patients, based on consensual reading. Visualization score of the 5 imaging criteria and artifacts are calculated using a 4-point scale as detailed in the method section.

*** =0.002**

Fig. 1 FCD2 detected at 3T but not at 1.5T. Coronal reformats of 3D T1-weighted MRI at 1.5T (A) and 3T (B). Blurred thickening of the cortex in the right anterior frontal region (arrow) is visible at 3T but not at 1.5T.

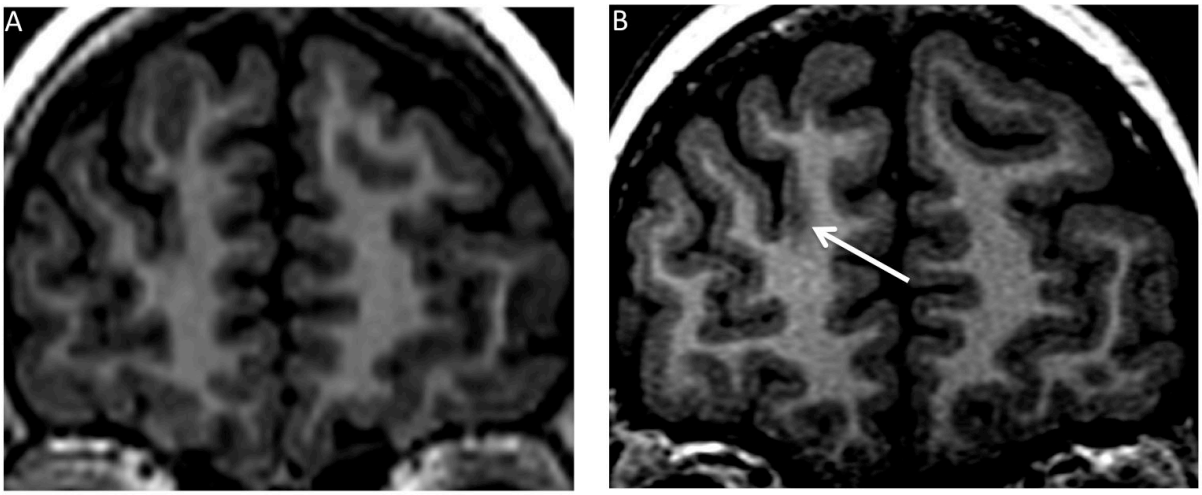

Fig. 2 Other patient with FCD2 visible at 3T and overlooked at 1.5T: axial FLAIR images at 1.5T (A) and at 3T (B). Sub-cortical hyper intensity with a transmantle sign (arrow) is seen at 3T but not at 1.5T.

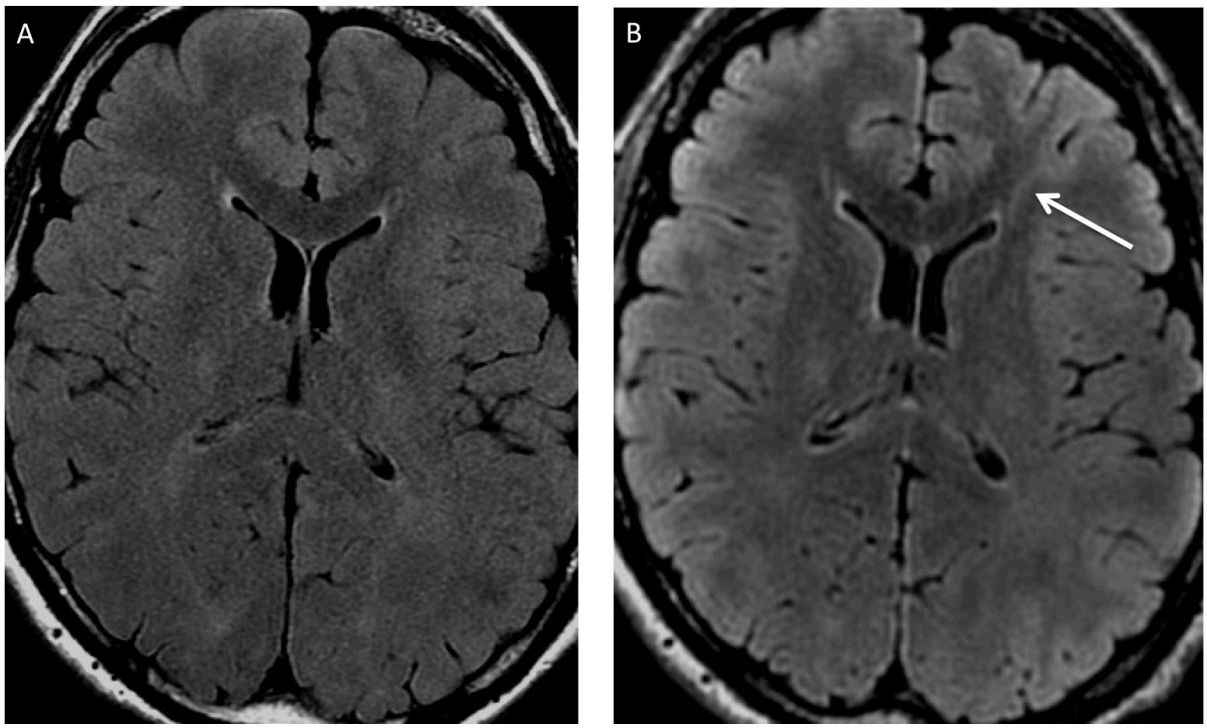

Fig. 3 Comparison of 1.5T and 3T in 4 different patients. Cases 1 to 3 illustrate a transmantle sign better visible at 3T than at 1.5T. Coronal reformats of 3D FLAIR sequences (case 1) Coronal T2-weighted images (case 2), and axial 2D FLAIR (case 3) show a well-delineated transmantle sign at 3T that is not or barely visible at 1.5T (double arrows). Of note, cortical and subcortical signal changes are visible at both magnetic fields, although more obvious at 3T. Case 4 illustrates a negative MRI on 3D FLAIR images at each magnetic field of a histologically confirmed FCD2 in the cingular gyrus (arrow).

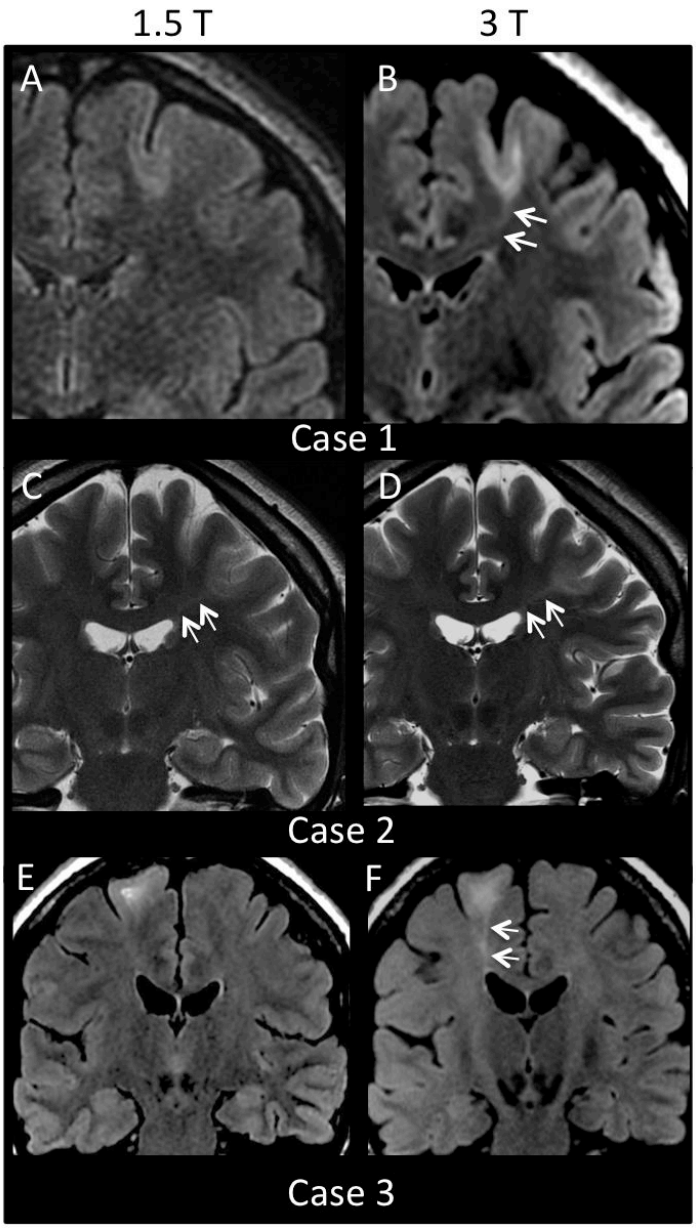

Discussion

We report here the first study comparing the diagnostic performance of 1.5T and 3T MR imaging in a homogenous series of 25 patients with FCD2. In this series, 3T MRI improved

FCD2 characterization owing to the transmantle sign being more clearly seen at 3T. This point is of interest since this feature is considered an MR signature of FCD2.7, 24-26

One of the strengths of our study is that the same patients were scanned at both magnetic fields on a magnet from the same manufacturer, using similar head coils and similar acquisition time. 3T MRI allows a high spatial resolution in a given acquisition time with isotropic millimetric voxels. This small voxel size helps in delineating and characterizing a cortical lesion, particularly for subtle signs, such as blurring of the gray-white matter interface, a cardinal feature of FCD2.7, 21, 25 Reformatting images is particularly helpful to search for cortical thickening, avoiding partial volume effect by observing the cortical surface in a plane orthogonal to the sulcus. Nevertheless, 3D T1 sequences are also available at 1.5T with an excellent spatial resolution. This likely explains the limited difference between the two magnetic fields for detection of cortical features (thickness, blurring), which relies almost exclusively on T1 contrast.

The most striking finding in our study is the contribution of 3T MRI for detection of the transmantle sign. This improvement has direct consequences for the MRI report since it allows not only the detection of FCD2 but also its characterization,7, 21, 24-26 given that the transmantle sign has not been described in other developmental or acquired cortical lesions. Moreover, the detection of the transmantle sign has been recently associated to a positive prognosis, with highly favorable seizure-free outcome after surgical treatment.27 The systematic use of 3D-FLAIR largely explains the increased detection of the transmantle sign at 3T. Multiplanar reformatting mainly benefits the detection of this linear T2 signal abnormality, which does not systematically taper in the acquisition plane and can thus be overlooked with 2D FLAIR/T2 images. Better visualization of the transmantle sign might have resulted simply from a transition from 2D FLAIR on 1.5T, to 3D FLAIR on 3T. A study indeed illustrated the benefit of 3D FLAIR over conventional sequences for detection and

delineation of FCD in 9 patients.28 In our study, only 4 patients had 3D FLAIR at both magnetic field strength, among which 2 were negative, preventing from drawing firm conclusion. However, in the 2 other patients, 3D FLAIR at 3T best detected the transmantle sign. From a practical point of view, 3D FLAIR at 1.5T suffers from a limited signal-to-noise ratio, for fixed acquisition duration compatible with routine clinical practice (5-6 minutes). To equal the SNR at 3T, one should theoretically double the acquisition time at 1.5T,29 resulting in a long acquisition time (> 10 min) at 1.5T increasing the risk of motion artifacts.

When all signs of FCD2 were considered together, the proportion of positive MRI at 3T was only slightly better than at 1.5T, with two cases being visible only at 3T in our series of patients. Accordingly, a recent study on 91 patients with FCD who underwent either 1.5T or 3T MRI, found similar visual detection rates at both magnetic fields.30 However, we also found a benefit of 3T MRI for improved FCD characterization. 3T MRI was able to clarify equivocal features generated by the 1.5T magnet, including abnormal signal from the bottom of the gyri to the ventricle surface without clearly showing the "transmantle line". Thus, ambiguous pattern at 1.5T became typical and convincing at 3T. This could partly explain the increased sensitivity for the detection of FCD reported at a higher magnetic field in previous studies, although these studies analyzed patients with focal intractable epilepsy regardless of the causal lesion, with only a few suspected FCD cases (respectively 9, 8 and 7 cases)12-14, half of which lacked histologic confirmation.

Taken together, our results and these previous studies may help to estimate the sample size for a larger prospective study comparing 1.5T to 3T with similar acquisition time for FCD2 detection. We found a difference between proportion of lesion detected at 3T and at 1.5T of approximately 10% (2 out of 25 patients). Based on a power analysis using a McNemar test to achieve 80% power at 0.05 significance with 10% of FCD2 switching from undetected to detected, the sample size required would be equal to 77 patients.

The limitations of high-field-strength imaging include a propensity to certain types of imaging artifacts, such as susceptibility and a perceived sensitivity to motion, as shown in our study. Disadvantages of imaging at 3T also include longer T1, increased acoustic noise, greater power deposition, and device incompatibility.31, 32 Aliasing artifact, only seen at 3T in our study, may mimic the transmantle sign on 3D FLAIR images, as observed here in one case. This reinforces the need to integrate all MRI features when searching for FCD.

Finally, our findings illustrate that even with an appropriate magnetic field and imaging protocol, with precise information regarding electro-clinical data and a meticulous analyze, about 30% of FCD2 remain overlooked. This strengthens the need for new sequences, such as double inversion recovery imaging,33 arterial spin labeling,34 and refinement of morphometric post processing tool,6, 30 which may also benefit from imaging at high field.

Our study has some limitations. First, it is retrospective, based on a small sample of patients and lacks a control group that would allow determination of specificity. This also likely introduces a bias in interpretations given that readers searched thoroughly for signs of FCD with no risk of over-diagnosis. Yet, we did not find any false positive cases (i.e. in erroneous location). The fact that reading was guided by clinical and electro-clinical data, according to guidelines,35 might in part explain that no lesion was detected elsewhere than in the area corresponding to the site of the FCD2. Second, the acquisition times were short and similar at both field strengths. By using longer times, the image quality could have been improved at 1.5 or at 3T. Third, readers could not be completely blind for magnetic field strengths, given that images are visually distinguishable. This limitation is inherent to all studies comparing 3T and 1.5T images.

In conclusion, we have shown that the detection and characterization of FCD2 is better at 3T than at 1.5T with similar head coils and acquisition time, owing to greater ability to detect the

transmantle sign. The use of 3T MRI may help to improve the selection of candidates for epilepsy surgery.

Disclosure

None of the authors has any conflict of interest to disclose.

We confirm that we have read the Journal's position on issues involved in ethical publication and affirm that this report is consistent with those guidelines.

References

1. Chassoux F, Rodrigo S, Semah F, et al. FDG-PET improves surgical outcome in negative MRI Taylor-type focal cortical dysplasias. Neurology. 2010 Dec 14;75:2168-75.

2. Chassoux F, Landre E, Mellerio C, et al. Type II focal cortical dysplasia: electroclinical phenotype and surgical outcome related to imaging. Epilepsia. 2012 Feb;53:349-58.

3. Jeha LE, Najm I, Bingaman W, et al. Surgical outcome and prognostic factors of frontal lobe epilepsy surgery. Brain. 2007 Feb;130:574-84.

4. McGonigal A, Bartolomei F, Regis J, et al. Stereoelectroencephalography in presurgical assessment of MRI-negative epilepsy. Brain. 2007 Dec;130:3169-83.

5. Chapman K, Wyllie E, Najm I, et al. Seizure outcome after epilepsy surgery in patients with normal preoperative MRI. J Neurol Neurosurg Psychiatry. 2005 May;76:710-3.

6. Bernasconi A, Bernasconi N, Bernhardt BC, et al. Advances in MRI for 'cryptogenic' epilepsies. Nat Rev Neurol. 2011 Feb;7:99-108.

7. Mellerio C, Labeyrie MA, Chassoux F, et al. Optimizing MR Imaging Detection of Type 2 Focal Cortical Dysplasia: Best Criteria for Clinical Practice. AJNR Am J Neuroradiol. 2012 May 3;33:1932-8.

8. Lerner JT, Salamon N, Hauptman JS, et al. Assessment and surgical outcomes for mild type I and severe type II cortical dysplasia: a critical review and the UCLA experience. Epilepsia. 2009 Jun;50:1310-35.

9. Hauptman JS, Mathern GW. Surgical treatment of epilepsy associated with cortical dysplasia: 2012 update. Epilepsia. 2012 Sep;53 Suppl 4:98-104.

10. Krsek P, Maton B, Jayakar P, et al. Incomplete resection of focal cortical dysplasia is the main predictor of poor postsurgical outcome. Neurology. 2009 Jan 20;72:217-23.

11. Madan N, Grant PE. New directions in clinical imaging of cortical dysplasias. Epilepsia. 2009 Oct;50 Suppl 9:9-18.

12. Knake S, Triantafyllou C, Wald LL, et al. 3T phased array MRI improves the presurgical evaluation in focal epilepsies: a prospective study. Neurology. 2005 Oct 11;65:1026-31.

13. Phal PM, Usmanov A, Nesbit GM, et al. Qualitative comparison of 3-T and 1.5-T MRI in the evaluation of epilepsy. AJR Am J Roentgenol. 2008 Sep;191:890-5.

14. Zijlmans M, de Kort GA, Witkamp TD, et al. 3T versus 1.5T phased-array MRI in the presurgical work-up of patients with partial epilepsy of uncertain focus. J Magn Reson Imaging. 2009 Aug;30:256-62.

15. Orbach DB, Wu C, Law M, et al. Comparing real-world advantages for the clinical neuroradiologist between a high field (3 T), a phased array (1.5 T) vs. a single-channel 1.5-T MR system. J Magn Reson Imaging. 2006 Jul;24:16-24.

16. Hashiguchi K, Morioka T, Murakami N, et al. Utility of 3-T FLAIR and 3D short tau inversion recovery MR imaging in the preoperative diagnosis of hippocampal sclerosis: direct comparison with 1.5-T FLAIR MR imaging. Epilepsia. 2010 Sep;51:1820-8.

17. Strandberg M, Larsson EM, Backman S, et al. Pre-surgical epilepsy evaluation using 3T MRI. Do surface coils provide additional information? Epileptic disorders. 2008 Jun;10:83-92.

18. Craven IJ, Griffiths PD, Hoggard N. Magnetic resonance imaging of epilepsy at 3 Tesla. Clin Radiol. 2011 Mar;66:278-86.

19. Doelken MT, Mennecke A, Huppertz HJ, et al. Multimodality approach in cryptogenic epilepsy with focus on morphometric 3T MRI. J Neuroradiol. 2012 May;39:87-96.

20. Craven IJ, Griffiths PD, Bhattacharyya D, et al. 3.0-tesla MRI of 2000 consecutive patients with localisation-related epilepsy. Br J Radiol. 2012 May 9;85:1236-42.

21. Kim DW, Kim S, Park SH, et al. Comparison of MRI features and surgical outcome among the subtypes of focal cortical dysplasia. Seizure. 2012 Oct 3;21:789-94.

22. Focke NK, Symms MR, Burdett JL, et al. Voxel-based analysis of whole brain FLAIR at 3T detects focal cortical dysplasia. Epilepsia. 2008 May;49:786-93.

23. Fonseca Vde C, Yasuda CL, Tedeschi GG, et al. White matter abnormalities in patients with focal cortical dysplasia revealed by diffusion tensor imaging analysis in a voxelwise approach. Front Neurol. 2012;3:121.

24. Barkovich AJ, Kuzniecky RI, Bollen AW, et al. Focal transmantle dysplasia: a specific malformation of cortical development. Neurology. 1997 Oct;49:1148-52.

25. Colombo N, Citterio A, Galli C, et al. Neuroimaging of focal cortical dysplasia: neuropathological correlations. Epileptic Disord. 2003 Sep;5(suppl 2):S67-72.

26. Colombo N, Tassi L, Deleo F, et al. Focal cortical dysplasia type IIa and IIb: MRI aspects in 118 cases proven by histopathology. Neuroradiology. 2012 Oct;54:1065-77.

27. Wang DD, Deans AE, Barkovich AJ, et al. Transmantle sign in focal cortical dysplasia: a unique radiological entity with excellent prognosis for seizure control. J Neurosurg. 2013 Feb;118:337-44.

28. Saini J, Singh A, Kesavadas C, et al. Role of three-dimensional fluid-attenuated inversion recovery (3D FLAIR) and proton density magnetic resonance imaging for the detection and evaluation of lesion extent of focal cortical dysplasia in patients with refractory epilepsy. Acta Radiol. 2010 Mar;51:218-25.

29. Lu H, Nagae-Poetscher LM, Golay X, et al. Routine clinical brain MRI sequences for use at 3.0 Tesla. J Magn Reson Imaging. 2005 Jul;22:13-22.

30. Wagner J, Weber B, Urbach H, et al. Morphometric MRI analysis improves detection of focal cortical dysplasia type II. Brain. 2011 Oct;134:2844-54.

31. Pattany PM. 3T MR imaging: the pros and cons. AJNR Am J Neuroradiol. 2004 Oct;25:1455-6.

32. Schmitz BL, Aschoff AJ, Hoffmann MH, et al. Advantages and pitfalls in 3T MR brain imaging: a pictorial review. AJNR Am J Neuroradiol. 2005 Oct;26:2229-37.

33. Rugg-Gunn FJ, Boulby PA, Symms MR, et al. Imaging the neocortex in epilepsy with double inversion recovery imaging. Neuroimage. 2006 May 15;31:39-50.

34. Pendse N, Wissmeyer M, Altrichter S, et al. Interictal arterial spin-labeling MRI perfusion in intractable epilepsy. J Neuroradiol. 2010 Mar;37:60-3.

35. Guidelines for neuroimaging evaluation of patients with uncontrolled epilepsy considered for surgery. Commission on Neuroimaging of the International League Against Epilepsy. Epilepsia. 1998 Dec;39:1375-6.

Chapitre 3 : Détection automatique des anomalies sulcales associées aux DCF2 de la région centrale.

Cette étude a fait l'objet d'un article soumis le 10 Juillet 2014 à la revue *Epilepsia*. Le manuscrit est inséré ci-après et les principaux résultats sont ici résumés :

Introduction

La localisation préférentielle des DCF2 est le lobe frontal et plus particulièrement la région centrale. Cette région a la particularité de ne présenter qu'une faible variabilité interindividuelle de la morphologie des sillons, en comparaison aux autres régions corticales, ce qui facilite la détection d'anomalies de configuration des sillons. Les anomalies sulco-gyrales font partie des critères de détection des DCF2, en dépit d'une description imprécise. Notre objectif principal était de tester la possibilité de détecter automatiquement les anomalies sulcales associées au DCF2 de la région centrale. Pour ceci, nous avons adapté un outil de labellisation automatique des sillons (Morphologist – Brainvisa) aux besoins de notre étude. Celle-ci était basée sur: 1- un nouveau descripteur de sillons corticaux appelé « énergie sulcale » reflétant la divergence d'un sillon avec une base d'apprentissage ; 2- trois groupes de sujets: les patients à IRM positive (IRM+) (n=17), à IRM négative (IRM-) (n=12) et des volontaires sains (n=29) ; 3- la présence d'une DCF2 prouvée histologiquement située dans la région centrale. Notre objectif secondaire était d'évaluer la pertinence des cartes z-score de l'énergie d'un sillon pour localiser la lésion épileptogène à un niveau individuel.

Résumé des principaux résultats

- L'analyse de groupe confirme une anomalie du motif du sillon central chez les patients porteurs de DCF2, de manière bilatérale. Cette anomalie se traduit par une « énergie sulcale » plus élevé chez les patients que chez les contrôles (p=0,006).
- Cette anomalie sulcale existe également de manière indépendante dans le groupe IRM+ (p=0,0033) mais également dans le groupe IRM- (p=0,0034) confirmant l'intérêt d'utiliser ce critère comme outil de détection supplémentaire des DCF2.

- Une analyse du sillon central du côté de la DCF2 retrouve également une différence d'énergie entre patients et témoins (p=0,032) ce qui n'est pas le cas du sillon central controlatéral à la lésion (p=0,019).
- L'analyse individuelle montre quant à elle une association entre la localisation de la DCF2 et le sillon pour lequel le z-score de l'énergie sulcale est le plus élevé (p=0,0046).
- Cette association est de manière surprenante vérifiée chez les patients à IRM- (p=0,024) mais pas chez les patients à IRM+ (p=0,058).
- Le z-score le plus élevé peut être utilisé comme outil de détection de la lésion chez 4/12 patients à IRM- et 5/17 patients à IRM+, en pointant sur le sillon porteur de la DCF2.

Conclusion

L'analyse automatisée des sillons basés sur l'« énergie sulcale » permet d'identifier des motifs sulcaux anormaux chez les patients porteurs de DCF2 dans la région centrale en comparaison aux sujets sains. Ce résultat souligne l'importance d'une étude des sillons chez les patients adressés pour EPPR de la région centrale. A l'échelle individuelle, le lien entre z-score maximum de l'énergie du sillon et site de la DCF2, pourrait aider à la détection et à la localisation de la lésion chez des patients à IRM négative, en combinaison avec le reste du bilan préopératoire.

Sulcus-based MR analysis of focal cortical dysplasia located in the central region

Pauline Roca[1], Charles Mellerio[1], Francine Chassoux[2], Denis Rivière[3], Arnaud Cachia[4], Sylvain Charron[1], Jean-François Mangin[3], Bertrand Devaux[2], Jean-François Meder[1], Catherine Oppenheim[1]

[1]Department of Neuroimaging, Sainte-Anne Hospital Center, Université Paris Descartes Sorbonne Paris Cité, Center for Psychiatry & Neurosciences, UMR 894 INSERM, Paris, France

[2]Department of Neurosurgery, Sainte-Anne Hospital Center, Université Paris Descartes Sorbonne Paris Cité, Paris, France

[3]UNATI, Neurospin, CEA, Saclay, France

[4]Center for Psychiatry & Neurosciences, Sainte-Anne Hospital Center, UMR 894 INSERM/Université Paris Descartes & Laboratory for the Psychology of Child Development and Education, UMR 8240 CNRS/Université Paris Descartes Sorbonne Paris Cité, Paris, France.

Address correspondence to Dr. Pauline Roca, Service d'Imagerie Morphologique et Fonctionnelle, Centre Hospitalier Sainte-Anne, 1 rue Cabanis, 75014 Paris, France

Phone number: +33 1 45 65 86 05

Fax: +33 1 45 65 83 73

E-mail: p.roca@ch-sainte-anne.fr

Running title: Sulcus-based MR analysis of central FCD

Keywords: Epilepsy, Focal cortical dysplasia, Image processing, Sulcus-based analysis, Abnormal sulcal patterns

Number of text pages: 21

Number of words: 3794

Number of figures: 5

Number of tables: 2

ABSTRACT

OBJECTIVE: Focal cortical dysplasias (FCDs) are mainly located in the frontal region, with a particular tropism for the central sulcus. Up to 30% of lesions are undetected (magnetic resonance [MR]-negative FCD patients) or belatedly diagnosed by visual analysis of MR images. We propose an automated sulcus-based method to analyze abnormal sulcal patterns associated with central FCD, taking into account the normal interindividual sulcal variability.

METHODS: We retrospectively studied 29 right-handed patients with FCD in the central region (including 12 MR negative histologically-confirmed cases) and 29 right-handed controls. The analysis of sulcal abnormalities from T1-weighted MR imaging (MRI) was performed using a graph-based representation of the cortical folds and an automated sulci recognition system, providing a new quantitative criterion to describe sulcal patterns, termed sulcus energy.

RESULTS: Group analysis showed that the central sulcus in the hemisphere ipsilateral to the FCD exhibited an abnormal sulcal pattern compared with controls ($p=0.032$). FCDs were associated with bilateral abnormal patterns of the central sulcus compared with controls ($p=0.006$), a result that remained significant when MR-negative and MR-positive patients were considered separately, while the effects of sex, age and MR-field were not significant. At the individual level, we found a significant association between maximum z-scores and the site of FCD ($p=0.0046$) which remained significant in MR-negative ($p=0.024$) but not in MR-positive patients ($p=0.058$). The maximum z-score pointed to an FCD sulcus in four MR-negative and five MR-positive patients.

SIGNIFICANCE: We identified abnormal sulcal patterns in patients with FCD of the central region compared with healthy controls. The abnormal sulcal patterns ipsilateral to the FCD strengthen the interest of sulcal abnormalities in FCD patients. The link between sulcus energy and the location of the FCD in the individual analysis, especially in MR-negative cases, supports such fully-automated methods for the presurgical evaluation of patients with central epilepsy.

KEYWORDS: Epilepsy, Focal cortical dysplasia, Image processing, Sulcus-based analysis, Abnormal sulcal patterns

Abbreviations: FCD = focal cortical dysplasia; MR = magnetic resonance; MR- = MR negative; MR+ = MR positive; MRI = magnetic resonance imaging; PET = positron-emission tomography

Introduction

Focal cortical dysplasias (FCDs) are highly epileptogenic lesions due to abnormal neuroglial proliferation and cortical organization.(29,30) They represent one of the main causes of extra-temporal medically refractory yet surgically curable epilepsy. FCDs are predominantly located in the frontal lobe, with a particular tropism for the central region.(31) In the presurgical work-up, accurate detection of the lesion by magnetic resonance imaging (MRI) is crucial, with a better postoperative outcome when MRI findings are positive.(32) MRI features typical of FCD include abnormalities of the cortex (thickening, T2 signal increase, gyral abnormalities) and of subcortical white matter (blurring of the gray–white matter junction, T2 signal increase, "transmantle" sign).(31,33–37) However, despite advanced MRI protocols, up to 30% of FCDs are not detected by conventional visual analysis.(31,38,39) These patients (hereafter referred to as "MR-negative" [MR-]) may be excluded from surgery, especially if the lesion is suspected to involve highly functional areas such as the primary motor cortex.

Current computer-aided diagnosis tools are mostly based on a subset of the MR criteria typical of FCD (cortical thickening and blurred gray–white matter junction) analyzed with advanced MRI post-processing such as voxel-based morphometry.(40–43) These methods have mainly been tested in patients with FCD detectable by conventional visual analysis (hereafter referred to as MR-positive [MR+]). Additional computational models of FCD, combining analysis of cortical thickness, blurring and tissue intensity derived from T1-weighted imaging, also increase the sensitivity of visual identification of FCD while maintaining a high specificity.(44–46)

Unfortunately, when the MR signal of FCD differs only slightly from that of normal tissue, these morphometric methods based on signal intensities may fail. There is therefore a need to

look at alternative criteria, such as abnormalities of sulcal morphology.(41) FCDs are developmental lesions, appearing early during cortical maturation and have consequences for the thickness, morphology and gyral organization of the cortex. This results in sulcal abnormalities such as broadening, increased depth, altered orientation (33–35,47) and abnormal sulcal patterns not detectable by the human eye.(48) Although these criteria are not yet standardized, they have been reported in nearly half of the patients of a cohort of 23 MR-FCD cases (49) and confirmed in a larger cohort of histologically confirmed FCD.(31) However, only a few studies performed a quantitative analysis of such sulcal anomalies with a comparison with a group of healthy controls. Besson (50) showed in 43 patients that FCD lesions were preferentially located at the bottom of an abnormally deep sulcus. In addition, (51) performed a surface-based morphometry analysis of sulcal depth and additional criteria such as local gyrification and curvature in 11 patients (5 with MR+ FCD and other epileptogenic malformations), showing that surface-based morphometry successfully discriminated patients from controls but failed to adequately describe the extent of the lesion in most cases. Recently, automated multivariate supervised classifiers based on surface-based features (sulcal depth, curvature, cortical thickness) and intensity (52) provided a gain in sensitivity over standard radiologic assessment in MR- FCD patients.

In this study, our main aim was to perform a quantitative group-wise analysis of abnormal sulcal patterns associated with FCD in MR- and MR+ patients based on: (1) an automated quantitative analysis of sulcal abnormalities using a novel descriptor of cortical sulci called sulcus energy;(48) (2) three groups of subjects: MR+ patients, MR- patients, and healthy controls; (3) FCD located in the central region, one of the most stable regions in terms of sulcal patterns and a frequent location for FCD. Our second goal was to assess the relevance of sulcus energy z-score maps to localize the epileptogenic lesion at the individual level.

Methods

Study groups

We retrospectively studied all consecutive patients referred to our center for intractable epilepsy who fulfilled the following criteria: (1) patients operated from 2000 to 2013; (2) with intractable epilepsy of the central region; (3) and a final diagnosis of FCD, based on typical MRI features, histology and/or on a comprehensive presurgical work-up (including 18-fluorodeoxyglucose positron-emission tomography [PET] and Stereo-EEG). A total of 38 patients fulfilled these criteria. For the purposes of this study we restricted our analysis to the right-handed patients (n = 29). All patients systematically underwent an MR examination as part of their presurgical assessment. FCD lesions were confirmed by histological analysis in 25 of the 29 cases. The remaining 4 patients had typical MRI features making the diagnosis of FCD unquestionable. Twenty-nine right-handed controls without medical history composed the control group. Demographic details of each group are presented in Table 1. These characteristics were similar between groups except for age ($p = 0.05$ in univariate t-test). This study was found to conform to generally accept scientific principles and ethical standards by the Ethics Review Committee of Ile de France III.

MRI acquisition

Patients and controls were scanned using a 1.5 T (n = 41) or a 3 T (n = 17) MRI scanner (GE Healthcare Medical System, Milwaukee, WI, USA) with a three-dimensional T1-weighted inversion recovery fast spoiled gradient recalled MR pulse sequence. For the patient group, additional T2-weighted and fluid attenuated inversion recovery MR images were acquired as part of their clinical imaging work-up. 3D T1-weighted inversion recovery MR acquisition

parameters were as follows: FOV, 220–250 mm; matrix, 256 × 256; slice thickness, 1–1.4 mm; number of slices, 114–146.

Image post-processing

Characterization of the sulco-gyral anatomy was assessed using a four-step procedure (Fig. 1) with Morphologist 2012, a toolbox of BrainVisa software (http://brainvisa.info): (1) extraction of cortical folds; (2) automated recognition of standard sulci; (3) sulcus energy map generation, sulcus energy being a new criterion quantifying the degree of abnormality of cortical sulci;(48) and (4) computation of sulcus energy z-score maps, taking into account the variability of sulcus energy in controls (Fig. 1B).

Cortical fold extraction

Cortical folds were automatically extracted from T1-weighted MRI including the following sub-steps: (i) segmentation of main brain tissues: cerebrospinal fluid, gray and white matter;(53) (ii) extraction of gray–white matter interface, and gray matter and cerebrospinal fluid interface and generation of associated surfaces; (iii) fold extraction from the skeleton of the gray matter/cerebrospinal fluid mask. The final extracted folds were converted to a graph-based representation of the cortex containing for each fold a list of morphological descriptors (area, depth, length, etc.) and spatial organization relative to neighbors (position, orientation).(54)

Automated sulci recognition

For each brain, sulci recognition was achieved through labeling of the folds with an anatomical nomenclature. It was performed using an automated algorithm, based on a congregation of artificial neural networks trained on a learning database.(54,55) The

automated labeling followed an energy minimization performed using simulated annealing. In order to ensure the reliability of the labeling, ten automated recognitions were performed. The recognition with the lowest central sulcus/central region energy was chosen (for group/individual analysis respectively). This energy encodes a quantification of the similarities with the learning database. Hence, we made the hypothesis that the final minimal energy would be higher in FCD patients than in controls. In this study, we focused on this criterion without taking into account the accuracy of the recognition. For each subject, the final minimal energy reflects the best match with the learning database and provides a quantitative value of the matching quality, despite recognition errors in comparison with a manual recognition.

Sulcus energy map

For each subject, a sulcus energy map was generated from the above final minimal energy. It was split into a set of local energies for each sulcus depending on the sulcus itself and its relationship with its neighboring sulci. These local energies reflected the quality of the recognition: low local sulcus energy meant that the pattern of the sulcus and its neighbors matched the patterns of the learning database, whereas high local sulcus energy meant poor matching. Local sulcus energy therefore provides a new way to characterize abnormal sulco-gyral patterns.

Sulcus energy z-score map

In order to compare energy values between sulci, we normalized the sulcus energy map by taking into account the normal variability of each sulcus in controls.(56,57) Thus, for a given patient, we computed a z-score by dividing the difference between the sulcus energy of the

patient and the mean sulcus energy of controls by the standard deviation of controls (Fig. 1B). A z-score was computed sulcus by sulcus.

Visual inspection

MRIs were reviewed retrospectively by an experienced neuroradiologist (C.M., 9 years' experience in epilepsy MRI) blind to the sulco-gyral analysis but aware of all presurgical evaluation data, including PET. He was asked to look for four typical FCD MRI criteria:(31) (1) cortical thickening; (2) abnormal cortical signal intensity; (3) blurring of the gray–white matter junction; (4) abnormal signal intensity of subcortical and deep white matter. MR imaging was considered as positive (MR+) for the diagnosis of FCD when at least one of these criteria was present and as MR- otherwise. Each gray–white matter interface generated by BrainVisa was visually inspected and manually corrected if necessary. All labeled sulci were then reviewed by an expert (F.C. or C.M.), who identified the cortical sulci involved in the FCD (hereafter referred as the FCD sulci). "FCD sulci" included all automatically labelled sulci facing MR abnormalities in MR+ patients (Fig. 2) or based on complete presurgical evaluation (including PET and stereo-EEG) and surgical data confirmed by histology in MR- patients. The nomenclature of the sulci of the central region provided by BrainVisa is defined in Fig. 3.

Statistical analyses

Group-wise analysis

Group-wise statistical analyses were performed with R software (http://www.r-project.org).

Global FCD effect on central sulci In order to assess a global effect of FCD on the sulcal morphology, we compared energies of the central sulci between patients and controls using multivariate analysis of variance (MANOVA) with repeated measures for both hemispheres, followed by post hoc comparisons. To correct for potential confounding effects

of age,(58) gender,(59,60) and MR field on the sulco-gyral anatomy, these covariates were added in the linear models.

FCD effect on ipsilateral and contralateral central sulci In order to investigate whether FCD had an effect on sulcal patterns ipsilateral or contralateral to the lesion, we performed additional analyses. We first compared energies of the central sulcus ipsilateral to the lesion between patients and controls (ANOVA with age, gender, MR field and hemisphere as cofactors). We then compared energies of the central sulcus contralateral to the lesion between patients and controls (ANOVA with the same cofactors as previously).

Individual analysis: Identification of FCD sulci in patients

In order to assess the relevance of this sulcus energy z-score map to localize the FCD, we computed the proportion of patients in whom an FCD sulcus corresponded to the maximum of z-score (the most abnormal sulcus relative to the variability observed in controls, Fig. 1B). Given that the electroclinical characteristics of partial seizures originated from the central region typically point to one hemisphere, we restricted the analysis to the central region ipsilateral to the FCD. The significance of these results was tested using a permutation test (10 000 permutations) on the characteristics of sulci (FCD or not).

Results

Study groups - Visual MR analysis

FCD lesions were visually identified in 17 of the 29 (57%) patients and composed the MR+ subgroup. The segmentation was successful in all but three subjects, for whom a manual intervention excluded small parts of longitudinal venous sinus that were misclassified as gray matter. In the whole of the patient group, a total of 45 FCD sulci were identified, the lesion

being in the vicinity of several neighboring sulci in some patients. The FCD lesions were preferentially located on either the central sulcus (eight patients) or the marginal precentral sulcus (eight patients). The sulci involved in the remaining cases were the intermediate (five patients), superior (four patients) and inferior (four patients) branches of the precentral sulcus, the central branch of the median frontal sulcus (four patients), the paracentral sulcus (two patients), the paracentral lobule sulcus (three patients) and the median branch of the precentral sulcus (four patients), the central sylvian sulcus (two patients) and the inferior postcentral ramus of the intraparietal sulcus (one patient). The demographics and the FCD type of the MR+ and MR- subgroups are detailed in Table 2. These characteristics were similar between subgroups except for age ($p = 0.02$), related to a bias of recruitment for pediatric MR- cases.

Group-wise statistical analysis

Global FCD effect on central sulci

Patients had significantly higher central sulcus energy than controls ($p = 0.006$), whereas the main effect of sex ($p = 0.06$), age ($p = 0.12$) and MR field ($p = 0.07$) was not significant. Similarly, when considered separately, MR+ ($p = 0.033$) and MR- patients ($p = 0.034$) had higher central sulcus energy than controls.

FCD effect on ipsilateral and contralateral central sulci

Patients had higher central sulcus energy ipsilateral to the FCD compared to the central sulcus in controls ($p = 0.032$), whereas the main effect of sex ($p = 0.531$), age ($p = 0.683$), MR field ($p = 0.161$) and lesion side ($p= 0.195$) was not significant (see Fig. 4). The same result was found when only MR+ patients were compared with controls ($p = 0.038$) but not when MR- patients were compared with controls ($p = 0.186$). The central sulcus energy contralateral to the lesion did not differ between patients and controls ($p = 0.192$).

Individual analysis

In controls, the mean sulcus energy differed across the 13 sulci of the central region (Fig. 1) with expected sulcus energies reflecting the degree of anatomical variability: for instance, the central sulcus, known to be the most stable sulcus across individuals, had the lowest mean energy whereas the central sylvian sulcus, a small branch of the central sulcus, had the highest mean energy. Fig. 5 shows examples of sulcus energy z-score maps for six patients taking into account the above-mentioned normal inter-sulcus variability in controls. For patients, the analysis relied on 28 patients as in one MR- case, the FCD sulcus was mislabeled as outside the central region. In nine (four MR- and five MR+) of 28 patients (32%), the maximum z-score pointed to an FCD sulcus ($p = 0.0046$). When MR+ and MR- patients were analyzed separately, these results remained significant for MR- patients ($p = 0.024$) but not for MR+ patients ($p = 0.058$).

Discussion

We found abnormal sulcal patterns in patients with FCD located in the central region after correction for potential bias factors such as gender, age and MR field strength. This group finding provides proof of concept for studying sulcal abnormalities in FCD patients, even if these are not yet considered as a cardinal sign of FCD. At the individual level, the automated sulcal energy analysis we used takes into account normal interindividual sulcal variability through the use of a group of healthy controls. Our findings strengthen the previously reported association between subclinical abnormal sulcal patterns and the epileptogenic zone in MR- frontal FCD patients based on visual inspection of sulcus energy maps.(48)

In the group-wise comparison, patients with FCD had abnormal sulcal patterns of the central regions. This was observed for the whole FCD population and when MR+ and MR- patients were considered separately. Our results are consistent with the greater depth of FCD sulci compared with the corresponding sulci in controls reported in a previous study.(50) Our results also match the visually detectable sulcal abnormalities in FCD reported in several previous studies.(31,34,35,49) One study noted that, even if present in MR- patients, visually detectable unusual sulcal patterns were more prominent in MR+ than in MR- patients.(31) This may explain why sulcal patterns of the central sulcus ipsilateral to the FCD differed from controls for MR+ but not for MR- patients in our study.

Other results of the individual analysis deserve attention. First, although sulcus energy variability was present in controls, we found a link between the location of the FCD and the sulcus energy z-scores, supporting the relevance of this criterion for the identification of FCD in MR- patients. Indeed, in the whole of the patient group, the proportion of patients for whom the maximum energy z-scores identified an FCD sulcus was above the chance level. In line with this, the fact that maximum sulcus energy z-scores pointed to the lesion in 4 of the 11 MR- cases is very promising. Adding a new localizing criterion to the currently available tools could increase the number of candidates for surgery. These results encourage future studies combining the sulcus energy z-score map with other presurgical data, as previously done with voxel-based morphometry.(42) Second, there were false-positive sulci, with maximum z-score pointing to sulcus distant from FCD. This ties in with a previous study,(51) which reported that surface-based morphometry analysis failed to adequately describe lesion extent in patients with epileptogenic malformations. The presence of these false positives distant from the FCD is consistent with other imaging studies reporting extra-lesional abnormalities such as an abnormal sulcal pattern (48) or gray matter increase.(41) It is also consistent with the developmental origin of FCD. Indeed, FCD is a disorder occurring very

early in brain morphogenesis,(61) especially during the development of cortical sulci. Although the mechanisms of this sulcogenesis remain poorly understood, different models have been proposed.(62–64) Among them, the theory of tension-based morphogenesis (62) postulated that sulcogenesis relies on the global minimization over the brain of the tensions from white matter fibers connecting cortical areas. This link between connectivity and sulcal patterns is supported by experimental data indicating that alterations of thalamo-cortical or cortico-cortical connections affected the gyral patterns.(65) In this context, the extra-lesional high sulcus energy z-scores we observed are not surprising considering that recent results using diffusion MRI have also shown bilateral and widespread patterns of white matter microstructural abnormalities extending beyond the FCD lesion.(66) Multimodal studies combining conventional or advanced diffusion techniques (67) and morphological MR imaging data may bring further insight into the link between sulcal and anatomical connectivity impairments related to FCD.

Our study suffers from several limitations. First, our findings cannot currently be applied to left-handed patients, whereas a substantial proportion of patients with FCD are left-handed. In our center, although 24% of patients with FCD of the central region were left-handed, we chose to focus our study on right-handed subjects to avoid the confounding effect of handedness. Indeed, a recent study demonstrated that sinistrals differ from dextrals in the shape of certain cortical folds, especially the central sulcus.(68) In addition, in the Morphologist toolbox of BrainVisa, the learning database of healthy subjects was composed solely of right-handed subjects. Second, the brain segmentation could potentially be perturbed by signal intensity changes associated with the FCD, which could impact the reconstruction of the underlying sulci. However, we systematically controlled the segmentation results and did not identify any such disturbances. As opposed to other methods, such as voxel-based or surface-based morphometry, our methodology does not require registration between the

individual subjects and is therefore free from the potential effects of misregistration due to the lesion. Third, the sulcus-based method we used was not designed to detect epileptogenic lesions, but rather to automatically recognize cortical folds, and especially the sulcus energy. New tools have been proposed to characterize and quantify the shape variability of a single sulcus, based on shape similarity measurements and on manifold learning.(68) Combining such new techniques and clinical a priori knowledge could be of great help in improving the methodology.

Conclusion

In this study, we demonstrated the ability of an automated sulcus energy-based analysis to identify abnormal sulcal patterns in patients with FCD of the central region compared with healthy controls. At the group level, an abnormal sulcal pattern was found on the central sulcus ipsilateral to the FCD, strengthening the importance of studying sulcal patterns in FCD patients. At the individual level, we found a link between maximum sulcus energy z-scores and the site of FCD, a finding that has clinical relevance for MR- FCD patients. Combining the sulcus energy z-score map with other presurgical data may in future help to localize FCD lesions in patients with epilepsy of the central region.

Disclosure

None of the authors has any conflict of interest to disclose.

We confirm that we have read the Journal's position on issues involved in ethical publication and affirm that this report is consistent with those guidelines.

References

1. Barkovich AJ, Kuzniecky RI, Jackson GD, et al. A developmental and genetic classification for malformations of cortical development. Neurology 2005;65(12):1873–87.
2. Barkovich AJ, Guerrini R, Kuzniecky RI, et al. A developmental and genetic classification for malformations of cortical development: update 2012. Brain 2012;135(Pt 5):1348–69.
3. Mellerio C, Labeyrie M-A, Chassoux F, et al. Optimizing MR Imaging Detection of Type 2 Focal Cortical Dysplasia: Best Criteria for Clinical Practice. Am J Neuroradiol 2012;33(10):1932–8.
4. Bien CG, Szinay M, Wagner J, et al. Characteristics and surgical outcomes of patients with refractory magnetic resonance imaging-negative epilepsies. Arch Neurol 2009;66(12):1491–9.
5. Barkovich AJ, Raybaud CA. Neuroimaging in disorders of cortical development. Neuroimaging Clin N Am 2004;14(2):231–54, viii.
6. Abdel Razek AAK, Kandell AY, Elsorogy LG, et al. Disorders of cortical formation: MR imaging features. AJNR Am J Neuroradiol 2009;30(1):4–11.
7. Colombo N, Salamon N, Raybaud C, et al. Imaging of malformations of cortical development. Epileptic Disord 2009;11(3):194–205.
8. Lerner JT, Salamon N, Hauptman JS, et al. Assessment and surgical outcomes for mild type I and severe type II cortical dysplasia: a critical review and the UCLA experience. Epilepsia 2009;50(6):1310–35.
9. Oster JM, Igbokwe E, Cosgrove GR, et al. Identifying subtle cortical gyral abnormalities as a predictor of focal cortical dysplasia and a cure for epilepsy. Arch Neurol Am Med Assoc; 2011;69(2):257–61.
10. Kim D, Lee S, Chu K, et al. Predictors of surgical outcome and pathologic considerations in focal cortical dysplasia. Neurology 2009;72(3):211–6.
11. Colombo N, Tassi L, Deleo F, et al. Focal cortical dysplasia type IIa and IIb: MRI aspects in 118 cases proven by histopathology. Neuroradiology 2012;54(10):1065–77.
12. Kassubek J, Huppertz HJ, Spreer J, et al. Detection and Localization of Focal Cortical Dysplasia by Voxel-based 3-D MRI Analysis. Epilepsia 2002;43(6):596–602.
13. Colliot O, Bernasconi N, Khalili N, et al. Individual voxel-based analysis of gray matter in focal cortical dysplasia. Neuroimage 2006;29:162–71.
14. Wagner J, Weber B, Urbach H, et al. Morphometric MRI analysis improves detection of focal cortical dysplasia type II. Brain 2011;134(Pt 10):2844–54.
15. House PM, Lanz M, Holst B, et al. Comparison of morphometric analysis based on T1- and T2-weighted MRI data for visualization of focal cortical dysplasia. Epilepsy Res 2013;106(3):403–9.
16. Bernasconi A, Antel SB, Collins DL, et al. Texture analysis and morphological processing of magnetic resonance imaging assist detection of focal cortical dysplasia in extra-temporal partial epilepsy. Ann Neurol 2001;49(6):770–5.
17. Antel SB, Collins DL, Bernasconi N, et al. Automated detection of focal cortical dysplasia lesions using computational models of their MRI characteristics and texture analysis. Neuroimage 2003;19(4):1748–59.
18. Rajan J, Kannan K, Kesavadas C, et al. Focal Cortical Dysplasia (FCD) lesion analysis with complex diffusion approach. Comput Med Imaging Graph 2009;33(7):553–8.

19. Bronen RA, Spencer DD, Fullbright RK. Cerebrospinal Fluid Cleft with Cortical Dimple: MR Imaging Marker for Focal Cortical Dysgenesis. Radiology 2000;214(3):657–63.
20. Régis J, Tamura M, Park MC, et al. Subclinical Abnormal Gyration Pattern, a Potential Anatomic Marker of Epileptogenic Zone in Patients With Magnetic Resonance Imaging–Negative Frontal Lobe Epilepsy. Neurosurgery 2011;69(1):80–93.
21. Chassoux F, Rodrigo S, Semah F, et al. FDG-PET improves surgical outcome in negative MRI Taylor-type focal cortical dysplasias. Neurology 2010;75(24):2168–75.
22. Besson P, Andermann F, Dubeau F, et al. Small focal cortical dysplasia lesions are located at the bottom of a deep sulcus. Brain 2008;131:3246–55.
23. Thesen T, Quinn BT, Carlson C, et al. Detection of epileptogenic cortical malformations with surface-based MRI morphometry. PLoS One 2011;6(2):e16430.
24. Hong S-J, Kim H, Schrader D, et al. Automated detection of cortical dysplasia type II in MRI-negative epilepsy. Neurology 2014;
25. Mangin J-F, Rivière D, Cachia A, et al. A framework to study the cortical folding patterns. Neuroimage 2004;23:S129–38.
26. Rivière D, Mangin J-F, Papadopoulos-Orfanos D, et al. Automatic recognition of cortical sulci of the human brain using a congregation of neural networks. Med Image Anal 2002;6(2):77–92.
27. Perrot M, Rivière D, Mangin J. Cortical sulci recognition and spatial normalization. Med Image Anal 2011;15(4):529–50.
28. Fillard P, Arsigny V, Pennec X, et al. Measuring brain variability by extrapolating sparse tensor fields measured on sulcal lines. Neuroimage 2007;34(2):639–50.
29. Ono M, Kubik S, Abernathey CD. Atlas of the cerebral sulci. Thieme, editor. 1990.
30. Rettmann ME, Kraut MA, Prince JL, et al. Cross-sectional and longitudinal analyses of anatomical sulcal changes associated with aging. Cereb Cortex 2006;16(11):1584–94.
31. Luders E, Narr K, Thompson P, et al. Gender differences in cortical complexity. Nat Neurosci 2004;7(8):799–800.
32. Duchesnay E, Cachia A, Roche A, et al. Classification based on cortical folding patterns. IEEE Trans Med Imaging Med Imaging 2007;26(4):553–65.
33. Chen JC, Tsai V, Parker WE, et al. Detection of human papillomavirus in human focal cortical dysplasia type IIB. Ann Neurol 2012;72(6):882–92.
34. Van Essen DC. A tension-based theory of morphogenesis and compact wiring in the central nervous system. Nature 1997;385:313–8.
35. Toro R, Burnod Y. A morphogenetic model for the development of cortical convolutions. Cereb Cortex 2005;15(12):1900–13.
36. Lefèvre J, Mangin J-F. A reaction-diffusion model of human brain development. PLoS Comput Biol 2010;6(4).
37. Rakic P. Specification of cerebral cortical areas. Science 1988;241:170–6.
38. De Carvalho Fonseca V, Yasuda CL, Tedeschi GG, et al. White matter abnormalities in patients with focal cortical dysplasia revealed by diffusion tensor imaging analysis in a voxelwise approach. Front Neurol 2012;3.

39. Winston GP, Micallef C, Symms MR, et al. Advanced diffusion imaging sequences could aid assessing patients with focal cortical dysplasia and epilepsy. Epilepsy Res 2014;108(2):336–9.

40. Sun ZY, Klöppel S, Rivière D, et al. The effect of handedness on the shape of the central sulcus. Neuroimage 2012;60(1):332–9.

Figure legends

Fig. 1 Flowchart of the sulcus-based analysis. A) Processing steps for the controls. First, based on T1-weighted MRI (T1w MRI), cortical sulci were extracted. They were then automatically labeled (one color per label). The sulcus energy maps derived from this recognition process were then generated (blue to red colors, reflecting a sulcus pattern with a good match to the learning database and a bad match, respectively). These maps were averaged to obtain mean and standard deviation (SD) maps. B) Processing steps for a single FCD patient. Cortical sulci extraction, labeling, and generation of sulcus energy map were done as described in A. Finally, a sulcus energy z-score map was computed by dividing the difference between the sulcus energy of the patient and the mean sulcus energy of controls by the standard deviation of controls (blue to red colors, reflecting an increasing z-score).

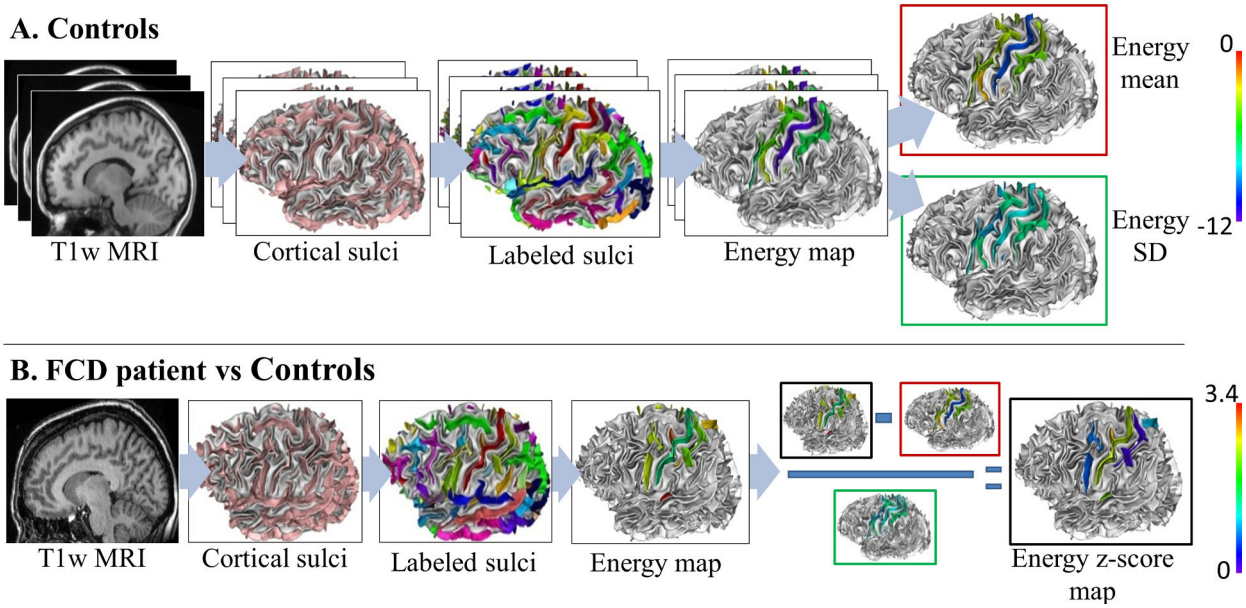

Fig. 2 Visual identification of FCD sulci in a MR+ patient. The hyperintensities in FLAIR (A) and the slight cortical thickening visible in T1 MRI (B) allowed to locate the lesion in the depth of an ascending branch of the left central sulcus (white arrows), at the intersection of the main branch of the central sulcus. These two sulci are automatically labelled (C): « superior branch of the pre-central sulcus» (orange) and « central sulcus » (red) and considered as FCD sulci.

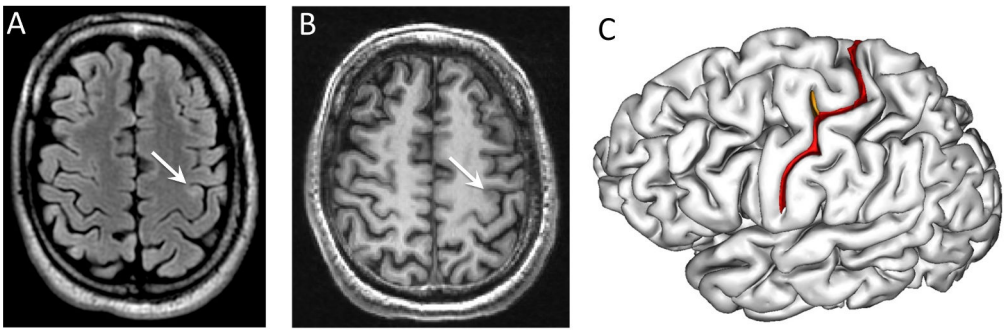

Fig. 3 Sulci of the left central area, based on BrainVisa nomenclature (http://brainvisa.info), lateral (A) and medial (B) views: The central sulcus (S.C.) is surrounded by the superior postcentral sulcus (S.Po.C.sup), the retrocentral transverse ramus of the lateral fissure (F.C.L.r.retroC.tr), the inferior postcentral ramus of the intraparietal sulcus (F.I.P.Po.C.inf), the median frontal sulcus (S.F.median) and the median (S.Pe.C.median), marginal (S.Pe.C.marginal), superior (S.Pe.C.sup.), intermediate (S.Pe.C.inter.) and inferior (S.Pe.C.inf.) branches of the pre-central sulcus. The ramifications of the central sulcus were composed of the central sylvian sulcus (S.C.sylvian), the paracentral lobule (S.C.LPC.) and the paracentral sulcus (S.p.C). Right hemisphere not shown.

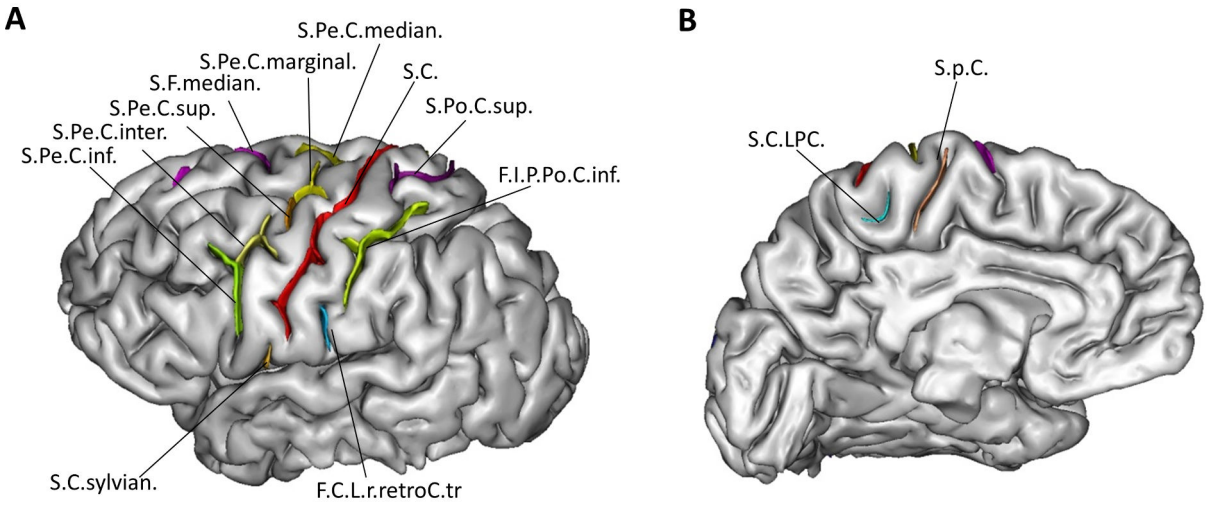

Fig. 4 Illustrative examples of patients with maximum z-scores pointing to an FCD sulcus. Z-score maps superimposed on gray–white matter interface surface models. For each patient, a color palette from blue to red was adjusted to the maximum z-score. Black arrow indicated the lesion. In Case 1, the maximum z-score (z = 3.4) pointed exactly to the FCD (red blob, arrow), in the depth of an ascending branch of the left central sulcus. In Case 2, the lesion was located on the right marginal precentral sulcus, which had a maximum z-score of 1.52. Of note, the right superior precentral sulcus (in red) also had a high, albeit not maximum, z-score (1.49). In Cases 3 and 4, the maximum z-scores (z = 2 and 0.4 respectively) pointed to the FCD sulcus, which stood-out from the neighboring sulci with much lower z-scores. In Case 5, the maximum z-score (z = 2.6) pointed to an FCD sulcus but there were other sulci with high local z-score beyond the FCD. In Case 6, even if the FCD was associated with a maximum z-score (z = 7.6), this high energy sulcus had a wide spatial extent, beyond the site of FCD.

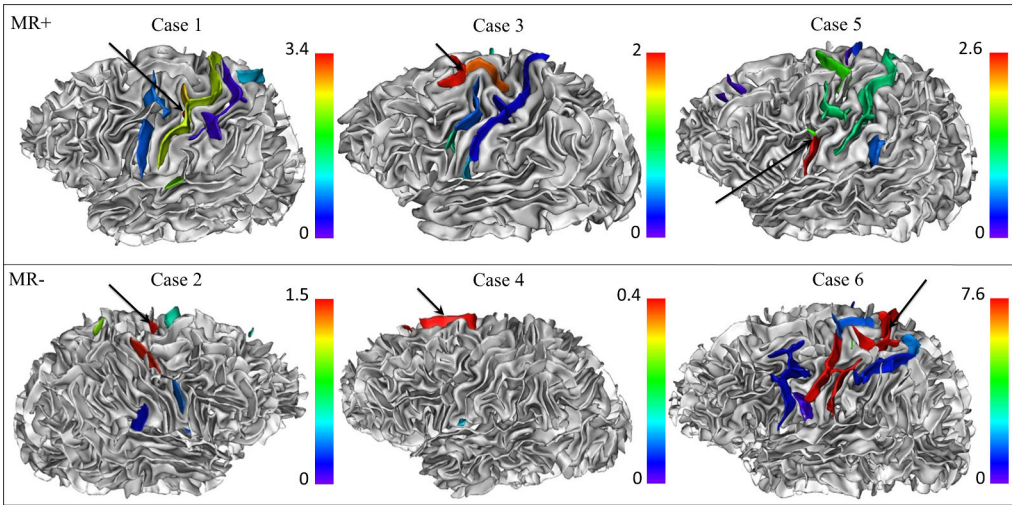

Chapitre 4 : Le « Power Button Sign »: un nouveau motif du sillon central en IRM 3D surfacique pour la détection des dysplasies corticales focales

Cette étude a fait l'objet d'un article accepté le 24 Juillet 2014 pour publication dans *Radiology,* dont le manuscrit est inséré ci-après et dont les principaux résultats sont ici résumés :

Introduction

Après avoir montré dans la précédente étude que les DCF2 en région centrale sont associées à des anomalies sulcales identifiables par une analyse automatisée des sillons, nous nous sommes interrogés sur la possibilité de détecter ces anomalies de manière reproductible à l'œil nu. Cette approche nécessite néanmoins l'utilisation d'un outil permettant une extraction du volume cérébral et une reconstruction surfacique du cortex avec un dessin des sillons (Anatomist – Brainvisa). Cette analyse visuelle consistait en la recherche des variations du sillon central (interruptions, nombre de branches latérales, de connexions) telle que décrite dans un atlas anatomique des sillons corticaux résultant d'une analyse post mortem (Ono et al.). L'analyse des sillons de cette région nous a permis de mettre en évidence un motif consistant en une interposition d'un segment du sillon précentral entre le sillon central et l'une de ses branches antérieurs ascendantes reproduisant le symbole du bouton « marche-arrêt » : le « Power Button Sign » (PBS). L'objectif de cette étude était donc de comparer les variations du sillon central et la présence du PBS chez patients et témoins. Cette analyse a été réalisée chez 37 patients (dont 13 avec IRM négative) ayant une DCF2 en région centrale, et chez 44 témoins.

Résumé des principaux résultats

- Le sillon central présente plus de branches latérales (nombre moyen = 2,05 vs. 1,12 ; p=0,008) de connexions au sillon précentral (38% vs. 11% ; p=0.0006) et de connexions avec la fissure latérale (35% vs. 15% ; p=0.001) chez les patients que chez les témoins.

- Le PBS est un motif sulcal spécifique (98,9%) de la présence d'une DCF2, car retrouvé chez un seul des 88 hémisphères témoins analysés.
- Ce signe bénéficie par ailleurs d'une excellente reproductibilité inter- et intra-observateur (0,88 and 0,93 respectivement).
- Ce motif est présent chez 62% des patients porteurs de DCF2, et en particulier chez 55% des patients à IRM négative. Ce résultat incite donc à la réalisation d'un reformatage 3D du cortex chez des patients adressés pour une EPPR de la région centrale à la recherche d'une anomalie sulcale.
- Lorsqu'il est visible, le PBS pointe sur la DCF2 dans 60% des cas. Il peut ainsi constituer une aide à la localisation d'une DCF2.

Conclusion

Chez les patients adressés pour EPPR, une attention particulière devrait être accordée à l'analyse tridimensionnelle des sillons. Nous avons décrit un nouveau marqueur diagnostique d'une DCF2 de la région centrale, appelé "Power Button Sign". Compte tenu de son excellente reproductibilité et de sa spécificité, le PBS, lorsqu'il est présent, pourrait devenir un nouveau critère diagnostique de DCF2 de la région centrale.

The Power Button Sign": a New Central Sulcal Pattern on Surface Rendering MRI of Type 2 Focal Cortical Dysplasia

Manuscript type: Original research

Advances in Knowledge:

1. In patients with type 2 focal cortical dysplasia (FCD2), the central sulcus differed significantly from controls, with more side branches (mean number: 2.05 vs. 1.12; p=0.0003), connections with pre-central sulcus (occurrence: 38% vs. 11%; p=0.0006) and sylvian fissure (occurrence: 35% vs. 15%; p=0.001).
2. The newly described "power button sign" is a specific (98.9%) sulcal pattern associated with FCD2.
3. This MR pattern is present in 62% of patients with FCD2, and particularly in 55% of patients without any other MR sign of FCD2.
4. When visible, this sign is on the same sulcus as the lesion (60%) or in its immediate vicinity (40%) and may thus help to localize FCD2.

Implications for Patient Care:

1. 3D reformats should be performed in patients referred for partial intractable epilepsy in order to look for an abnormal sulcal pattern and in particular for a "power button sign" (PBS).
2. When present, PBS confirms the presence of a FCD2 and allows diagnosing 55% of patients with an otherwise negative MRI.
3. This sign can serve as a guide to the site of FCD2.

Summary Statement

The power button sign, which enriches the MR semiology of FCD2, may increase diagnostic confidence when other cardinal MR criteria are visible or, more importantly, when these are lacking or doubtful.

Abstract

Purpose: Type 2 focal cortical dysplasia (FCD2), one of the main causes of refractory partial epilepsy of the central region, is often overlooked by magnetic resonance imaging (MRI). This study aimed to compare in patients and controls the occurrence of several central sulcus variants and to assess the reproducibility of a sulcal pattern named "power button sign" (PBS).

Materials and Methods: The local institutional review board approved the study. Four readers reviewed the 3D T1-weighted MRI of 37 patients (13 with negative MRI) with histologically proven FCD2 of the central region and 44 controls, based on the visual analysis of 3D reconstruction of cortical folds. They searched for central sulcus variations (interruptions, side branches, connections) and for a particular sulcal pattern, namely the interposition of a pre-central sulcal segment between the central sulcus and one of its hook-shaped anterior ascending branches, termed PBS by analogy to the on-off power button symbol. Inter- and intra-observer reliability, specificity, sensitivity were calculated.

Results: The central sulcus showed a greater number of side branches (p=0.0003) and was more frequently connected to the pre-central sulcus (p=0.0006) in patients than in controls. PBS was found in 23/37 (62%) patients (6/13 with negative MRI), but in only one control. Inter- and intra-observer rates were excellent (0.88 and 0.93) for the detection of PBS. FCD2 was located either in the depth of the ascending branch of the central sulcus (14/23=60%) or in its immediate vicinity (n=9).

Conclusion: Given its excellent reproducibility and specificity, the PBS, when present, could become a new major qualitative diagnostic MR criterion of FCD2 in the central region.

Abbreviations:

FCD = focal cortical dysplasia

FCD2 = type 2 focal cortical dysplasia

PBS = power button sign

18FDG-PET = 18 fludeoxyglucose positron emission tomography

EEG = electroencephalography

Introduction

Type 2 focal cortical dysplasia (FCD2) is one of the most common causes of extra-temporal drug-resistant partial epilepsy that is surgically curable. As excision of the dysplastic cortex directly influences postoperative outcome (1–4), detection of focal cortical dysplasia (FCD) has become one of the most challenging aims of the presurgical work-up. Owing to improved image quality, MRI has contributed to the steady increase in presurgical detection of FCD2. However, even with dedicated protocols, MR diagnosis remains difficult, with up to 30–40% of FCD2 cases either undetected or diagnosed late (5–8) even with 3 Tesla MR units (9). One of the most robust signs of FCD2 is the transmantle sign, spreading along the axis of the abnormal sulcus, and running perpendicular to the wall of the lateral ventricle along the path of migrating neuroblasts. This substantiates the developmental origin of FCD2 and is consistent with a disruption of early stages of embryogenesis (10). In line with this hypothesis, FCD2 is associated with abnormal gyral/sulcal morphology. These include deep and enlarged sulcus, gyral simplification and unusual angulation or shape of a sulcus (7,8,11–13) in the vicinity of the FCD. Furthermore, small FCDs are preferentially located at the bottom of abnormally deep sulci (14) and their detection may benefit from an automated sulcal pattern recognition tool (15).

Given that up to 40% of FCD2s are located in the central region (1,8,16), this area represents a challenge in FCD surgery because of the risk of permanent postoperative neurological deficit. While examining the brain surface of patients referred for MRI because of intractable seizures in the central region, we noticed the presence of unusual features of the central sulcus in close proximity to the FCD2, though at this stage there was no tangible evidence for abnormality rather than simply a variant of normal anatomy. This observation was recently reinforced by the use of three-dimensional (3D) reformatting of brain MRIs with drawing of the sulci, which enabled us to describe a particular sulcal pattern of the central sulcus, namely, the interposition of a pre-central sulcal segment between the central sulcus and a hook-shaped anterior ascending branch. By analogy to the shape of the power symbol on the button that turns an electronic device on or off (Fig 1), we termed this the “power button sign” (PBS). Interestingly, this unusual sulcal pattern has never been reported as a normal variant of the central sulcus in anatomical atlases (17,18) or in MRI observations of the central region (19,20). Our objective was to compare in patients and controls the occurrence of several central sulcus variants, such as interruptions, number of side branches and connections with adjacent sulci, which have been comprehensively described in an anatomical atlas in healthy

subjects (18). We also aimed to assess the reproducibility of PBS and evaluate its occurrence in both groups.

Figure 1: Typical "power button sign" (PBS). Sulcal graph on a 3D reconstruction of the brain surface of a 17 year-old male patient (A) and magnification of the PBS (B). The central sulcus is shown in red. The PBS, by analogy to the power symbol (C), corresponds to the interposition of a pre-central segment (in green) between the central sulcus and a hook-shaped anterior ascending branch (also in red).

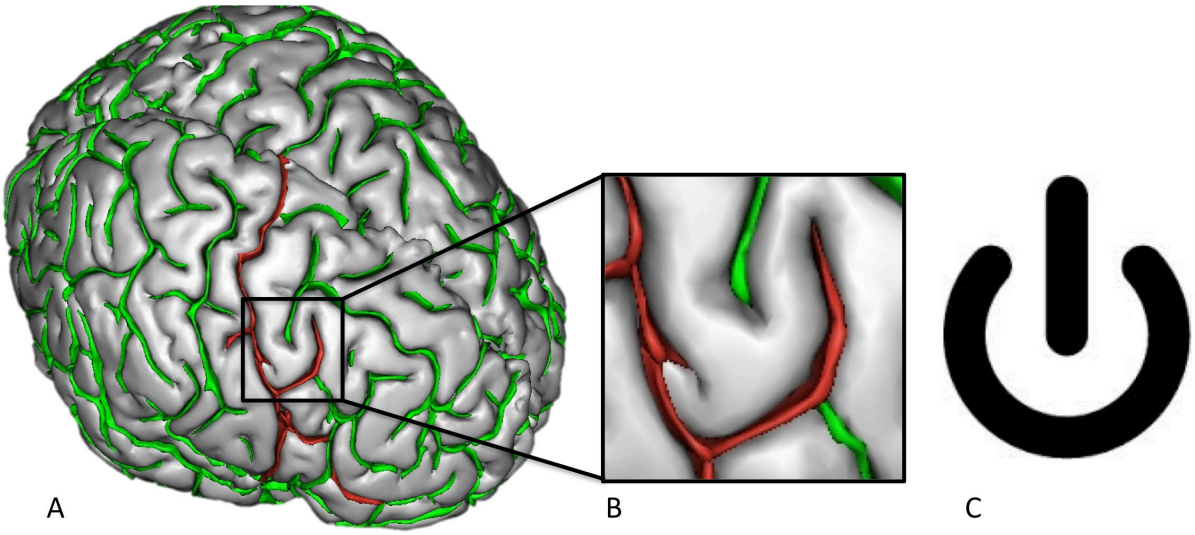

Materials and Methods

Patients and Controls

Among 265 consecutive patients with intractable epilepsy referred to our institution for a presurgical work-up between January 2006 and September 2013, we retrospectively identified all patients who fulfilled the following three inclusion criteria: 1) epilepsy of the central region; 2) preoperative MRI with 3D T1-weighted sequence in DICOM format; 3) histological confirmation of FCD2 (focal disorganization of the cortical cytoarchitecture and presence of giant dysmorphic neurons, associated or not with balloon cells). Thirty-seven patients fulfilled the above criteria and were included in the study; the remaining 218 patients failed to meet one or more of the criteria (see flow chart in Fig 2). In addition to MRI, presurgical evaluation included, ictal video-EEG and 18FDG–PET scans for all patients and stereo-EEG for 18 patients, which allowed lesion detection, particularly in patients with negative MRI (see below). Part of the population (n=25/37 patients) studied here has been published previously in original papers dealing with entirely different scientific questions (xxx). Based on a previously published method, we distinguished negative from positive MRI

for FCD2 (8). Briefly, MRI was considered positive when at least one of the cardinal MR signs (i.e. cortical thickening, blurring, cortical and/or subcortical signal changes, transmantle sign) of FCD2 was present. Patients were compared with a group of 44 right-handed controls (median age 26 years, inter-quartile range: 23–32; 22 males) without medical history. Patients did not differ from controls for age (p=0.22) or gender (p=0.89). This study was found to conform to generally accept scientific principles and ethical standards by the local Ethics Review Committee.

Figure 2: Flowchart of patients.

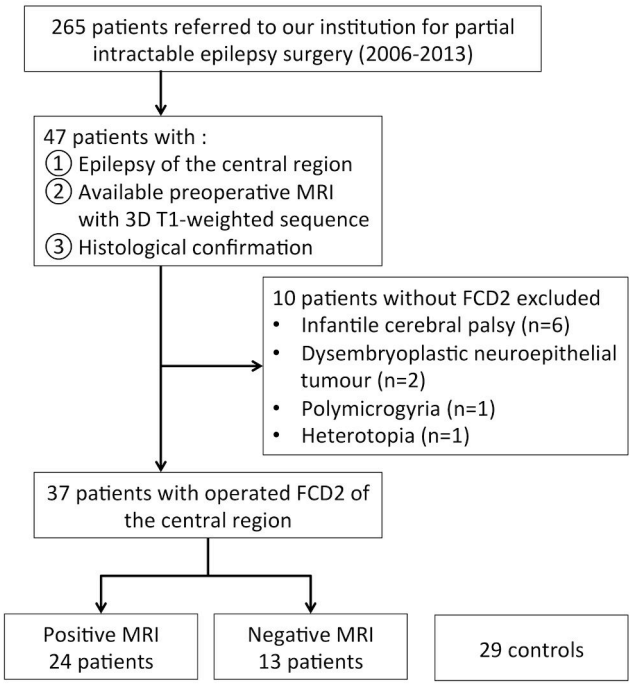

MRI Acquisition

Images were acquired on a 1.5 T Signa MR scanner (Signa 1.5T, General Electric Healthcare, Milwaukee, WI, USA) using an inversion recovery three-dimensional T1-weighted fast-spoiled gradient recalled acquisition (repetition time/echo time/flip angle: 10/2 ms/15°, matrix: 256 × 256, 1.2 mm slice thickness, no gap, in-plane resolution: 0.93 mm × 0.93 mm, acquisition time: 6 min 14 s).

Extraction of cortical folds

A sulcal graph was obtained using a 3D surface-based reconstruction of cortical folds provided by Morphologist 2012, a toolbox of BrainVisa software (http://brainvisa.info) as previously described (21). An automated pre-processing step skull-striped T1 MRI and segmented the brain tissues: cerebrospinal fluid, grey matter, and white matter. The two hemispheres were then separated and reconstructed in 3D brain surfaces corresponding to the grey–white matter and grey matter–cerebrospinal fluid interface. The cortical folds were then automatically segmented throughout the cortex from the skeleton of the grey matter/cerebrospinal fluid mask, with the cortical folds corresponding to the crevasse bottoms of the "landscape", the altitude of which is defined by intensity on MRI. This definition provides a stable and robust sulcal surface definition that is not affected by variations of the grey–white matter contrast (22). The cortical folds were then converted to a graph-based representation of the cortex. No spatial normalization was applied to the MRI data to overcome potential bias due to the sulcus shape deformations induced by the warping process.

Image Analysis

Four readers (1, 3, 8 and 20 years of experience) reviewed first separately then in consensus sulcal variations and abnormalities on 3D reconstruction of brain surface with sulcal representation provided by the BrainVisa software. Pairs of sulcal unlabeled graphs (right and left hemisphere) of patients and controls were presented in a random order. In each hemisphere, readers assessed five criteria adapted from Ono's description of anatomical variations of the central sulcus (18) based on different patterns: 1- interruption (when the central sulcus was discontinuous); 2- extension to the sylvian fissure; 3- presence of a connection with the pre-central sulcus or 4- with the post-central sulcus; 5- number of side branches. Readers also looked for a PBS with a binary (yes/no) assessment. This sign was defined as the interposition of a pre-central segment between a branch arising from central sulcus and the central sulcus itself (Fig 1). In order to check for intra-observer reproducibility, one reader examined all images again 6 months later, with the images being presented in a different randomized order from that of the first session.

After consensual reading, one reader checked all postoperative T1 MRIs and per-operative data to determine whether the FCD2 was located in the depth of the branch ascending from the central sulcus, in patients harboring the PBS.

Statistical Analysis

The occurrence of each sulcal criterion, including the PBS, was calculated separately for left and right hemisphere. These results were compared between patients and controls and between the index (ipsilateral to the FCD2) and the contralateral hemisphere using a Chi square test or a Mann-Whitney test, as appropriate. For the PBS, we calculated sensitivity and specificity, with true positives defined as present in the index hemisphere and true negatives as the absence of the sign in controls. We also computed the inter- and intra-observer concordance for each criterion using Fleiss' kappa index. In a post hoc analysis, we tested the association between the presence of PBS and visually assessed cortical thickening at the site of FCD2.

Results

The 37 patients (18 males, 29 right-handed) had a median age of 24 years (inter-quartile range: 19-32) at surgery. FCD2 was unilateral (left central region, n=19) and limited to a single lobe (35 frontal, 2 parietal) in all cases. Inter- and intra-observer agreement for detection of the PBS was respectively kappa=0.88 [IC95%=0.78–0.98] and 0.93 [IC95%=0.84–1]. Interobserver agreement was kappa=1, 0.76, 0.75, 0.81 and 0.85 for interruptions, extension to the sylvian fissure, side branches, post-central connection and pre-central connection, respectively.

Figure 3: Occurrence (as %) of criteria defining the central region including the "power button sign" for patients (on the side of the lesion and in the contralateral hemisphere, respectively) and controls.

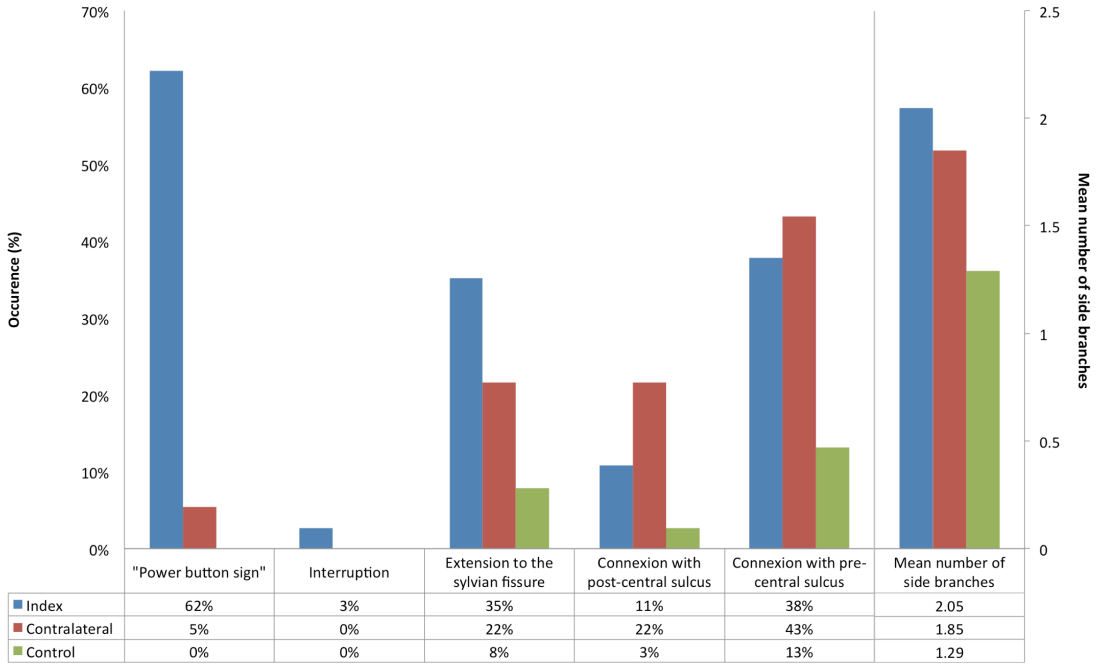

	"Power button sign"	Interruption	Extension to the sylvian fissure	Connexion with post-central sulcus	Connexion with pre-central sulcus	Mean number of side branches
Index	62%	3%	35%	11%	38%	2.05
Contralateral	5%	0%	22%	22%	43%	1.85
Control	0%	0%	8%	3%	13%	1.29

Patients with FCD2 did not differ from controls for interruptions (p=0.12) or connection with post-central sulcus (p=0.76) (Fig 3). Interestingly, the central sulcus ipsilateral to the FCD2 had significantly more side branches (mean number=2.05 in patients vs. 1.12 in controls; p=0.0003) and was more frequently connected to the pre-central sulcus (p=0.0006) or to the sylvian fissure (p=0.01) than controls. However, the frequency of occurrence for the five criteria derived from Ono's atlas did not significantly differ between the index and the contralateral hemisphere of patients.

Figure 4: Examples of central sulci with "power button sign" (PBS) in patients with positive MRI (second column, 24 year-old male, 19 y-old female and 32 y-old male, respectively) and negative MRI (third column, 11 year-old male, 42 year-old male and 17 year-old male, respectively) compared to controls (first column, 20 year-old female, 29 year-old male and 19 year-old female, respectively). Note that controls may present a small branch in the pre-central gyrus (second raw) or an ascending connection with the pre-central sulcus (third raw). In the absence of the interposition of a pre-central segment, these variations are not considered as PBS.

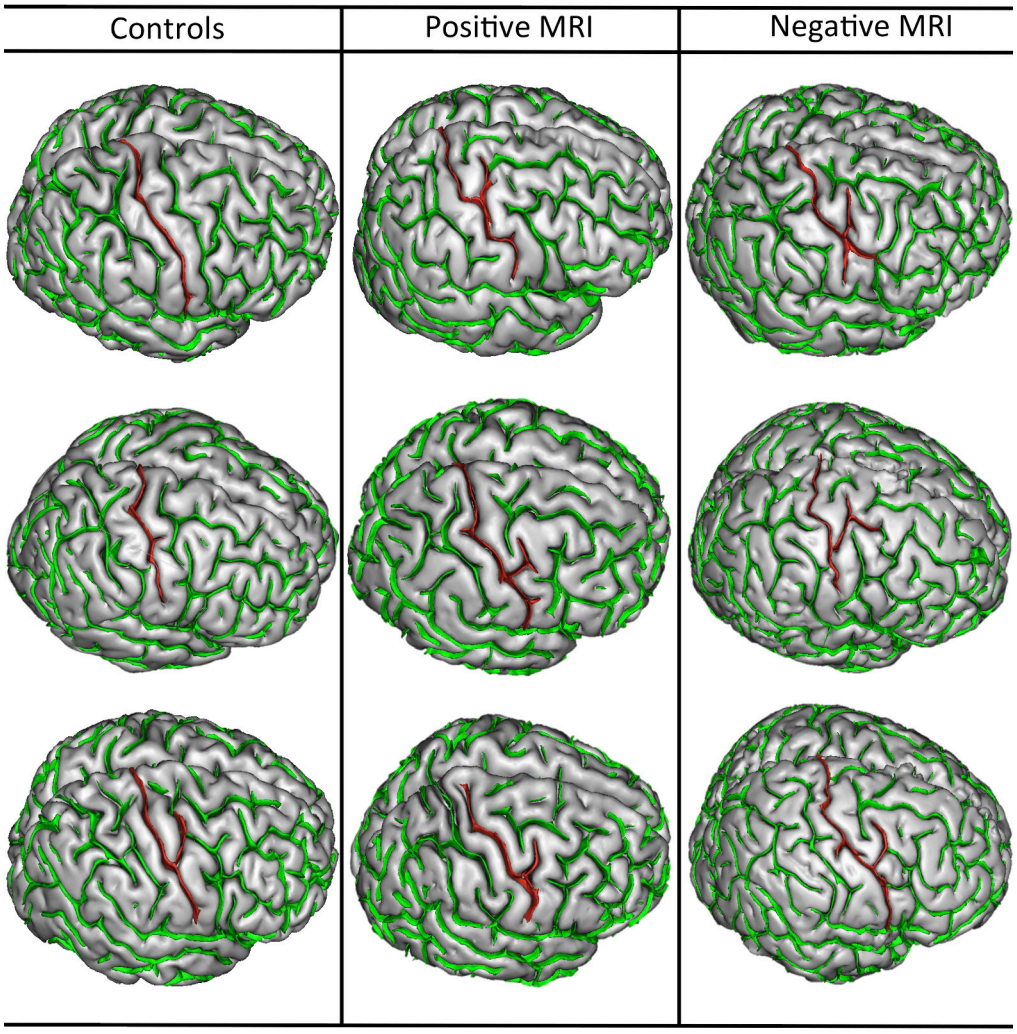

The PBS was observed in one of the 44 controls (88 hemispheres) whereas it was observed in 23 of the 37 patients, corresponding to a specificity of 98.9% and a sensitivity of 62% for the detection of patients with FCD2 (Fig 4). The PBS was bilateral in two patients. When unilateral (n=21), it was always located in the hemisphere ipsilateral to the FCD2. Of the 23 patients with a PBS, 17 (70%) had positive MRI and six had negative MRI using standard FCD2 criteria. PBS was present in left-handed patients (n=5/9; 55%) as in right-handed patients (n=18/28; 64%) in a similar proportion (p=0.8). Similarly, PBS was present in patients with cortical thickening (n=12/16; 75%) as well as in patients without cortical thickening (n=11/21; 52%), in a similar proportion (p=0.15). Patients with PBS did not differ from patients without PBS in terms of either age at epilepsy onset or duration from onset to surgery.

A comparison of PBS location with per-operative data, histological examination and postoperative MRIs revealed that FCD2 was located precisely in the depth of the hook-shaped anterior branch ascending from the central sulcus (Fig 5) in 14 of the 23 (60%) patients with a PBS. In the other nine cases, FCD2 was located in its immediate vicinity.

Figure 5: "Power button sign" (PBS) as a locating tool. FCD2 is located in the depth of the hook-shaped anterior ascending branch (arrow) from the central sulcus (A) in a 42 year-old male. PBS is consistent with other MR signs of FCD2 (here thickening and blurring of the cortex) on a surface (B) and deep (C) oblique sagittal reformat of the 3D T1-weighted MRI (arrow). PBS is also notable on pre-operative view (D, arrow). The diagnosis of FCD2 was confirmed after cortectomy (E).

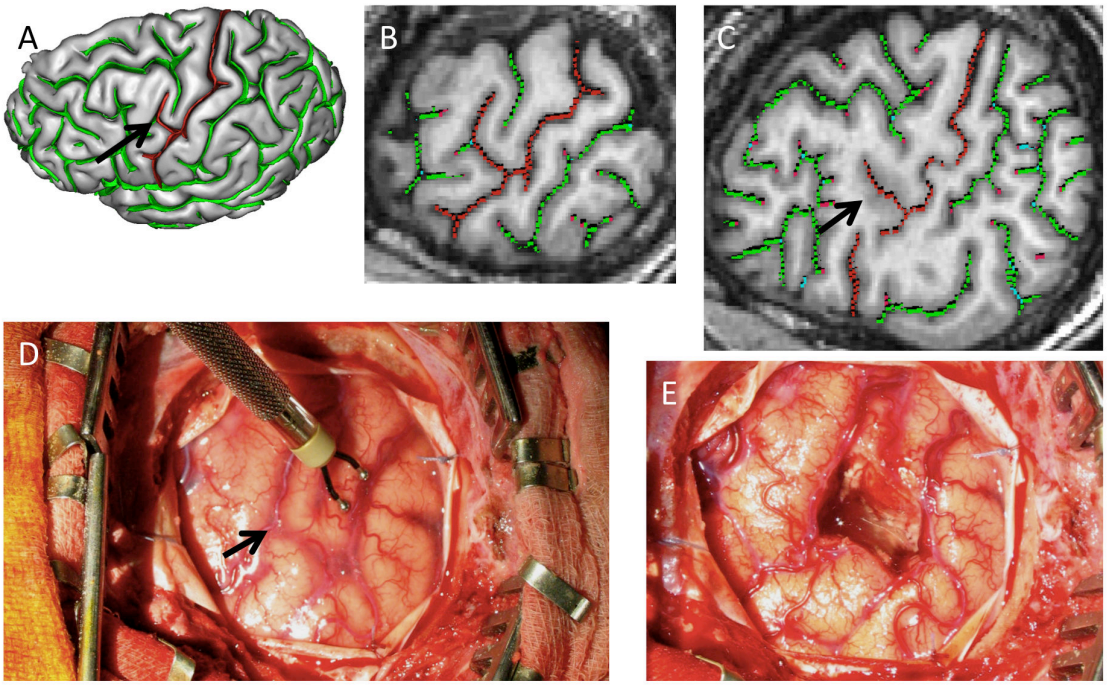

Discussion

In this retrospective case–control study of consecutive patients with FCD2 located in the central region, we described for the first time a new sulcal pattern, associated with FCD2 in this region. The absence of this sign in the control group confers excellent specificity. **The PBS, which enriches the MR semiology of FCD2, may increase diagnostic confidence when other cardinal MR criteria are visible or, more importantly, when these are lacking or doubtful.** Finally, the PBS can also serve as a guide to the site of FCD2. Taken together, these results are clinically relevant since negative or ambiguous MRI can preclude patients from being referred for surgery, although such patients are increasingly considered as potential candidates (7,23).

Using 3D visualization, we first showed that some anatomical variants of the central sulcus were more frequent in FCD2 than in controls. Known anatomical variants of the central sulcus are based on visual inspection of 2D MR images and on post mortem brains. For instance, Ono's atlas (18) provides a comprehensive analysis of all possible sulcal patterns of the central sulcus in 25 normal subjects. We focused our analysis on five anatomical variants described by Ono. Among these, side branches, connection with the pre-central sulcus and extension to the sylvian fissure were more frequent in FCD2 patients than in controls. The process of sulcation relies on multiple factors during the foetal period and may include tension between axons connecting different cortical areas (24). In addition, the link between sulcation and connectivity is supported by experimental data: alteration of the geniculo-cortical connections during early embryogenesis stages in monkeys leads to a reduction of the surface of the visual cortex and an increased number of sulci replacing the normal smooth cortical surface (25). In FCD, reduced connectivity between the lesion and underlying white matter is supported by decreased fractional anisotropy, increased mean diffusivity and, more recently, a reduced intracellular volume fraction based on advanced diffusion techniques (26). Accordingly, the increased sulcation that we, in line with others (14), found in the central region in patients, could result from a disruption of early corticogenesis inducing reduced white matter connectivity with a subsequent impact on cortical folding. Early disruption during cortical development is also expected to produce widespread sulcal abnormalities. This could explain the unexpected high frequency of sulcal variations in the hemisphere contralateral to the FCD2. It may also account for the bilateral occurrence of the PBS in two of our FCD2 patients.

The results concerning the PBS are undoubtedly the most clinically pertinent in our study. In the literature, reports of sulcal abnormalities in FCD are scarce (27) and their descriptions

often equivocal. Aberrant sulcal features reported in FCD2 relied on quantitative markers, such as alteration in the width, length, depth and size of the sulcus (11,12,14,27,28). A sulcus-based analysis automatically identified subclinical abnormal sulcal patterns in the epileptic zone for 9 of 12 patients with MRI-negative extra-temporal intractable epilepsy (15). We have shown here that sulcal changes can also be detected by the human eye in about two-thirds of FCD2 patients, and with high reproducibility. Interestingly, the PBS was seen in half of the MR-negative patients, i.e. without any other signs suggesting FCD2, whereas previously reported "major" unusual sulcal patterns (8) were never isolated. In the present study, the FCD2 was found precisely in the depth of the ascending branch of the central sulcus in 60% of patients with a PBS, in agreement with a study that found small FCD at the bottom of an abnormally deep sulcus (14). PBS is unlikely to be an epiphenomenon caused by cortical modification induced by the lesion, given that it was observed equally in patients with and patients without cortical thickening. This adds further weight to the argument that PBS is specific to FCD2. Given its excellent specificity, the PBS, when present, could be used as a new diagnostic MR criterion for FCD2 of the central region. Of note, before searching for the PBS, one should first identify the central sulcus, based on normal sulcal landmarks such as the "hand knob" (20), "pars bracket" (29) and "shepherd's crook" sign, which are not modified by the FCD2 in the central region (30).

Three dimensional surface visualization is increasingly performed for detection of developmental lesions, but also for planning the surgical approach to FCD2 and intraoperative guidance (31). We used a post-processing tool for 3D visualization of brain sulci that allowed for the identification of the PBS. Even if this tool is freely available and routinely exploitable, similar results might be obtained with commercial algorithms for 3D brain surface rendering, although these were not tested here. A possible alternative is curvilinear reformatting of 3D T1-weighted acquisition, which provides on a single plane a comprehensive view of the central region. This post-processing tool is available on most workstations, has been evaluated for anatomical MR description of the central region (32) and improves the detection of MR signal changes in subtle FCD (33).

Our study has limitations. First, the excellent specificity we report should be interpreted with care given that our control group consisted of healthy subjects. Consequently, we cannot be certain that the PBS would not be observed in epileptogenic lesions other than FCD2, particularly developmental lesions. Yet, lesions associated with epilepsy of the central regions (Fig 2), such as infantile cerebral palsy, dysembryoplastic neuroepithelial tumor and

polymicrogyria, would be easily diagnosed using standard diagnostic criteria. Second, all our controls were right-handed whereas 25% of the patients were left-handed. We cannot exclude the possibility that these handedness differences could partly explain the group differences we found, given that the shape of the central sulcus depends on handedness (34). Nevertheless, the PBS was found in a similar proportion in left-handed and right-handed patients. Third, the cardinal signs of FCD2 were absent in 35% of patients using 1.5T MRI. This is likely explained by the fact that, in these patients, surgery was based on a combination of FDG-PET and stereo-EEG. One might argue that the detection rate would have increased with the use of a higher magnetic field. This is unlikely, however, given that 3T MRI only marginally increases the detection of FCD2 (9). Nevertheless, we cannot extrapolate our results regarding abnormal sulcal patterns to 3T images, since grey matter–cerebrospinal fluid interface segmentation can be affected by increased intensity inhomogeneity (bias field) at higher magnetic field (35). Finally, our study is limited to the central region, which accounts for fewer than half of the patients with FCD2. A similar method of sulcal analysis should also be tested in regions other than the central area.

Conclusion

In patients referred for intractable partial epilepsy, special attention should be given to 3D sulci analyses. We have described a new qualitative MR imaging finding for the diagnosis of FCD2: the “power button sign”. This sign was present in half of the FCD2 patients with normal conventional MRI. Given its excellent reproducibility and specificity, the PBS, when present, could be used as a new major diagnostic MR criterion of FCD2 of the central region, if confirmed by future studies.

References

1. Chassoux F, Devaux B, Landré E, et al. Stereoelectroencephalography in focal cortical dysplasia A 3D approach to delineating the dysplastic cortex. Brain 2000;123(8):1733–1751.
2. Urbach H, Scheffler B, Heinrichsmeier T, et al. Focal Cortical Dysplasia of Taylor's Balloon Cell Type: A Clinicopathological Entity with Characteristic Neuroimaging and Histopathological Features, and Favorable Postsurgical Outcome. Epilepsia 2002;43(1):33–40.
3. Fauser S, Bast T, Altenmüller D-M, et al. Factors influencing surgical outcome in patients with focal cortical dysplasia. J Neurol Neurosurg Psychiatry 2008;79(1):103–105.
4. Lerner JT, Salamon N, Hauptman JS, et al. Assessment and surgical outcomes for mild type I and severe type II cortical dysplasia: a critical review and the UCLA experience. Epilepsia 2009;50(6):1310–1335.
5. McGonigal A, Bartolomei F, Régis J, et al. Stereoelectroencephalography in presurgical assessment of MRI-negative epilepsy. Brain 2007;130(12):3169–3183.
6. Kim DW, Lee SK, Chu K, et al. Predictors of surgical outcome and pathologic considerations in focal cortical dysplasia. Neurology 2009;72(3):211–216.
7. Chassoux F, Rodrigo S, Semah F, et al. FDG-PET improves surgical outcome in negative MRI Taylor-type focal cortical dysplasias. Neurology 2010;75(24):2168–2175.
8. Mellerio C, Labeyrie M-A, Chassoux F, et al. Optimizing MR Imaging Detection of Type 2 Focal Cortical Dysplasia: Best Criteria for Clinical Practice. Am J Neuroradiol 2012;33(10):1932–1938.
9. Mellerio C, Labeyrie M-A, Chassoux F, et al. 3T MRI improves the detection of transmantle sign in type 2 focal cortical dysplasia. Epilepsia 2014;55(1):117–122.
10. Barkovich AJ, Kuzniecky RI, Bollen AW, Grant PE. Focal transmantle dysplasia: A specific malformation of cortical development. Neurology 1997;49(4):1148–1152.
11. Yagishita A, Arai N, Maehara T, Shimizu H, Tokumaru AM, Oda M. Focal cortical dysplasia: appearance on MR images. Radiology 1997;203(2):553–559.
12. Raymond AA, Fish DR, Sisodiya SM, Alsanjari N, Stevens JM, Shorvon SD. Abnormalities of gyration, heterotopias, tuberous sclerosis, focal cortical dysplasia, microdysgenesis, dysembryoplastic neuroepithelial tumour and dysgenesis of the archicortex in epilepsy: Clinical, EEG and neuroimaging features in 100 adult patients. Brain 1995;118(3):629–660.
13. Krsek P, Maton B, Korman B, et al. Different features of histopathological subtypes of pediatric focal cortical dysplasia. Ann Neurol 2008;63(6):758–769.
14. Besson P, Andermann F, Dubeau F, Bernasconi A. Small focal cortical dysplasia lesions are located at the bottom of a deep sulcus. Brain J Neurol 2008;131(Pt 12):3246–3255.
15. Régis J, Tamura M, Park MC, et al. Subclinical abnormal gyration pattern, a potential anatomic marker of epileptogenic zone in patients with magnetic resonance imaging-negative frontal lobe epilepsy. Neurosurgery 2011;69(1):80–93.
16. Palmini A, Gambardella A, Andermann F, et al. Intrinsic epileptogenicity of human dysplastic cortex as suggested by corticography and surgical results. Ann Neurol 1995;37(4):476–487.
17. Cunningham DJ. Text-book of anatomy. New York: W. Wood and company; 1905.
18. Ono M, Kubik S, Abernathey CD. Atlas of the Cerebral Sulci. Stuttgart: Thieme; 1990.
19. Hamasaki T, Imamura J, Kawai H, Kuratsu J. A three-dimensional MRI study of variations in central sulcus location in 40 normal subjects. J Clin Neurosci 2012;19(1):115–120.
20. Yousry TA, Schmid UD, Alkadhi H, et al. Localization of the motor hand area to a knob on the precentral gyrus. A new landmark. Brain J Neurol 1997;120 (Pt 1):141–157.
21. Gay O, Plaze M, Oppenheim C, et al. Cortex Morphology in First-Episode Psychosis Patients With Neurological Soft Signs. Schizophr Bull 2012;39(4):820–829.
22. Mangin J-F, Rivière D, Cachia A, et al. A framework to study the cortical folding patterns. NeuroImage 2004;23:S129–S138.
23. Chassoux F, Landré E, Mellerio C, et al. Type II focal cortical dysplasia: electroclinical phenotype and surgical outcome related to imaging. Epilepsia 2012;53(2):349–358.
24. Van Essen DC. A tension-based theory of morphogenesis and compact wiring in the central nervous system. Nature 1997;385(6614):313–318.
25. Rakic P. Specification of cerebral cortical areas. Science 1988;241(4862):170–176.
26. Winston GP, Micallef C, Symms MR, Alexander DC, Duncan JS, Zhang H. Advanced diffusion imaging sequences could aid assessing patients with focal cortical dysplasia and epilepsy. Epilepsy Res [Internet] 2013 [cited 2013 Dec 17]; Available from: http://linkinghub.elsevier.com/retrieve/pii/S092012111300288X
27. Bronen RA, Spencer DD, Fulbright RK. Cerebrospinal Fluid Cleft with Cortical Dimple: MR Imaging Marker for Focal Cortical Dysgenesis1. Radiology 2000;214(3):657–663.

28. Colombo N, Tassi L, Deleo F, et al. Focal cortical dysplasia type IIa and IIb: MRI aspects in 118 cases proven by histopathology. Neuroradiology 2012;54(10):1065–1077.
29. Naidich TP, Brightbill TC. The pars marginalis. 1. A"bracket"sign for the central sulcus in axial plane CT and MRI. Int J Neuroradiol 1996;2(1):3–19.
30. Hingwala D, Thomas B, Radhakrishnan A, Suresh Nair N, Kesavadas C. Correlation between anatomic landmarks and fMRI in detection of the sensorimotor cortex in patients with structural lesions. Acta Radiol Stockh Swed 1987 2014;55(1):107–113.
31. Yang JC, Aronson JP, Dunn GP, Codd PJ, Buchbinder BR, Eskandar EN. Three-dimensional brain surface visualization for epilepsy surgery of focal cortical dysplasia. J Clin Neurosci Off J Neurosurg Soc Australas 2013;
32. Wagner M, Jurcoane A, Hattingen E. The U Sign: Tenth Landmark to the Central Region on Brain Surface Reformatted MR Imaging. Am J Neuroradiol 2012;34(2):323–326.
33. Montenegro MA, Min Li L, Guerreiro MM, Guerreiro CAM, Cendes F. Focal Cortical Dysplasia: Improving Diagnosis and Localization With Magnetic Resonance Imaging Multiplanar and Curvilinear Reconstruction. J Neuroimaging 2002;12(3):224–230.
34. Sun ZY, Klöppel S, Rivière D, et al. The effect of handedness on the shape of the central sulcus. NeuroImage 2012;60(1):332–339.
35. Vovk U, Pernus F, Likar B. A review of methods for correction of intensity inhomogeneity in MRI. IEEE Trans Med Imaging 2007;26(3):405–421.

Troisième partie : Synthèse et perspectives

Les nouvelles techniques en IRM sont un élément clé du diagnostic et de la prise en charge des DCF2, mais sont également utile à la compréhension de leur physiopathologie. Dans la première partie de cette synthèse, nous discuterons nos résultats à la lumière des mécanismes développementaux à l'origine des DCF2. Dans la seconde partie, nous proposerons des solutions pratiques pour optimiser leur détection et leur caractérisation. Nous tâcherons pour finir de dégager des perspectives de travaux pour améliorer davantage les outils diagnostiques de cette pathologie.

1. Les dysplasies corticales focales : un modèle d'anomalie développementale

Au gré des quatre études présentées ci-dessus, il se dégage un point commun propre aux DCF2. Ces lésions résument par leur présentation en imagerie les différentes étapes du développement cortical.

Le développement normal du cortex cérébral au cours de l'embryogénèse s'effectue en plusieurs étapes successives et enchevêtrées, à l'origine des classifications des malformations du développement cortical. Ces trois étapes se résument ainsi : prolifération, migration et organisation corticale. La première étape de multiplication des précurseurs neuronaux issus de la plaque germinative ventriculaire se déroule de la 4ème à la 16ème semaine de gestation. La phase de migration de ces précurseurs depuis les zones germinatives profondes (péri-ventriculaires) jusqu'au cortex lui succède de la 6ème semaine jusqu'à la 20ème semaine. Cette migration est un phénomène complexe nécessitant la participation de cellules gliales spécialisées. Elle se réalise de manière radiale d'une part pour aboutir à la superposition des différentes couches de populations neuronales au sein du cortex et de manière tangentielle d'autre part, conduisant au développement d'interneurones. Enfin, l'organisation corticale post migratoire s'effectue en seconde partie de grossesse et se prolonge après la naissance.

Durant cette phase vont se différencier les cellules neuronales avec l'apparition de dendrites, d'axones, et de connections synaptiques.

Parmi les nombreuses classifications des malformations du développement cortical (MDC), la plus utilisée (18,24) est celle de Barkovich et al. (Tableau 4). Elle se base sur le délai de survenue de l'anomalie dans la chronologie de ces 3 étapes de maturation du cortex.

I. Malformations liées à une prolifération neuronale et gliale ou une apoptose anormale
A. Prolifération diminuée/apoptose augmentée (Microcéphalies)
B. Prolifération augmentée avec cellule normale/apoptose diminuée (Mégalencephalies)
C. Prolifération anormale avec cellules anormales
1. Non-néoplasique (tuber, DCF avec cellules ballonisées, Hemimégalencephalie)
2. Néoplasique (Tumeur neuroépitheliale dysembryoplasique, gangliogliome, gangliocytome)
II. Malformations liées à une migration neuronale anormale
A. Lissencephalie/Bande d'hétérotopie subcorticale
B. Cobblestone complex
C. Hétérotopie
III. Malformations liées à une organisation corticale anormale
A. Polymicrogyrie and schizencephalie
B. DCF sans cellules ballonisées
C. Microdysgenesis
IV. Malformations non classifiées

Tab. 4 : Malformations du développement cortical (d'après la classification de Barkovich et al. 2001)

Les DCF2 résulteraient d'une atteinte précoce de la gestation pendant la phase de prolifération cellulaire, responsable de profondes anomalies cellulaires à la fois neuronales et gliales. Néanmoins, il existe également une répercussion sur les phases plus tardives illustrée par les différentes parties de cette étude, en particulier la phase de migration (« transmantle sign ») et d'organisation du cortex (anomalies sulcales).i

1.1. Les anomalies de signal : témoins de l'aberration cellulaire

Les anomalies de signal en IRM retrouvées dans notre série (partie 1 et 2) sont typiques des DCF2 décrites dans la littérature.

L'épaississement cortical et **l'aspect flou** de la jonction gris-blanc, bien que difficilement perceptibles, font partie des signes cardinaux des DCF2 dans la littérature (9,38–40), en raison de leur caractère typique. Histologiquement, ils pourraient correspondre à la présence de neurones ectopiques, de cellules ballonisées, ou de neurones géants dans le cortex et à la jonction gris-blanc ou encore d'une perte axonale (4). Leur fréquence dans notre série est semblable à celle décrite dans la littérature. Néanmoins, nous retrouvons des anomalies peu marquées et subtiles, contrastant avec les épaississements caricaturaux des séries les plus anciennes. Les données histologiques corroborent cette notion que l'épaississement est le plus souvent minime voire imperceptible, et suggèrent l'existence de pseudo-épaississements à l'IRM (40), en rapport avec des anomalies de signal de la substance blanche sous-corticale proches du signal du cortex.

L'hypersignal cortical en T2 ou FLAIR du cortex des DCF2 est un signe connu et rapporté dans la littérature mais inconstamment décrit (3,10). Il est retrouvé dans notre série dans 38% des cas de patients à IRM positive. Il est particulièrement visible sur les séquences FLAIR sous la forme d'un signal modérément hyperintense au cortex normal. Histologiquement, cette anomalie pourrait être en rapport avec une densité importante de cellules ballonisées dans le cortex (10).

Les anomalies de la substance blanche sous corticale sont constantes dans notre série. Elles sont aussi plus faciles à détecter que les autres anomalies, tout particulièrement en pondération FLAIR. Histologiquement, elles correspondraient plutôt à la dysplasie elle-même (notamment les cellules ballonisées et les anomalies de la myélinisation) qu'à des lésions de gliose secondaires à la récurrence des crises comitiales (4,7,10,40).

1.2. Le « transmantle sign » : traceur de la migration neuronale

Le « transmantle sign » a été décrit initialement par Barkovich et al. en 1997 à propos de 18 patients présentant une DCF2 (38). Sa signification histologique a fait l'objet de peu d'études du fait de la fréquente fragmentation des prélèvements et de l'exérèse souvent limitée de la substance blanche. Barkovich en 1997 puis Urbach en 2002 considérèrent que ce signe est la conséquence de l'hypomyélinisation et de la présence de cellules ballonisées dans la substance blanche sous-jacente à la lésion corticale (7,38). La topographie tout à fait particulière de ce signe qui s'étend radialement du bord supéro-externe du ventricule latéral

jusqu'au cortex dysplasique, correspond au trajet de migration des neuroblastes du toit des vésicules cérébrales vers le néocortex durant l'embryogénèse. Cela va dans le sens d'une **perturbation précoce de la corticogénèse affectant la phase de migration des neuroblastes** (25). Il est intéressant de remarquer que cette disposition radiaire des régions sous-épendymaires vers le cortex peut se rencontrer dans d'autres anomalies du développement telles que certaines malformations artério veineuses (41). Ce signe est présent dans notre étude chez 4/5 patients à IRM positive. Sa fréquence dans notre série est nettement supérieure au taux de 30% rapporté dans les études les plus anciennes, suggérant que ce signe ait pu être sous-estimé (40,42,43). Les progrès techniques (antennes multiphasées en réseau, séquences 3D) se sont accompagnés d'une augmentation de la fréquence de ce signe dans les séries les plus récentes. Ainsi parmi 83 patients porteurs de DCF2, Colombo et al. (44) retrouvent ce signe dans 92% des cas avec un taux significativement plus important dans la population de DCF2 avec cellules ballonisées (95%) que sans (75% ; p=0,003). Dans cette même étude, le « transmantle sign » était spécifique du type 2 car n'était retrouvé dans aucune des DCF qui n'étaient pas de type 2.

Nous avons montré que le passage de 1,5T a 3T améliorait la détection du « transmantle sign ». Ce résultat a des conséquences cliniques directes, étant donné que ce signe n'a pas été rapporté dans d'autres lésions corticales acquises. En outre, la détection du « transmantle sign » a récemment été **associée à un bon pronostic après chirurgie** (45). Hormis l'augmentation du champ magnétique, l'utilisation systématique d'une séquence FLAIR volumique à 3T explique en grande partie l'amélioration de la détection du « transmantle sign » dans notre deuxième étude. La détection de cet hypersignal T2 linéaire subtil bénéficie particulièrement du reformatage multiplanaire dans la mesure où son orientation correspond rarement au plan d'acquisition axial ou coronal strict (figure 4) et peut donc être invisible sur des séquences FLAIR/T2 en 2D.

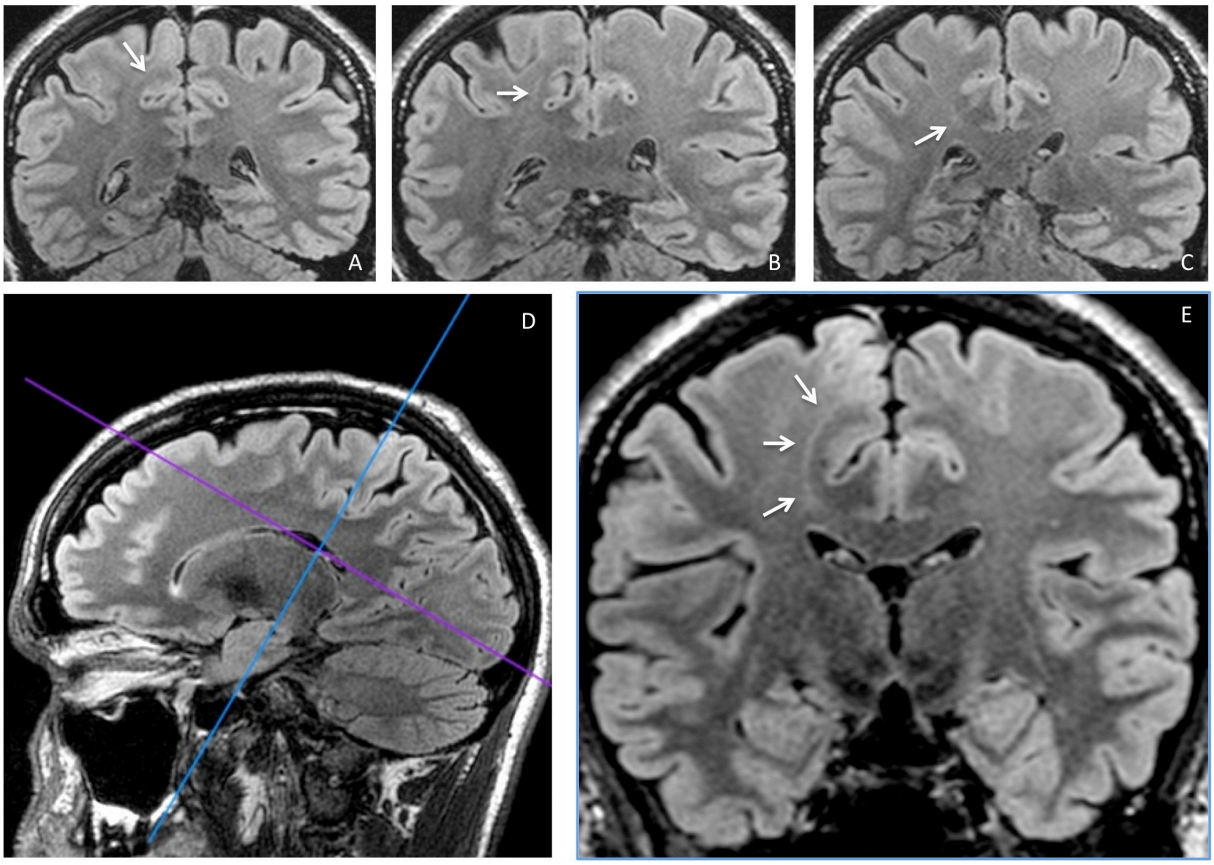

Figure 4 : Intérêt d'un plan d'acquisition oblique pour une meilleure visualisation du « transmantle sign ». Patient de 32 ans adressé pour EPPR de l'aire motrice supplémentaire droite. Les coupes A, B et C acquises dans un plan coronal strict permettent difficilement de suivre une anomalie de signal très subtile de la substance blanche sous corticale rejoignant le ventricule latéral droit (flèches). En réalisant un plan d'acquisition coronal oblique (D) le « transmantle sign » apparaît clairement et son trajet facilement reconnaissable (flèches).

1.3. Anomalies sulcales : marqueurs du retentissement sur l'organisation du cortex

Les anomalies sulcales associées aux DCF2 ont fait l'objet d'une appréciation de la largeur, la profondeur et l'angulation des sillons. Outre ces anomalies quantitatives, des anomalies qualitatives concernent le dessin des sillons. Ces dernières, bien que décrites dans la littérature, et mises en évidence dès notre première étude, sont le plus souvent subtiles et/ou subjectives et leur description assez floue (par exemple dans Colombo et al. 2012 (44): « *Abnormal cortical gyrations and sulcations - which can be better evaluated by means of 3D-volume sequences and surface rendering reconstructions - are frequently encountered, ranging from focal enlargement of the subarachnoid spaces to highly dysmorphic cortical*

convolutions with deeply running sulci. »). Par ailleurs leur prévalence n'a pas été évaluée isolément dans les principales séries, y compris les plus récentes (3,9,22,44). L'intérêt en imagerie de ces anomalies du motif sulcal dans la détection et la caractérisation des DCF2 de la région centrale nous a tout d'abord été suggéré par l'observation de configurations aberrantes des sillons lors de l'exposition peropératoire du cortex environnant la lésion avant sa cortectomie. Suite à cette observation, nous nous sommes tout d'abord intéressés à une étude de l'anatomie sulcale en IRM de 60 hémisphères chez des sujets sains (résultats non encore publiés – Annexe 3) pour rechercher si ces configurations aberrantes existaient chez le sujet sain. Cette étude comparative de la reconstruction corticale surfacique avec dessin des sillons par le même outil que celui utilisé dans les parties 3 et 4 (Morphologist – Brainvisa) avec un atlas de l'anatomie sulcale basé sur l'observation post-mortem de cerveaux (46) nous a permis de confirmer la **stabilité interindividuelle de la région centrale**. Cette analyse nous a ainsi fourni une description des variations « normales » des sillons de la région centrale, préalable essentiel à la détection d'anomalies sulcales associées aux DCF2. Nous nous sommes limités à la région centrale, dont nous avions ainsi confirmé la stabilité interindividuelle, telle que rapportée dans la littérature (47–50). C'est d'ailleurs à partir du sillon central qu'ont été conçus les principaux repères anatomiques utilisables en clinique, en particulier le signe de l' « *oméga inversé* » ou « *hand knob* » pour repérer la région de la motricité de la main (51).

Dans les parties 3 et 4, nous avons montré que certaines variantes anatomiques du sillon central sont plus fréquentes dans les DCF2 que chez les volontaires sains et que ce phénomène peut trouver son explication dans l'origine développementale des dysplasies. De telles variantes anatomiques du sillon central ont été largement étudiées à partir de description radio-anatomiques en IRM et surtout par l'étude post-mortem de la surface du cerveau. C'est à partir de l'atlas de Ono (46), qui fournit une analyse complète de tous les motifs sulcaux possibles du sillon central que nous avons extrait les cinq variantes anatomiques sur laquelle s'est basée notre analyse. Parmi ceux-ci, le nombre de branches latérales, de connexion entre sillon central et pré-central et son extension à la fissure sylvienne était plus fréquent chez les patients que chez les témoins. Bien que les mécanismes de « sulcogénèse » soient encore mal identifiés, différents modèles ont été proposés (52–54). Le processus de sulcation au cours de la période fœtale repose sur plusieurs facteurs, dont la description par Van Essen et al. de phénomènes de « tension » entre les axones reliant les différentes zones corticales (52). Ce lien entre sulcation et connectivité est également conforté par des données expérimentales : la

modification des connexions géniculo-corticales pendant les stades de l'embryogenèse précoce chez le singe entraîne une réduction de la surface du cortex visuel associée à une augmentation du nombre de sillons de la corticale (55). Ainsi, **trouble précoce du développement cortical et nombre de sillon/connexion sont liés**. De plus, cette relation connectivité/sulcation dans le cas particulier des DCF2 trouve également son interprétation dans les études récentes en tenseur de diffusion. Une diminution de la fraction d'anisotropie témoignant d'une réduction de la connectivité est retrouvée dans la substance blanche sous-jacente à la lésion, associée à une augmentation de la diffusivité moyenne et une réduction de la fraction du volume intracellulaire (56). En somme, **cette augmentation du nombre de sillons à proximité des DCF2 dans notre analyse réaffirme l'hypothèse d'une perturbation précoce du développement cortical induisant une diminution de la connectivité locale avec un effet direct sur la sulcation**. Cette précocité de la perturbation du développement cortical est également sous-tendue par la dispersion des anomalies sulcales au-delà de la dysplasie. Cela pourrait expliquer la fréquence élevée inattendue des variations sulcales dans l'hémisphère controlatéral à la DCF2.

2. Optimisation de la détection des dysplasies corticales focales en IRM

2.1. Optimisation du protocole et des critères de sémiologie en IRM

La partie 1 porte sur une analyse qualitative systématique du signal et de la morphologie de DCF2 prouvées histologiquement, à travers une série de 42 (59%) patients à IRM positive. Certains résultats de cette étude ont un intérêt en pratique clinique pour caractériser les DCF2

2.1.1. Axe de symétrie et gradient d'anomalie du centre vers la périphérie

Dans la moitié des cas, les anomalies IRM sont disposées de manière symétrique par rapport à un axe perpendiculaire au cortex et passant par le fond du sillon centrant la dysplasie (article 1 – figure 1), s'estompant progressivement en s'éloignant de cet axe. Cette symétrie concerne à la fois les anomalies corticales (épaississement, signal) et de la substance blanche sous-corticale. Il est intéressant de constater que l'axe de symétrie correspond au trajet du

« transmantle sign », s'il est visible. Cette symétrie pourrait traduire un **gradient de sévérité** de l'atteinte corticale du centre vers la périphérie, hypothèse renforcée par les données histologiques qui retrouvent un gradient centripète : le centre de la lésion contient le plus de neurones géants, de cellules ballonisées et d'anomalie de la myélinisation, alors que prédominent en périphérie les anomalies de la lamination et les neurones ectopiques proches des DCF de type 1.

2.1.2. Valeur diagnostique des anomalies IRM

- **L'épaississement cortical, l'aspect flou de la jonction cortico-sous-corticale et le transmantle sign sont caractéristiques des DCF2**. Cependant, considérés isolément, aucun n'est spécifique.
- Les anomalies de la différenciation cortico-sous-corticale peuvent se rencontrer dans d'autres pathologies en particulier les tumeurs infiltratives du cortex telles que l'oligodendrogliome ou la tumeur dysembryoplasique neuro-épithéliale, ce d'autant que ces tumeurs ne prennent pas nécessairement le contraste. Il est important de préciser à ce propos que la spectroscopie par résonance magnétique du proton des DCF met en évidence des anomalies non spécifiques, parfois proche des lésions tumorales (57).
- Les anomalies de signal de la substance blanche sous-corticale, bien que très sensibles car retrouvées chez tous les patients dont l'IRM est positive, n'ont aucune spécificité et peuvent être rencontrées dans le cadre de lésions tumorales, séquellaires ou simplement d'une leucopathie sous-corticale aspécifique bien que rare chez les sujets jeunes. En revanche, **une anomalie de signal isolée chez un patient ne pourra être considérée comme une DCF2**.
- Le « transmantle sign » a été peu étudié dans la littérature en dehors des DCF2 et de la sclérose tubéreuse de Bourneville (STB) (4). Ses caractéristiques sémiologiques doivent être rigoureusement analysées pour ne pas le confondre avec une dilatation d'un espace de Virchow-Robin sous-cortical qui a également une orientation radiaire mais de signal liquidien.

2.1.3. Optimisation des protocoles d'acquisition et de lecture

A la lumière de nos résultats et des données de littératures, quelques recommandations pratiques peuvent être formulées :

- Les **acquisitions volumiques** sont indispensables aussi bien en T1 qu'en FLAIR afin de limiter les effets de volume partiel et de faciliter la détection des petites anomalies par un reformatage adapté. Une étude récente a ainsi montré la supériorité de l'acquisition FLAIR 3D par rapport au FLAIR 2D, à champ magnétique identique, pour la détection de petites DCF (58).
- La **symétrie** des DCF2 par rapport sillon au fond duquel se situe la lésion invite à les analyser avec des reconstructions multiplanaires suivant l'axe perpendiculaire au cortex dysplasique et passant par le fond du sillon.
- La mise en évidence du «transmantle sign» est améliorée par une **reconstruction MIP** (maximal intensity projetion) à partir d'une séquence 3D FLAIR (données non publiées) (figure 5).

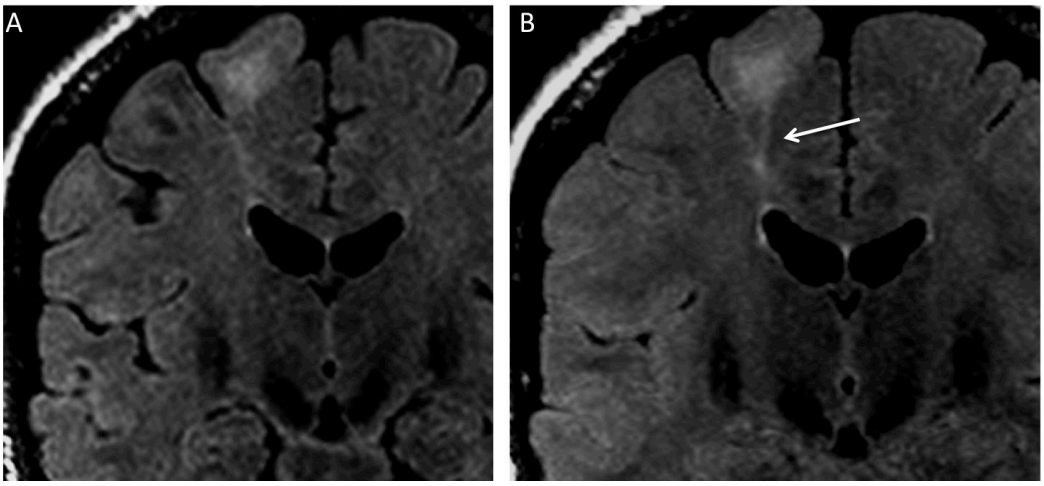

Figure 5 : Intérêt de l'utilisation du MIP pour la détection du Transmantle Sign. Reformatage coronal d'une séquence 3D FLAIR sans (A) puis avec utilisation du MIP (B), chez un patient porteur d'une DCF2 frontale supérieure droite. Le « transmantle sign » (flèche) est mieux visible après application de cet algorithme.

- Un **reformatage 3D de la surface corticale** doit être effectué afin de chercher un motif sulcal anormal et en particulier un PBS en cas de symptômes pointant vers la région centrale

2.2. Choix du champ magnétique

Nous rapportons dans la partie 2 les performances diagnostiques de deux champs magnétiques différents sur une population homogène de 25 patients porteurs de DCF2. Dans cette série, l'augmentation du champ magnétique s'est accompagnée d'une meilleure caractérisation des DCF2 grâce à une meilleure définition du « transmantle sign ». Ce point est d'autant plus intéressant que, comme montré plus haut, ce signe pourrait être considéré comme une signature de la DCF2. Un des points forts de cette étude est que les mêmes patients ont été explorés sur deux aimants du même fabricant (General Electric), en utilisant des antennes et un temps d'acquisition similaire.

L'apport de l'IRM à 3T permet d'obtenir une acquisition avec des voxels millimétriques et isotropes pour des temps d'acquisition similaire à une acquisition 2D à la 1,5T. Cette meilleure résolution spatiale permettant la délimitation et la caractérisation de modifications corticales subtiles, tels que l'aspect « flou » de l'interface gris-blanc. Par ailleurs, la possibilité d'un reformatage multiplanaire est particulièrement utile pour rechercher un épaississement cortical, évitant ainsi l'effet de volume partiel grâce à l'observation de la surface corticale dans un plan non orthogonal mais perpendiculaire au sillon. Néanmoins, les acquisitions 3D T1 à 1,5T ont également une bonne résolution ce qui explique sans doute la faible supériorité du 3T pour ces 2 critères.

En revanche, le résultat le plus marquant de cette étude comparative est l'apport du champ magnétique à 3T pour la détection du « transmantle sign » dont nous avons déjà précisé l'importance en pratique clinique. L'utilisation systématique du FLAIR 3D explique en grande partie la détection accrue du « transmantle sign » à 3T (cf. figure 4). Le reformatage multiplanaire profite principalement à la détection de cet hypersignal T2 linéaire de trajet rarement orthogonal et qui peut donc être négligée sur une acquisition 2D. Sa meilleure visualisation aurait pu résulter tout simplement d'un passage du FLAIR 2D à 1,5T au FLAIR 3D à 3T. Une étude a bien illustré l'avantage de la 3D sur des séquences FLAIR classiques pour la détection et la délimitation des DCF2 chez 9 patients (58). Dans notre étude, néanmoins, quatre patients ont été exploré en FLAIR 3D avec les deux champs magnétiques, avec une meilleure détection du « transmantle sign » à 3T. D'un point de vue pratique, le FLAIR 3D à 1,5T souffre d'un rapport signal-sur-bruit limité, pour la durée d'acquisition compatible avec la pratique clinique (5-6 min).

2.3. Des outils de post-traitement avancé : analyse des sillons

2.3.1. Analyse qualitative

Dans la partie 4, l'étude rétrospective incluant 37 patients consécutifs porteurs de DCF2 situées en région centrale nous a permis, outre la description de variantes anatomiques discutées dans le chapitre précédent, de décrire pour la première fois un nouveau motif sulcal associé aux DCF2 dans cette région. La quasi-absence de ce signe dans le groupe de contrôle lui confère une excellente spécificité. Ce signe, le « power button sign » (PBS), pourrait donc être considéré comme un nouveau critère sémiologique de détection afin d'améliorer la fiabilité diagnostique, en particulier lorsque les autres critères de détection en IRM sont douteux ou font défaut. Nous avons également montré que le PBS pourrait servir de guide vers l'emplacement précis de la lésion. Ainsi, dans la présente étude, la DCF2 a été retrouvé précisément dans la profondeur de la petite branche ascendante du sillon central constituant le PBS chez 60% des patients, en accord avec une étude montrant que les petites dysplasies se situent au fond d'un sillon anormalement profond (42).

2.3.2. Analyse quantitative

Dans la partie 3, l'utilisation d'un outil de labélisation automatique des sillons a permis de confirmer l'existence d'une configuration sulcale anormale chez les patients atteints de DCF2 de la région centrale, en comparaison avec un groupe de témoin. Cette constatation fournit une preuve supplémentaire de l'intérêt d'explorer la configuration des sillons en cas d'épilepsie partielle pharmacorésistante. Par ailleurs, à l'échelle individuelle, plusieurs résultats montrent l'intérêt de cette technique comme aide complémentaire à la détection des DCF2. Premièrement, bien qu'une variabilité de l'énergie sulcale soit également observée chez les témoins, nous avons mis en évidence un lien entre le site de la dysplasie et le z-score de l'énergie du sillon qui lui est associé. Ainsi, la proportion de patients pour lesquels un z-score d'énergie maximale était associé au sillon porteur de la DCF était au-dessus du niveau du hasard. Le fait que ce z-score maximal soit associé à la lésion chez 4 des 11 patients à IRM négatives est un élément prometteur : l'incorporation d'un nouveau critère de localisation en plus des outils actuellement disponibles permettrait ainsi d'augmenter le nombre de candidats à la chirurgie. Ces résultats encouragent la réalisation d'études combinant carte de z-score des énergies sulcales avec d'autres données préopératoires, de manière similaires aux études de détection des DCF en morphométrie basée sur l'analyse voxel par voxel (59).

3. Perspectives

3.1. Séquences IRM : quelles nouveautés ?

3.1.1. Séquences 3D Spin Echo rapide en Double Inversion Récupération (CUBE DIR)

Parmi les signes sémiologiques de détection des DCF2 en IRM, l'hypersignal sous-cortical est le signe le plus sensible. En revanche, l'hypersignal cortical n'est retrouvé que chez la moitié d'entre eux, sans doute en raison de l'hypersignal spontané du cortex résultant de l'absence de neurone myélinisé, qui rend la distinction de cette anomalie plus difficile. Cette difficulté explique l'intérêt pour les séquences accentuant les différences de contraste à l'interface du contraste blanc-gris. C'est le cas par exemple des séquences volumique T2 Double Inversion Récupération (CUBE DIR). La séquence CUBE™ est une séquence 3D Spin Echo rapide qui applique des impulsions radiofréquence de refocalisation, en modulant les angles de bascules. Ce procédé permet d'obtenir des trains d'échos très longs avec un taux d'absorption spécifique réduit. Elle produit des images de tissu cérébral avec une augmentation du rapport signal/bruit sans modulation d'angle de bascule. La Double Inversion Récupération (DIR) consiste en deux impulsions pour supprimer le signal de la substance blanche et du liquide céphalorachidien. **Cette technique permettrait ainsi une meilleure visualisation des anomalies de signal dans la substance grise en atténuant le signal des structures adjacentes**.

Des séquences 3D DIR ont déjà fait l'objet d'études dans la détection de lésions cérébrales, comme la sclérose en plaque (60), mais également dans la maladie épileptique, en particulier pour le dépistage de sclérose de l'hippocampe (61). L'étude des malformations du développement cortical grâce à une séquence similaire, mais en 2D (donc analyse uniquement possible dans un plan), a également fait l'objet d'une étude quantitative voxel par voxel en comparaison avec des témoins, montrant qu'il existait des variations significatives du signal à proximité de lésions corticales subtiles (62).

Une séquence prototype est installée sur l'IRM 3T de notre institution dans le cadre d'une étude prospective (Soins courants – ID RCB : 2013-A00784-41 (D13-P002) – Réf. CPP S.C. 3076 – Investigateur principal : Charles MELLERIO) dont l'objectif principal est de déterminer si la séquence CUBE DIR est plus sensible que les séquences conventionnelles

pour la détection de lésions corticales épileptogènes. En date du 15 Juillet 2014, 5 patients souffrant d'épilepsie pharmacorésistante ont été inclus. Un de ces patients avait une forte suspicion clinique et paraclinique de DCF de la région centrale gauche et une IRM avec séquence conventionnelle normale. La séquence CUBE DIR montrait un hypersignal de l'interface blanc-gris dans la région suspectée (figure 6). Il est intéressant de noter qu'une anomalie sulcale de type PBS était également présente en lieu et place de cet hypersignal précentral.

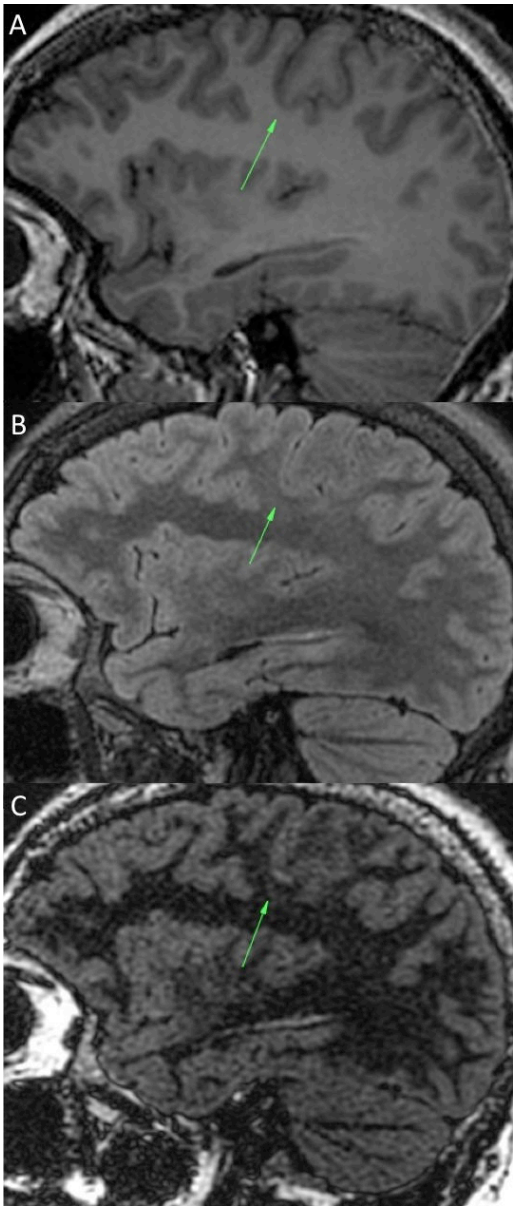

Figure 6a (à gauche) : patient de 26 ans admis dans notre centre pour exploration pré-chirurgicale d'une épilepsie partielle pharmacorésistante de la région centrale gauche. Les reconstructions sagittales passant par le sillon central gauche en 3D FLAIR (A) et 3D T1 (B) ne montrent pas d'anomalie de signal ni de l'interface blanc-gris. La séquence Cube DIR (C) dans la même orientation montre un hypersignal subtil de l'interface blanc-gris d'une branche antérieure du sillon central gauche (flèche).

Figure 6b (ci dessous) : Diagramme de la séquence Cube DIR et méthode de choix du temps d'inversion (TI). (*Remerciements M. Uettwiller*)

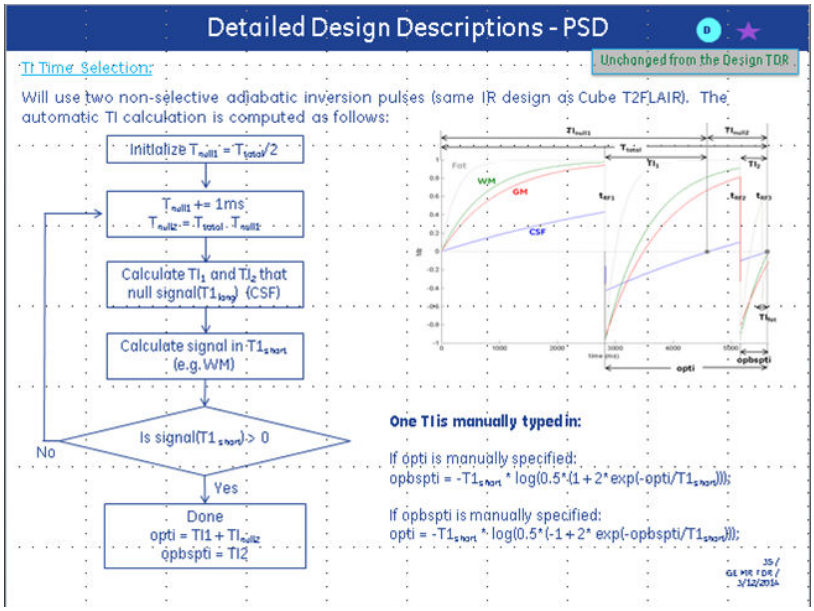

3.1.2. Imagerie par marquage de spin artériel

L'ASL (Arterial Spin Labeling) est une technique non invasive d'imagerie de perfusion en IRM qui permet de produire une carte de flux sanguin cérébral sans injection de produit de contraste. Cette séquence (4-5 minutes) peut s'intégrer dans le protocole d'exploration des EPPR en clinique avec comme principal avantage la possibilité de fusionner facilement ces données paramétriques avec une séquence anatomique acquises dans la même session. Les

données de perfusion ainsi obtenues se rapprochent en théorie de celle obtenues en imagerie nucléaire et en particulier de la scintigraphie (SPECT), et pourrait également fournir des résultats se confondant aux données de l'imagerie métabolique, en particulier du TEP-scanner.

L'imagerie de perfusion permet de latéraliser et, dans certains cas, de localiser le foyer épileptogène. Ainsi dans le cas de malformation du développement cortical, et en particulier celui des DCF, le foyer épileptogène va se manifester par une zone corticale en hypoperfusion en comparaison avec le cortex sain (figure 7). Dans de rares cas, l'imagerie de perfusion peut être acquise au cours d'une crise (état de mal partiel par exemple) et le « foyer » sera en hyperperfusion. Les données provenant de la scintigraphie démontrent que l'imagerie en période ictale est nettement supérieure en terme de fiabilité que l'imagerie interictale seule (63,64) et que cette sensibilité est encore augmentée par le recalage avec l'imagerie anatomique (65). Malheureusement, contrairement à la scintigraphie, l'ASL est une imagerie reflétant l'état de perfusion au moment de l'acquisition des images et ne permet, à l'exception de rares cas, que de fournir des données interictales. Malgré cet obstacle, plusieurs études ont montré l'intérêt de l'ASL en pratique clinique dans la **détection et la localisation du foyer épileptogène dans le cas de DCF2 à IRM négative en montrant un foyer d'hypoperfusion focal** (66,67). Cette séquence IRM est donc très prometteuse dans cette indication.

Depuis 2012, une séquence 3D PC ASL (pseudo-continuous arterial spin labelling) est intégrée à notre protocole d'exploration préopératoire de patients adressés pour EPPR. Notre expérience de cette séquence est cohérente avec les données préliminaires de la littérature citées ci-dessus. Une hypoperfusion superposable aux anomalies de signal en regard des dysplasies corticales focales, mais également d'autres malformations du développement corticales (tumeurs dysembryoplasiques neuroépithéliales en particulier) est habituellement visible. En cas d'acquisition per-ictale, une zone d'hyperperfusion focale correspondant au foyer épileptogène est observée. Plusieurs cas de patients ayant une IRM par ailleurs négative (figure 8) présentant également des anomalies de perfusion focale cohérente avec les données cliniques et électro-cliniques incitant à une étude de sensibilité et spécificité de cette méthode. La technique de référence chez ces patients à IRM négative pourrait être une combinaison de données cliniques, électro-cliniques, métaboliques (TEP-scanner) et chirurgicales (SEEG, données peropératoires).

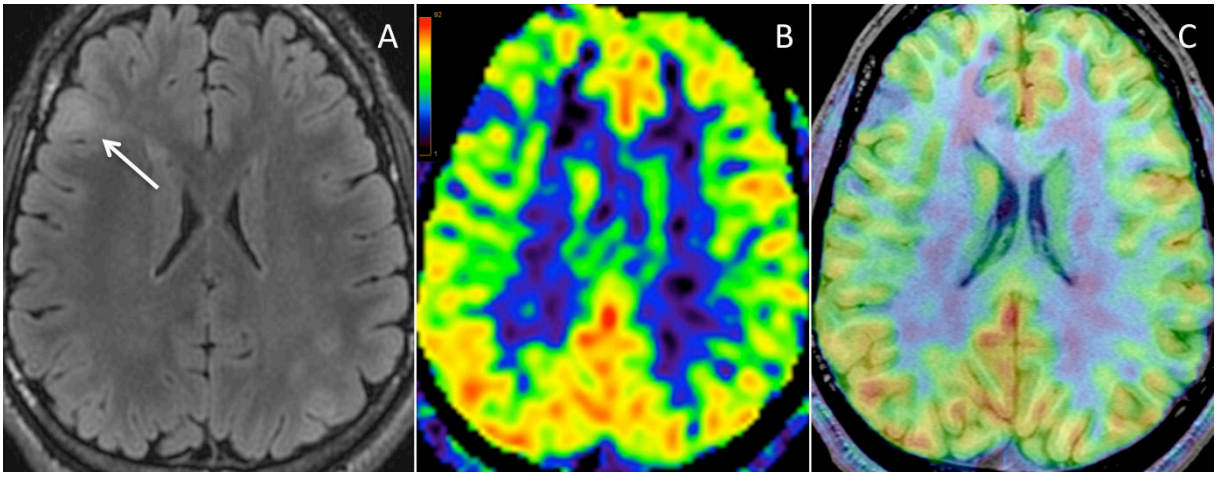

Figure 7 : Imagerie par marquage de spin artériel à 3Tesla : Dysplasie corticale focale fronto-operculaire droite visible sur une coupe axiale FLAIR (A). Cartographie du débit sanguin cérébral (DSC) montrant une baisse du DSC du cortex en regard de la lésion, mieux identifiable sur l'image recalée sur l'anatomie en 3DT1 (C) que sur l'image native (B).

3.1.3. Tenseur de diffusion

Le tenseur de diffusion (DTI) procure une information sur l'amplitude et la direction de la diffusion de l'eau. Le coefficient apparent de diffusion (ADC) traduit l'amplitude moyenne de la diffusion dans un voxel donné. La fraction d'anisotropie (FA), un des index obtenus à partir de l'image en tenseur de diffusion, reflète quant à elle la contrainte directionnelle moyenne des molécules dans un voxel donné. Une FA diminuée correspond à une contrainte directionnelle basse de la diffusion et une FA très élevée correspond théoriquement à une limitation de la diffusion dans une seule direction. Dans la substance blanche, la direction des molécules d'eau est contrainte et déterminée par l'orientation des gaines de myéline et de la membrane cellulaire des axones.

En analysant la contrainte directionnelle de diffusion de voxels adjacents, le trajet des principaux faisceaux de substance blanche peut en être déduit. Il existe ainsi de nombreux algorithmes pour aligner les voxels d'orientation identique. Ainsi une représentation des faisceaux de substance blanche en trois dimensions permet de la subdiviser en régions fonctionnellement pertinentes. Une limitation majeure du DTI est que son hypothèse n'autorise qu'une seule direction de diffusion au sein de chaque voxel et ne tient donc pas compte des croisements de fibres. Des techniques plus récentes telles que l'imagerie de diffusion à haute résolution angulaire (HARDI) et l'imagerie de diffusion spectrale (DSI)

permettent de remédier partiellement à cette limite. Grâce à la robustesse du DSI, de nouveau faisceaux de fibres plus fins ont pu être également identifiés (68).

Dans notre institution, une séquence de tenseur de diffusion est intégrée au protocole d'IRM préopératoire des patients adressés pour EPPR (couplée à l'acquisition des données d'IRM fonctionnelle). En pratique quotidienne, cette séquence permet, en adéquation avec les données de la littérature, de matérialiser le foyer épileptogène au sein de la substance blanche sous corticale en regard et au delà de DCF subtiles (figure 8), procurant un outil de détection en complément du reste bilan (69–73). Un axe de recherche intéressant sur le plan physiopathologique serait de **confirmer l'altération de la connectivité par une chute de l'anisotropie sous jacente aux anomalies sulcales**, comme stipulé dans la discussion des parties 3 et 4. Une analyse du faisceau pyramidal de patients porteurs de DCF2 de la région central associé à un PBS souffrirait d'un facteur confondant. En effet, les éventuelles anomalies en tenseur de diffusion pourraient être imputables à la lésion et non à l'anomalie sulcale elle-même. Une étude préliminaire sur une base de données d'un très grand nombre de témoins (n>200) nous a permis d'identifier un PBS chez environ 1% des sujets sains mais surtout l'existence de formes intermédiaires, plus fréquentes (5% des sujets). Une analyse en tenseur de diffusion à haute résolution angulaire (HARDI) chez ces patients permettrait d'établir un lien entre ces formes frustres d'anomalies sulcales dont on sait qu'elles sont fortement corrélées à une anomalie du développement cortical en pathologie, et une anomalie de connectivité infraclinique. Pour explorer ces anomalies subtiles, un modèle plus précis que le tenseur de diffusion serait utile. En particulier, l'obtention d'une cartographie de la fonction de distribution des orientations (ODF) par une méthode de calcul analytique individuel de type Q-ball (74) permettrait de rendre compte d'anomalies structurelles. Ces thématiques ont déjà fait l'objet de réunions scientifiques et pourraient s'effectuer dans le cadre d'une collaboration avec l'équipe du Pr. JF Mangin (Neurospin – CEA) et l'ingénieur de recherche travaillant dans notre institution, Pauline Roca.

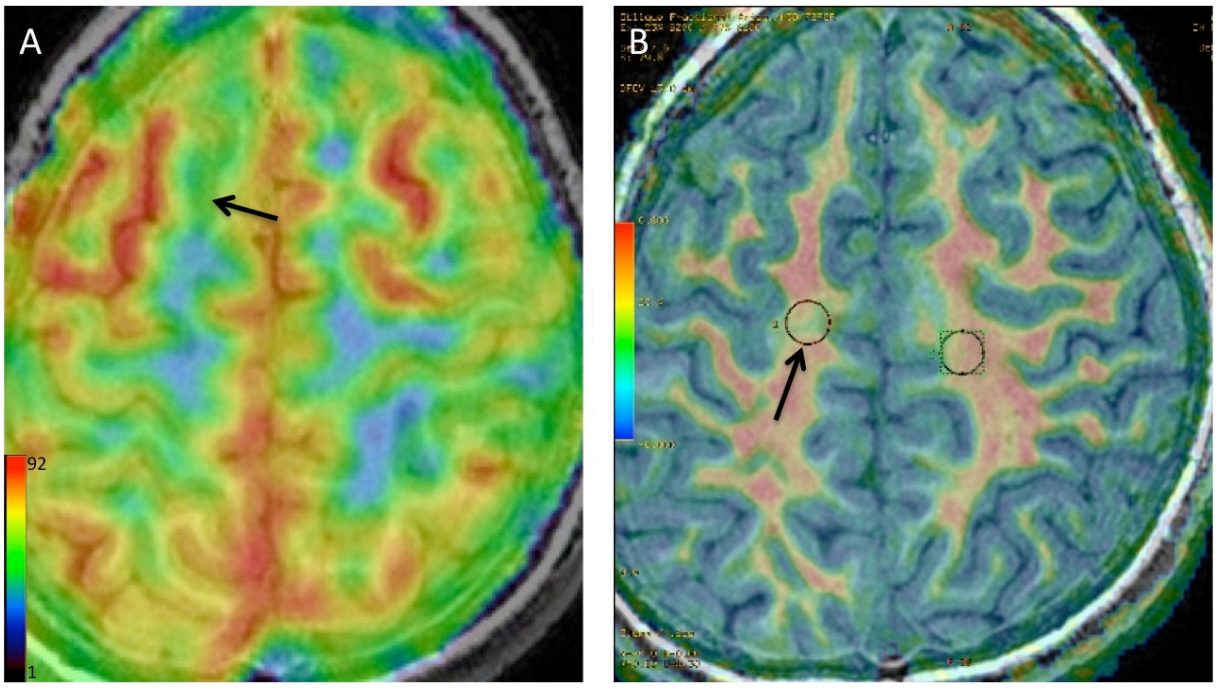

Figure 8 : Intérêt de 2 techniques avancées complémentaires en pratique clinique pour l'évaluation d'épilepsie réfractaire cryptogénique. L'ASL procure une information du débit sanguin du cortex tandis que le DTI est une imagerie de la substance blanche sous corticale. Patient de 24 ans porteur d'une DCF2 frontale supérieure droite invisible sur les séquences conventionnelles en IRM. (A) Cartographie du débit sanguin cérébral en ASL recalée sur la séquence anatomique 3D T1 montrant une hypoperfusion du sillon porteur de la dysplasie (flèche). (B) Cartographie de FA en DTI recalé sur l'anatomie montrant une chute focale de la FA de la substance blanche sous-corticale en regard de la lésion, en comparaison avec le côté sain (chute de 40%).

3.2. Champ magnétique à 1,5T, à 3T : peut-on aller plus loin ?

Nous avons montré dans la partie 2 de notre étude que la transition 1,5 vers 3T, même si elle permet une meilleur caractérisation des DCF2 en particulier par une meilleure définition du « transmantle sign », ne s'accompagne pas d'un taux de détection idéal avec toujours un haut pourcentage d'IRM négatives. Dans la littérature, l'expérience de la 7 Tesla a également montré que la montée en puissance du champ améliore considérablement le rapport signal-sur-bruit et la résolution avec une plus petite taille de voxel (de l'ordre du dixième de millimètre) avec une meilleure délimitation et caractérisation des DCF et autres malformations du développement cortical (75). Les premières images à 7 Tesla disponibles (figure 9) dans la littérature confirment en particulier sur des séquences volumiques T2 Echo

de gradient rapide à faible angle de bascule (FLASH) la très haute résolution et l'obtention d'un contraste cortico-sous-corticale permettant de se rapprocher de la structure corticale, qui pourrait s'avérer utile dans la détection et la caractérisation des DCF subtiles.

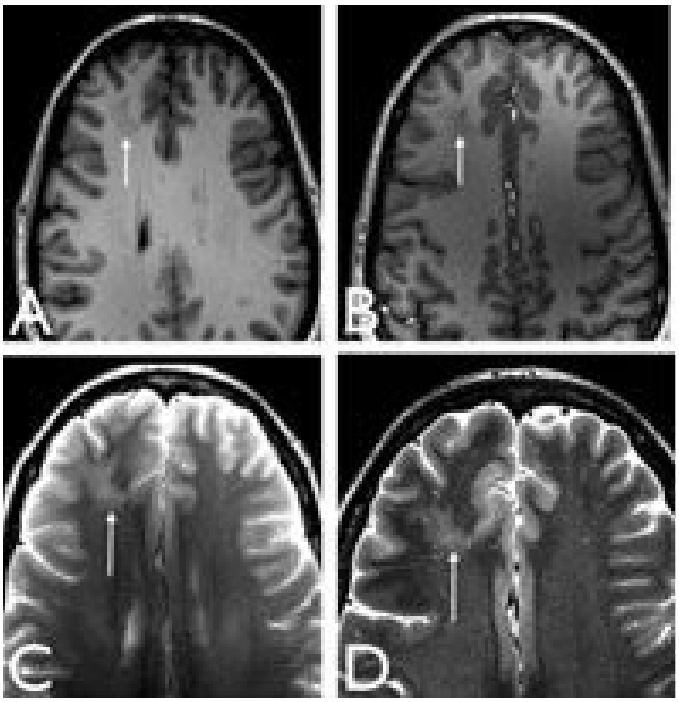

D'après Madan et al. - Epilepsia 2009

Figure 9 : imagerie à 3T (A et C) et à 7T (B et D) respectivement en 3DT1 et Axial T2 spin echo chez un patient épileptique. Même si la dysplasie corticale focale (flèche) est visible aussi bien à 3T qu'à 7T, il est à espérer que l'amélioration de la résolution spatiale et en contraste permettra dans le futur de mieux détecter les petites lésions subtiles.

Néanmoins, le réglage des paramètres d'acquisition et le développement de séquences adaptées seront indispensables en raison de l'importante hétérogénéité du champ magnétique et de la non uniformité des angles de bascule qui sont un problème à 3T et le seront d'autant plus à 7T.

3.3. Vers une imagerie combinée : le TEP-IRM

La tomographie par émission de positrons (TEP) tient une place prépondérante dans l'évaluation pré-chirurgicale de l'épilepsie réfractaire, et ce depuis de nombreuses années (11). L'hypométabolisme cortical inter-critique après injection de ^{18}fluoro-désoxyglucose (FDG) permet de localiser un foyer épileptogène. Toutefois, en raison de la faible résolution spatiale de cette modalité d'imagerie, la TEP-FDG en elle-même n'est pas suffisamment précise pour localiser le foyer épileptogène. Plusieurs études récentes (8,76,77) ont démontré que le recalage ou la fusion de la cartographie du métabolisme cérébral acquis en TEP avec l'IRM

structurelle améliore nettement l'identification des DCF. Le bénéfice attribuable à la TEP en pratique quotidienne est capital en particulier chez les patients dont l'IRM conventionnelle est négative, et permet d'identifier la lésion causale, de guider le geste chirurgical, et d'améliorer le pronostic postopératoire, en évitant, le cas échéant, le recours aux techniques invasives d'exploration en Stéréo-EEG (11). La sensibilité et la spécificité de la TEP-FDG peuvent encore renforcées en pratique clinique dans la population des patients à IRM négative par l'utilisation d'outils d'analyse basés sur le voxel, tels que SPM (statistical parametric mapping), afin de détecter de manière objective les anomalies de métabolisme liés à la lésion en comparaison avec une population témoin (13). Enfin le couplage de cet outil avec les données d'autre techniques non invasives tel que la magnétoencéphalographie (MEG) permet encore l'amélioration de sa fiabilité, en particulier dans les cas litigieux (14).

L'acquisition simultanée des données métaboliques en TEP et des données structurelles de l'IRM dans un système couplé TEP-IRM, permet non seulement **d'améliorer le recalage** (78), mais fournit d'autres atouts permettant de faire bénéficier des avantages d'une technique pour palier les imprécisions de l'autre et inversement. Par exemple, la meilleure correction de mouvement en IRM peut être utilisée pour déterminer celle nécessaire à une amélioration de la précision des données en TEP. Ce procédé serait particulièrement utile pour la population pédiatrique pour laquelle le risque d'artéfacts de mouvements nécessite fréquemment l'usage de sédation. En outre, il devient possible **d'obtenir des informations multimodales** pour l'analyse de processus physiologiques en combinant par exemple l'ASL, la spectroscopie par résonance magnétique, ou l'imagerie fonctionnelle BOLD (blood oxygenation level dependant) avec la fixation de traceurs en TEP (79). Une des limites de cette technique est la nécessité d'estimer une carte d'atténuation des données brutes de la TEP, habituellement fournie automatiquement par les données du scanner lors d'acquisition en TEP-scanner. Des méthodes alternatives d'algorithmes utilisant les données de l'IRM sont néanmoins développées pour pallier cet écueil avec des résultats prometteurs (80).

Peu d'études ont analysé à ce jour la fiabilité de l'exploration simultanée en TEP-IRM pour la détection et la caractérisation de lésions épileptogènes (81). Son intérêt dans l'analyse des DCF2 semble néanmoins évident compte-tenu de la place actuelle du TEP-scanner. L'acquisition prochaine d'appareil de TEP-IRM en Ile-de-France (Neurospin – CEA ; Créteil) laisse envisager la possibilité de collaborations sur notre thématique.

3.4. Evaluation préopératoire du risque chirurgical : intérêt de l'IRM fonctionnelle d'activation

Un des enjeux de la chirurgie des DCF est la résolution d'un compromis entre l'exérèse complète de la lésion, qui est associé à un pronostique postopératoire favorable (3,7,26,82), et l'absence de déficit iatrogène si la zone de cortectomie implique une zone fonctionnelle adjacente. Ce risque est important dans la mesure où les DCF impliquent systématiquement le cortex et que leur localisation en zone fonctionnelle et en particulier à proximité du cortex sensori-moteur est fréquente, comme nous l'avons vu tout au cours de ce travail. L'IRM fonctionnelle (IRMf) d'activation reposant sur l'effet BOLD (blood oxygenation level dependent) est une technique de cartographie fonctionnelle non invasive qui s'est largement développée dans la planification préopératoire de patients atteints d'une lésion cérébrale (15) et est maintenant recommandée avant l'exérèse des tumeurs gliales situées en zone éloquente (83). Dans cette indication, l'IRMf s'est révélée être très sensible à l'identification du cortex moteur primaire (84,85). Peu d'études se sont intéressées à l'apport de l'IRMf dans le cadre des malformations du développement cortical et en particulier des DCF. Ces études portent pour la plupart sur une faible cohorte de groupes hétérogènes de patients, mêlant différentes étiologies de lésions épileptogènes (86–89). Néanmoins, elles concordent sur un **lien entre la précocité de l'atteinte au cours de la maturation corticale et le degré de réorganisation fonctionnelle**. Ainsi, des lésions intervenant tardivement pendant la période fœtale, comme la polymicrogyrie, s'accompagnent habituellement d'une activation fonctionnelle au sein du cortex lésionnel. Inversement, les atteintes des phases précoces comme la phase prolifération ne s'accompagnent pas de réponse fonctionnelle dans la lésion, témoignant d'un certain degré de réorganisation fonctionnelle. Ainsi, Janszky et al. n'a retrouvé d'activation fonctionnelle lors de tâches de motricité que chez 1 sur 7 patients porteurs de DCF2, tandis que des réponses étaient visualisées en zone lésionnelle chez 10 des 11 patients souffrant de polymicrogyrie ou de schizencéphalie (87).

Dans notre institution, 25 patients ont été adressés pour une IRMf motrice dans le bilan préopératoire d'une DCF2 de la région centrale. Tous ces patients ont été opérés et 6 d'entre eux ont également été explorés en IRMf à distance du geste chirurgical. A partir des données cliniques et neuropsychologiques pré- et postopératoires, et des données des sites de stimulation électrique peropératoire du cortex comparées aux données d'IRM fonctionnelles, nous tentons d'explorer ce degré de plasticité du cortex sensori-moteur en présence d'une

DCF de la région centrale (Travail en cours. Thèse de médecine de Volodia Dangouloff ; co-encadrement Catherine Oppenheim et Charles Mellerio). Nous tâcherons en outre de réaliser un classement de la réorganisation fonctionnelle, si présente, de type intra-gyral, intra-hémisphérique ou inter-hémisphérique. L'absence d'activation au sein de la lésion sur l'IRMf préopératoire, le haut degré de réorganisation, ainsi que l'absence de modification des réponses postopératoires permettraient de confirmer que le tissu dysplasique en région centrale n'a pas de fonction, et donc d'élargir les indications opératoires (figure 10). Enfin, les données de l'IRMf postopératoire par une technique de recalage anatomique et la comparaison avec le score clinique à long terme nous permettront également de valider cette technique comme outil pronostique de prédiction du déficit postopératoire.

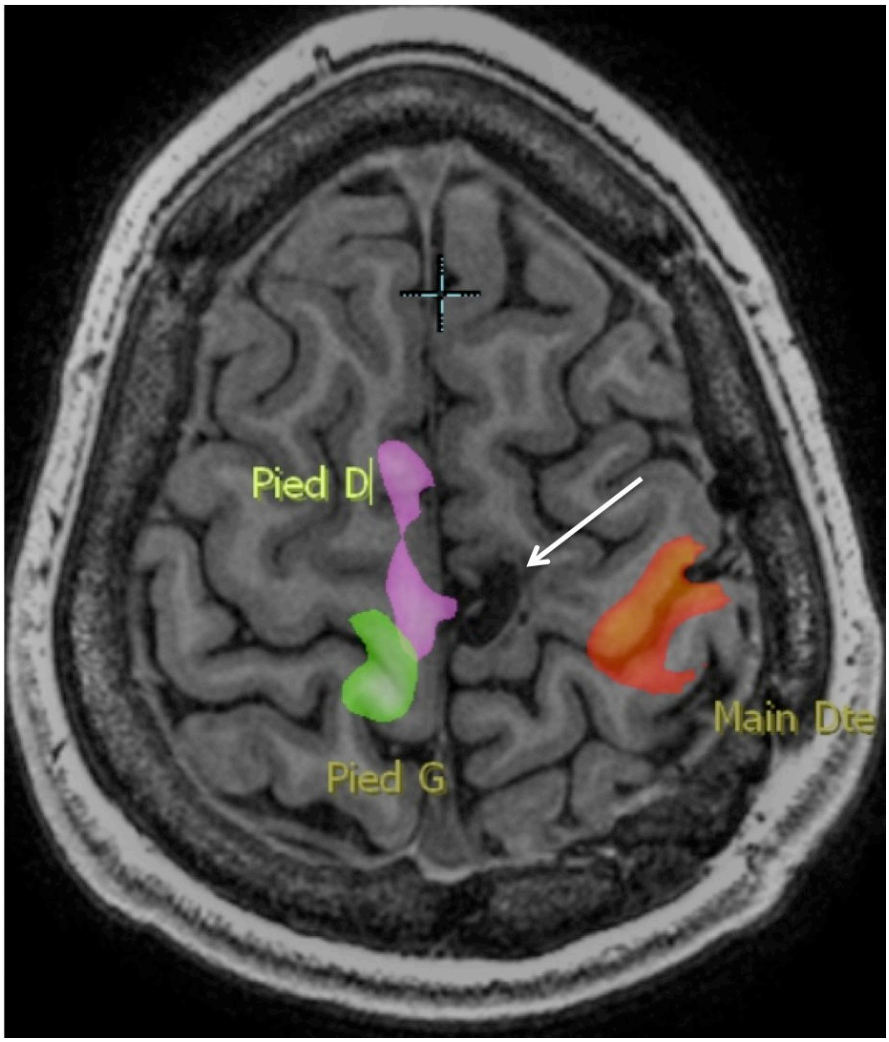

Figure 10 : Réorganisation fonctionnelle en zone motrice chez un patient de 17 ans présentant de crises partielles motrices depuis l'âge de 4 ans ayant fait découvrir une DCF2 à IRM normale du lobule para-central gauche (flèche), opérée avec disparition des crises en postopératoire. L'IRM fonctionnelle post opératoire objective une réorganisation fonctionnelle de type inter-hémisphérique. Des réponses sont observées en

situation anatomique lors des mouvements de la main droite (en rouge) et du pied gauche (en vert), à distance de la lésion. En revanche, lors des mouvements du pied droit (en violet), les réponses attendues en situation lobulaire para-centrale gauche en regard de la lésion sont en fait observées de manière controlatérale avec une activation du lobule para-central droit et de l'AMS droite.

Bibliographie

1. Banerjee PN, Filippi D, Allen Hauser W. The descriptive epidemiology of epilepsy—a review. Epilepsy Res. 2009;85(1):31-45.

2. Devaux B, Chassoux F, Guenot M, Haegelen C, Bartolomei F, Rougier A, et al. La chirurgie de l'épilepsie en France: Évaluation de l'activité. Neurochirurgie. 2008;54(3):453-65.

3. Lerner JT, Salamon N, Hauptman JS, Velasco TR, Hemb M, Wu JY, et al. Assessment and surgical outcomes for mild type I and severe type II cortical dysplasia: a critical review and the UCLA experience. Epilepsia. 2009;50(6):1310-35.

4. Tassi L, Colombo N, Garbelli R, Francione S, Russo GL, Mai R, et al. Focal cortical dysplasia: neuropathological subtypes, EEG, neuroimaging and surgical outcome. Brain. 2002;125(8):1719-32.

5. Krsek P, Maton B, Korman B, Pacheco-Jacome E, Jayakar P, Dunoyer C, et al. Different features of histopathological subtypes of pediatric focal cortical dysplasia. Ann Neurol. juin 2008;63(6):758-769.

6. Jeha LE, Najm I, Bingaman W. Surgical outcome and prognostic factors of frontal lobe epilepsy surgery. Brain; 2007.

7. Urbach H, Scheffler B, Heinrichsmeier T, Von Oertzen J, Kral T, Wellmer J, et al. Focal Cortical Dysplasia of Taylor's Balloon Cell Type: A Clinicopathological Entity with Characteristic Neuroimaging and Histopathological Features, and Favorable Postsurgical Outcome. Epilepsia. 2002;43(1):33-40.

8. Salamon N, Kung J, Shaw SJ, Koo J, Koh S, Wu JY, et al. FDG-PET/MRI coregistration improves detection of cortical dysplasia in patients with epilepsy. Neurology. 2008;71(20):1594-601.

9. Widdess-Walsh P, Diehl B, Najm I. Neuroimaging of Focal Cortical Dysplasia. J Neuroimaging. 2006;16(3):185-96.

10. Widdess-Walsh P, Kellinghaus C, Jeha L. Electro-clinical and imaging characteristics of focal cortical dysplasia: correlation with pathological subtypes. Epilepsy Res. 2005.

11. Chassoux F, Rodrigo S, Semah F, Beuvon F, Landre E, Devaux B, et al. FDG-PET improves surgical outcome in negative MRI Taylor-type focal cortical dysplasias. Neurology. 2010;75(24):2168-75.

12. Conférence de Consensus. Prise en charge de l'Epilepsie Partielle Pharmaco Résistante. ANAES; 2004.

13. Kumar A, Juhász C, Asano E, Sood S, Muzik O, Chugani HT. Objective detection of epileptic foci by 18F-FDG PET in children undergoing epilepsy surgery. J Nucl Med. 2010;51(12):1901-7.

14. Widjaja E, Shammas A, Vali R, Otsubo H, Ochi A, Snead OC, et al. FDG-PET and magnetoencephalography in presurgical workup of children with localization-related nonlesional epilepsy. Epilepsia. 2013;54(4):691-9.

15. Matthews PM, Honey GD, Bullmore ET. Applications of fMRI in translational medicine and clinical practice. Nat Rev Neurosci. 2006;7(9):732-44.

16. De Vanssay-Maigne A, Noulhiane M, Devauchelle AD, Rodrigo S, Baudoin-Chial S, Meder JF, et al. Modulation of encoding and retrieval by recollection and familiarity: mapping the medial temporal lobe networks. Neuroimage. 2011;58(4):1131-8.

17. Chamberlain WA, Cohen ML, Gyure KA. Interobserver and intraobserver reproducibility in focal cortical dysplasia (malformations of cortical development). Epilepsia; 2009. 50–12 p.

18. Barkovich AJ, Guerrini R, Kuzniecky RI, Jackson GD, Dobyns WB. A developmental and genetic classification for malformations of cortical development: update 2012. Brain J Neurol. mai 2012;135(Pt 5):1348-1369.

19. Blümcke I, Thom M, Aronica E, Armstrong DD, Vinters HV, Palmini A, et al. The clinicopathologic spectrum of focal cortical dysplasias: A consensus classification proposed by an ad hoc Task Force of the ILAE Diagnostic Methods Commission1. Epilepsia. 2011;52(1):158-74.

20. Palmini A, Najm I, Avanzini G, Babb T, Guerrini R, Foldvary-Schaefer N, et al. Terminology and classification of the cortical dysplasias. Neurology. 2004;62(6 suppl 3):S2-S8.

21. Coras R, de Boer OJ, Armstrong D, Becker A, Jacques TS, Miyata H, et al. Good interobserver and intraobserver agreement in the evaluation of the new ILAE classification of focal cortical dysplasias. Epilepsia. 2012;53(8):1341-8.

22. Kim DW, Lee SK, Chu K, Park KI, Lee SY, Lee CH, et al. Predictors of surgical outcome and pathologic considerations in focal cortical dysplasia. Neurology. 2009;72(3):211-6.

23. Taylor DC, Falconer MA, Bruton CJ, Corsellis JAN. Focal dysplasia of the cerebral

cortex in epilepsy. J Neurol Neurosurg Psychiatry. 1971;34(4):369-87.

24. Barkovich AJ, Kuzniecky RI, Jackson GD. Classification system for malformations of cortical development: update. 2001.

25. Sisodiya SM. Malformations of cortical development: burdens and insights from important causes of human epilepsy. Lancet Neurol; 2004.

26. Chassoux F, Devaux B, Landré E, Turak B, Nataf F, Varlet P, et al. Stereoelectroencephalography in focal cortical dysplasia A 3D approach to delineating the dysplastic cortex. Brain. 2000;123(8):1733-51.

27. Palmini A, Gambardella A, Andermann F, Dubeau F, da Costa JC, Olivier A, et al. Intrinsic epileptogenicity of human dysplastic cortex as suggested by corticography and surgical results. Ann Neurol. avr 1995;37(4):476-487.

28. Yeung RS, Xiao G-H, Everitt JI, Jin F, Walker CL. Allelic loss at the tuberous sclerosis 2 locus in spontaneous tumors in the Eker rat. Mol Carcinog. 1 sept 1995;14(1):28-36.

29. Yeung RS, Katsetos CD, Klein-Szanto A. Subependymal astrocytic hamartomas in the Eker rat model of tuberous sclerosis. Am J Pathol. 1997;151(5):1477.

30. Chae T, Kwon YT, Bronson R, Dikkes P, Li E, Tsai L-H. Mice lacking p35, a neuronal specific activator of Cdk5, display cortical lamination defects, seizures, and adult lethality. Neuron. 1997;18(1):29-42.

31. Tschuluun N, Wenzel JH, Katleba K, Schwartzkroin PA. Initiation and spread of epileptiform discharges in the methylazoxymethanol acetate rat model of cortical dysplasia: functional and structural connectivity between CA1 heterotopia and hippocampus/neocortex. Neuroscience. 2005;133(1):327-42.

32. Schwartzkroin PA, Wenzel HJ. Are developmental dysplastic lesions epileptogenic? Epilepsia. 2012;53(s1):35-44.

33. Boonyapisit K, Najm I, Klem G, Ying Z, Burrier C, LaPresto E, et al. Epileptogenicity of focal malformations due to abnormal cortical development: direct electrocorticographic–histopathologic correlations. Epilepsia. 2003;44(1):69-76.

34. André VM, Cepeda C, Vinters HV, Mathern GW, Levine MS. Interneurons, GABA currents, and subunit composition of the GABAA receptor in type I and type II cortical dysplasia. Epilepsia. 2010;51(s3):166-70.

35. Calcagnotto ME, Paredes MF, Tihan T, Barbaro NM, Baraban SC. Dysfunction of synaptic inhibition in epilepsy associated with focal cortical dysplasia. J Neurosci.

2005;25(42):9649-57.

36. Cepeda C, André VM, Wu N, Yamazaki I, Uzgil B, Vinters HV, et al. Immature neurons and GABA networks may contribute to epileptogenesis in pediatric cortical dysplasia. Epilepsia. 2007;48(s5):79-85.

37. Wagner J, Urbach H, Niehusmann P, von Lehe M, Elger CE, Wellmer J. Focal cortical dysplasia type IIb: completeness of cortical, not subcortical, resection is necessary for seizure freedom. Epilepsia. 2011;52(8):1418-24.

38. Barkovich AJ, Kuzniecky RI, Bollen AW, Grant PE. Focal transmantle dysplasia: A specific malformation of cortical development. Neurology. 10 janv 1997;49(4):1148-1152.

39. Bronen RA, Vives KP, Kim JH. Focal cortical dysplasia of Taylor, balloon cell subtype: MR differentiation from low-grade tumors. AJNR Am J Neuroradiol. 1997;

40. Colombo N, Salamon N, Raybaud C. Imaging of malformations of cortical development. Epileptic Disord. 2009. 11–3 p.

41. Lasjaunias P, Manelfe C, Terbrugge K. Endovascular treatment of cerebral arteriovenous malformations.

42. Besson P, Andermann F, Dubeau F, Bernasconi A. Small focal cortical dysplasia lesions are located at the bottom of a deep sulcus. Brain J Neurol. déc 2008;131(Pt 12):3246-3255.

43. Widjaja E, Otsubo H, Raybaud C, Ochi A, Chan D, Rutka JT, et al. Characteristics of MEG and MRI between Taylor's focal cortical dysplasia (type II) and other cortical dysplasia: surgical outcome after complete resection of MEG spike source and MR lesion in pediatric cortical dysplasia. Epilepsy Res. 2008;82(2):147-55.

44. Colombo N, Tassi L, Deleo F, Citterio A, Bramerio M, Mai R, et al. Focal cortical dysplasia type IIa and IIb: MRI aspects in 118 cases proven by histopathology. Neuroradiology. 1 oct 2012;54(10):1065-1077.

45. Wang DD, Deans AE, Barkovich AJ, Tihan T, Barbaro NM, Garcia PA, et al. Transmantle sign in focal cortical dysplasia: a unique radiological entity with excellent prognosis for seizure control: Clinical article. J Neurosurg. févr 2013;118(2):337-344.

46. Ono 45. Atlas of the cerebral sulci. Editions Thieme; 1990.

47. Cykowski MD, Coulon O, Kochunov PV, Amunts K, Lancaster JL, Laird AR, et al. The Central Sulcus: an Observer-Independent Characterization of Sulcal Landmarks and Depth Asymmetry. Cereb Cortex. 10 déc 2007;18(9):1999-2009.

48. Hamasaki T, Imamura J, Kawai H, Kuratsu J. A three-dimensional MRI study of

variations in central sulcus location in 40 normal subjects. J Clin Neurosci. 2012;19(1):115-20.

49. Hayashi N, Sakuta K, Minehiro K, Takanaga M, Sanada S, Suzuki M, et al. Development of identification of the central sulcus in brain magnetic resonance imaging. Radiol Phys Technol. 29 sept 2010;4(1):53-60.

50. Mirjalili SA, Hale SJM, Stringer MD, Wilson B. The surface anatomy of the central sulcus. J Clin Neurosci. oct 2012;19(10):1467.

51. Yousry TA, Schmid UD, Alkadhi H, Schmidt D, Peraud A, Buettner A, et al. Localization of the motor hand area to a knob on the precentral gyrus. A new landmark. Brain J Neurol. janv 1997;120 (Pt 1):141-157.

52. Van Essen DC. A tension-based theory of morphogenesis and compact wiring in the central nervous system. Nature. 23 janv 1997;385(6614):313-318.

53. Toro R, Burnod Y. A morphogenetic model for the development of cortical convolutions. Cereb Cortex. 2005;15(12):1900-13.

54. Lefèvre J, Mangin J-F. A reaction-diffusion model of human brain development. PLoS Comput Biol. 2010;6(4):e1000749.

55. Rakic P. Specification of cerebral cortical areas. Science. 8 juill 1988;241(4862):170-176.

56. Winston GP, Micallef C, Symms MR, Alexander DC, Duncan JS, Zhang H. Advanced diffusion imaging sequences could aid assessing patients with focal cortical dysplasia and epilepsy. Epilepsy Res [Internet]. nov 2013 [cité 17 déc 2013]; Disponible sur: http://linkinghub.elsevier.com/retrieve/pii/S092012111300288X

57. Leite CC, Lucato LT, Sato JR, Valente KD, Otaduy MCG. Multivoxel proton MR spectroscopy in malformations of cortical development. Am J Neuroradiol. 2007;28(6):1071-5.

58. Saini J, Singh A, Kesavadas C, Thomas B, Rathore C, Bahuleyan B, et al. Role of three-dimensional fluid-attenuated inversion recovery (3D FLAIR) and proton density magnetic resonance imaging for the detection and evaluation of lesion extent of focal cortical dysplasia in patients with refractory epilepsy. Acta Radiol. 2010;51(2):218-25.

59. Hong S-J, Kim H, Schrader D, Bernasconi N, Bernhardt BC, Bernasconi A. Automated detection of cortical dysplasia type II in MRI-negative epilepsy. Neurology. 1 juill 2014;83(1):48-55.

60. Geurts JJG, Roosendaal SD, Calabrese M, Ciccarelli O, Agosta F, Chard DT, et al.

Consensus recommendations for MS cortical lesion scoring using double inversion recovery MRI. Neurology. 2011;76(5):418-24.

61. Li Q, Zhang Q, Sun H, Zhang Y, Bai R. Double inversion recovery magnetic resonance imaging at 3 T: diagnostic value in hippocampal sclerosis. J Comput Assist Tomogr. 2011;35(2):290-3.

62. Rugg-Gunn FJ, Boulby PA, Symms MR, Barker GJ, Duncan JS. Imaging the neocortex in epilepsy with double inversion recovery imaging. Neuroimage. 2006;31(1):39-50.

63. Kim JT, Bai SJ, Choi KO, Lee YJ, Park H-J, Kim DS, et al. Comparison of various imaging modalities in localization of epileptogenic lesion using epilepsy surgery outcome in pediatric patients. Seizure. 2009;18(7):504-10.

64. Ho SS, Berkovic SF, Berlangieri SU, Newton MR, Egan GF, Tochon-Danguy HJ, et al. Comparison of ictal SPECT and interictal PET in the presurgical evaluation of temporal lobe epilepsy. Ann Neurol. juin 1995;37(6):738-745.

65. Matsuda H, Matsuda K, Nakamura F, Kameyama S, Masuda H, Otsuki T, et al. Contribution of subtraction ictal SPECT coregistered to MRI to epilepsy surgery: a multicenter study. Ann Nucl Med. 2009;23(3):283-91.

66. Storti SF, Galazzo IB, Del Felice A, Pizzini FB, Arcaro C, Formaggio E, et al. Combining ESI, ASL and PET for quantitative assessment of drug-resistant focal epilepsy. NeuroImage [Internet]. 2013 [cité 25 sept 2013]; Disponible sur: http://www.sciencedirect.com/science/article/pii/S1053811913006654

67. Pendse N, Wissmeyer M, Altrichter S, Vargas M, Delavelle J, Viallon M, et al. Interictal arterial spin-labeling MRI perfusion in intractable epilepsy. J Neuroradiol J Neuroradiol. mars 2010;37(1):60-63.

68. Hagmann P, Jonasson L, Maeder P, Thiran J-P, Wedeen VJ, Meuli R. Understanding Diffusion MR Imaging Techniques: From Scalar Diffusion-weighted Imaging to Diffusion Tensor Imaging and Beyond 1. Radiographics. 2006;26(suppl_1):S205-S223.

69. Lee S-K, Kim DI, Mori S, Kim J, Kim HD, Heo K, et al. Diffusion tensor MRI visualizes decreased subcortical fiber connectivity in focal cortical dysplasia. Neuroimage. 2004;22(4):1826-9.

70. Widjaja E, Zarei Mahmoodabadi S, Otsubo H, Snead OC, Holowka S, Bells S, et al. Subcortical Alterations in Tissue Microstructure Adjacent to Focal Cortical Dysplasia: Detection at Diffusion-Tensor MR Imaging by Using Magnetoencephalographic Dipole

Cluster Localization 1. Radiology. 2009;251(1):206-15.

71. Eriksson Sh, Rugg-Gunn FJ, Symms MR, Barker GJ, Duncan JS. Diffusion tensor imaging in patients with epilepsy and malformations of cortical development. Brain. 2001;124(3):617-26.

72. Gross DW, Bastos A, Beaulieu C. Diffusion tensor imaging abnormalities in focal cortical dysplasia. Can J Neurol Sci. 2005;32(4):477-82.

73. De la Roque AD, Oppenheim C, Chassoux F, Rodrigo S, Beuvon F, Daumas-Duport C, et al. Diffusion tensor imaging of partial intractable epilepsy. Eur Radiol. 2005;15(2):279-85.

74. Descoteaux M, Angelino E, Fitzgibbons S, Deriche R. Regularized, fast, and robust analytical Q-ball imaging. Magn Reson Med. 2007;58(3):497-510.

75. Madan N, Grant PE. New directions in clinical imaging of cortical dysplasias. Epilepsia. 2009;50(s9):9-18.

76. Chandra PS, Salamon N, Huang J, Wu JY, Koh S, Vinters HV, et al. FDG-PET/MRI Coregistration and Diffusion-Tensor Imaging Distinguish Epileptogenic Tubers and Cortex in Patients with Tuberous Sclerosis Complex: A Preliminary Report. Epilepsia. 2006;47(9):1543-9.

77. Rastogi S, Lee C, Salamon N. Neuroimaging in Pediatric Epilepsy: A Multimodality Approach 1. Radiographics. 2008;28(4):1079-95.

78. Schlemmer H-PW, Pichler BJ, Schmand M, Burbar Z, Michel C, Ladebeck R, et al. Simultaneous MR/PET imaging of the human brain: feasibility study 1. Radiology. 2008;248(3):1028-35.

79. Pichler BJ, Judenhofer MS, Pfannenberg C. Multimodal imaging approaches: Pet/ct and pet/mri. Molecular Imaging I [Internet]. Springer; 2008 [cité 15 juill 2014]. p. 109-32. Disponible sur: http://link.springer.com/chapter/10.1007/978-3-540-72718-7_6

80. Hofmann M, Pichler B, Schölkopf B, Beyer T. Towards quantitative PET/MRI: a review of MR-based attenuation correction techniques. Eur J Nucl Med Mol Imaging. 1 mars 2009;36(1):93-104.

81. Garibotto V, Heinzer S, Vulliemoz S, Guignard R, Wissmeyer M, Seeck M, et al. Clinical Applications of Hybrid PET/MRI in Neuroimaging: Clin Nucl Med. janv 2013;38(1):e13-e18.

82. Fauser S, Bast T, Altenmüller D-M, Schulte-Mönting J, Strobl K, Steinhoff BJ, et al. Factors influencing surgical outcome in patients with focal cortical dysplasia. J Neurol

Neurosurg Psychiatry. 1 janv 2008;79(1):103-105.

83. Soffietti R, Baumert BG, Bello L, Von Deimling A, Duffau H, Frénay M, et al. Guidelines on management of low-grade gliomas: report of an EFNS–EANO* Task Force. Eur J Neurol. 2010;17(9):1124-33.

84. Bizzi A, Blasi V, Falini A, Ferroli P, Cadioli M, Danesi U, et al. Presurgical Functional MR Imaging of Language and Motor Functions: Validation with Intraoperative Electrocortical Mapping 1. Radiology. 2008;248(2):579-89.

85. Lehéricy S, Duffau H, Cornu P, Capelle L, Pidoux B, Carpentier A, et al. Correspondence between functional magnetic resonance imaging somatotopy and individual brain anatomy of the central region: comparison with intraoperative stimulation in patients with brain tumors. J Neurosurg. 2000;92(4):589-98.

86. Vitali P, Minati L, D'Incerti L, Maccagnano E, Mavilio N, Capello D, et al. Functional MRI in Malformations of Cortical Development: Activation of Dysplastic Tissue and Functional Reorganization. J Neuroimaging. juill 2008;18(3):296-305.

87. Janszky J, Ebner A, Kruse B, Mertens M, Jokeit H, Seitz RJ, et al. Functional organization of the brain with malformations of cortical development. Ann Neurol. juin 2003;53(6):759-767.

88. Chang BS, Walsh CA. Mapping form and function in the human brain: the emerging field of functional neuroimaging in cortical malformations. Epilepsy Behav. déc 2003;4(6):618-625.

89. Marusic P, Najm IM, Ying Z, Prayson R, Rona S, Nair D, et al. Focal Cortical Dysplasias in Eloquent Cortex: Functional Characteristics and Correlation with MRI and Histopathologic Changes. Epilepsia. 1 janv 2002;43(1):27-32.

Annexes 1 : Article publié de l'étude n°1

Published May 3, 2012 as 10.3174/ajnr.A3081

ORIGINAL RESEARCH

Optimizing MR Imaging Detection of Type 2 Focal Cortical Dysplasia: Best Criteria for Clinical Practice

C. Mellerio
M.-A. Labeyrie
F. Chassoux
C. Daumas-Duport
E. Landre
B. Turak
F.-X. Roux
J.-F. Meder
B. Devaux
C. Oppenheim

BACKGROUND AND PURPOSE: Type 2 FCD is one of the main causes of drug-resistant partial epilepsy. Its detection by MR imaging has greatly improved surgical outcomes, but it often remains overlooked. Our objective was to determine the prevalence of typical MR imaging criteria for type 2 FCD, to provide a precise MR imaging pattern, and to optimize its detection.

MATERIALS AND METHODS: We retrospectively reviewed 1.5T MR imaging of 71 consecutive patients with histologically proved type 2 FCD. The protocol included millimetric 3D T1-weighted, 2D coronal and axial T2-weighted, and 2D or 3D FLAIR images. Two experienced neuroradiologists looked for 6 criteria: cortex thickening, cortical and subcortical signal changes, blurring of the GWM interface, the "transmantle" sign, and gyral abnormalities. The frequency of each sign and their combination were assessed. We compared the delay between epilepsy onset and surgery, taking into account the time of type 2 FCD detection by MR imaging.

RESULTS: Only 42 patients (59%) had positive MR imaging findings. In this group, a combination of at least 3 criteria was always found. Subcortical signal changes were constant. Three characteristic signs (cortical thickening, GWM blurring, and transmantle sign) were combined in 64% of patients, indicating that MR imaging can be highly suggestive. However, typical features of type 2 FCD were overlooked on initial imaging in 40% of patients, contributing to a delay in referral for surgical consideration (17 versus 11.5 years when initial MR imaging findings were positive).

CONCLUSIONS: A combination of 3 major MR imaging signs allows type 2 FCD to be recognized in clinical practice, thereby enabling early identification of candidates for surgery.

ABBREVIATIONS: EEG = electroencephalography; ^{18}FDG = fluorine 18 FDG; GWM = gray-white matter; type 2 FCD = type 2 focal cortical dysplasia

BRAIN

ORIGINAL RESEARCH

Type 2 FCD is one of the main causes of extratemporal drug-resistant partial epilepsy that is surgically curable. It corresponds to Taylor-type focal cortical dysplasia, according to recent classifications,[1,2] a more homogeneous pathologic entity than other subtypes of cortical dysplasia, especially type 1 FCD. The major predictor of a favorable surgical outcome is complete removal of the dysplastic cortex,[3-7] and accurate presurgical assessment of the lesion extent is crucial to improve surgical results. During the past decade, the development of MR imaging protocols specifically designed for type 2 FCD detection has contributed to the steady increase of candidates for surgery and to a favorable outcome, with a remission rate of up to 90% when MR imaging findings are positive compared with 40%–60% when MR imaging findings are negative.[3,6-9] The MR imaging diagnosis remains difficult, however, even in specialized centers by using appropriate protocols, with up to 50% of type 2 FCD cases remaining undetected or being diagnosed late, thereby depriving patients of effective treatment for years.[3] Despite severe and intractable epilepsy, the average time from onset of seizures to surgery is around 14 years in most reported series.[3,10-12]

Typical MR imaging features have previously been described.[3,6,7,13-21] These include abnormalities of the cortex (thickening, T2 signal increase, gyral abnormalities) and of the subcortical white matter (blurring of the GWM interface, T2 signal increase, "transmantle" sign). Initial MR imaging descriptions relied on a limited sample of patients.[7,15] However, more recent larger series do not provide a comprehensive analysis of all reported MR imaging signs and the prevalence of each sign varies considerably between studies (Table 1). In addition, the proportion of negative MR imaging findings in type 2 FCD differs widely, likely because of differences in imaging protocols and selection bias.

We performed a retrospective study on a large cohort of surgically treated patients with type 2 FCD investigated with high-resolution MR imaging during the past decade. Our goal was to determine the prevalence of each previously described MR imaging criterion for type 2 FCD and to define a precise MR imaging pattern so as to optimize its detection in clinical practice. Our second goal was to determine the influence of MR imaging positivity on delay to surgical referral.

Materials and Methods

Patients

We retrospectively reviewed the MR imaging data of 71 consecutive patients (40 males, 24 children) with a histologic diagnosis of type 2 FCD who underwent surgery for intractable epilepsy between May

Received December 18, 2011; accepted after revision January 25, 2012.

From the Departments of Neuroimaging (C.M., M.-A.L., J.-F.M., C.O.), Neurosurgery (F.C., E.L., B.T., F.-X.R., B.D.), and Neuropathology (C.D.-D.), Centre Hospitalier Sainte-Anne, Paris, France; and Université Paris Descartes (C.M., M.-A.L., F.C., J.-F.M., C.O.), Paris, France.

Please address correspondence to Charles Mellerio, MD, Service d'Imagerie Morphologique et Fonctionnelle, Centre Hospitalier Sainte-Anne, 1 rue Cabanis 75014-Paris; e-mail: c.mellerio@ch-sainte-anne.fr

http://dx.doi.org/10.3174/ajnr.A3081

Table 1: Frequency of typical MR imaging signs of histologically proved type 2 FCD reported in the literature

	Urbach et al, 2002[7]	Colombo et al, 2003[15]	Widdess-Walsh et al, 2005[14]	Besson et al, 2008[26]	Widjaja et al, 2008[28]	Kim et al, 2009[4]	Krsek et al, 2009[6]	Lerner et al, 2009[3]	This Study
Period of study	1996–2000	1996–2000	1990–2002	NA	1991–2005	1995–2005	2002–2005	2000–2007	2000–2011
No. of patients	22	15	48	26	13	28	16	64	71
Negative findings on MRI	0	5 (33%)	10 (21%)	0	2 (15%)	6 (21%)	0	1	29 (41%)
Cortical thickening	18 (81%)	10 (67%)	NA	NA	8 (61%)	NA	8 (50%)	43 (67%)	30 (71%)
Blurring of GWM junction	8 (36%)	13 (87%)	NA	NA	11 (84%)	NA	11 (69%)	47 (73%)	38 (90%)
Cortical signal changes	NA	6 (40%)	NA	NA	2 (15%)	NA	10 (62%)	22 (35%)	21 (50%)
Subcortical signal changes	22 (100%)	13 (87%)	27 (56%)	NA	11 (84%)	NA	14 (87%)	64 (100%)	42 (100%)
Transmantle sign	18 (81%)	3 (20%)	NA	5 (19%)	8 (72%)	NA	6 (37%)	NA	35 (83%)
Sulcal abnormalities	NA	NA	NA	NA	3 (23%)	NA	11 (69%)	NA	22 (52%)
Atrophy	NA	3 (20%)	NA	NA	2 (15%)	NA	7 (44%)	11 (17%)	0

Note:—NA indicates not available.

2000 and May 2011. Presurgical evaluation included ictal video-EEG, high-resolution MR imaging, functional MR imaging, and ^{18}FDG-PET scans for all patients and stereo-EEG for 43 of them (60%). Median age was 6 years (range, 1–20 years) at epilepsy onset and 20 years (range, 8–52 years) at surgery. No patient had clinical criteria for tuberous sclerosis. The study was approved by the Ethics Committee of Ile de France III and was found to conform to generally accepted scientific principles and ethical standards.

MR Imaging Acquisition

Brain MRI was performed on a 1.5T MR imaging scanner (Signa Excite; GE Healthcare, Milwaukee, Wisconsin) and included the following sequences: a volumetric gradient-echo T1-weighted inversion recovery acquisition (section thickness = 1.2 mm, FOV = 240 × 240 mm, 256 × 192 matrix, NEX = 1), coronal and axial 2D fast spin-echo T2-weighted acquisitions (thickness = 4 mm, no gap, FOV = 240 × 240 mm, 512 × 256 matrix, NEX = 2), FLAIR by using 2D contiguous sections (thickness = 5 mm, FOV = 240 × 240 mm, matrix = 256 × 192, NEX = 1), or a 3D acquisition (section thickness = 1.2 mm, FOV = 240 × 240 mm, 256 × 226 matrix, NEX = 1). A 3D T1 fast gradient-echo acquisition after injection of gadolinium was also performed; this was not part of the epilepsy presurgical standard protocol but was needed for accurate identification of vascular landmarks with neuronavigational guidance during intracranial recordings or surgery.

Data Analysis

Two neuroradiologists (7 and 9 years' experience), aware of the final localization of the operated lesion, retrospectively reviewed all MRI in consensus to look for structural abnormalities. They analyzed 6 criteria: 1) abnormal cortical thickness, defined as a thickening (or thinning) of at least 50% of the normal cortex, visible on T1WI and T2WI sequences, on at least 2 orthogonal planes, to rule out partial volume effects (when visible on 1 sequence only, it was defined as a "pseudothickening"); 2) abnormal cortical signal intensity on T1WI, T2WI, and/or FLAIR, defined as signal changes involving the entire thickness of the cortex; 3) blurring of the GWM junction, visible on at least 1 sequence and in 2 orthogonal planes; and 4) abnormal signal intensity of subcortical white matter relative to normal cortex (this latter abnormality was further classified as either "marked," when the subcortical white matter signal was at least identical to that of the normal cortex, or "subtle " otherwise (Fig 1); 5) abnormal signal intensity of deep white matter, the so-called transmantle sign, defined as a subcortical white matter signal-intensity change, tapering toward the ventricle on T1WI and/or T2WI (Fig 1);[22] and 6) a major abnormality of sulcal morphology, defined as an abnormality of the depth, angulation, or shape of a sulcus, compared with the contralateral side, on reformatted 3D T1WI or on T2WI sequences.

The presence of calcifications, cysts, contrast enhancement, atrophy or mass effect, and vascular abnormalities was also recorded. MR imaging was considered negative for the diagnosis of type 2 FCD when none of the above abnormalities were present and positive when at least 1 of the 6 MR imaging criteria was present. In addition, we looked for minor sulcal abnormalities in patients with negative MR imaging finding (ie, unusual sulci patterns not discernible enough to be classified as major). Because these findings were regarded as nonspecific or doubtful, MR imaging findings were still considered negative.

To determine the influence of MR imaging positivity on referring the patient for a presurgical work-up, we compared the time from epilepsy onset to surgery between the groups with positive and negative MR imaging findings by using a Wilcoxon test. In addition, in the subgroup of patients with positive MR imaging findings, we reviewed all previous MRI with negative findings available in the medical records to retrospectively detect the lesion and compared the time from epilepsy onset to surgery with that of patients whose first MR imaging findings were considered positive, by using a Wilcoxon test.

Results

Among the 71 patients, type 2 FCD was located in the frontal lobe ($n = 60$, including 28 in the central region limited by the pre- and postcentral sulci and 3 in the insula); parietal lobe ($n = 7$); occipital lobe ($n = 2$); or temporal ($n = 2$) lobe. All lesions were limited to a single lobe and were unilateral, with a right/left hemisphere ratio of 1:3. Histologic confirmation of type 2 FCD was based on a focal disorganization of the cortical cytoarchitecture with giant dysmorphic neurons. Balloon cells were present in 63 patients (type 2b FCD) and were not found in the cortical specimen in the remaining patients (type 2a FCD).

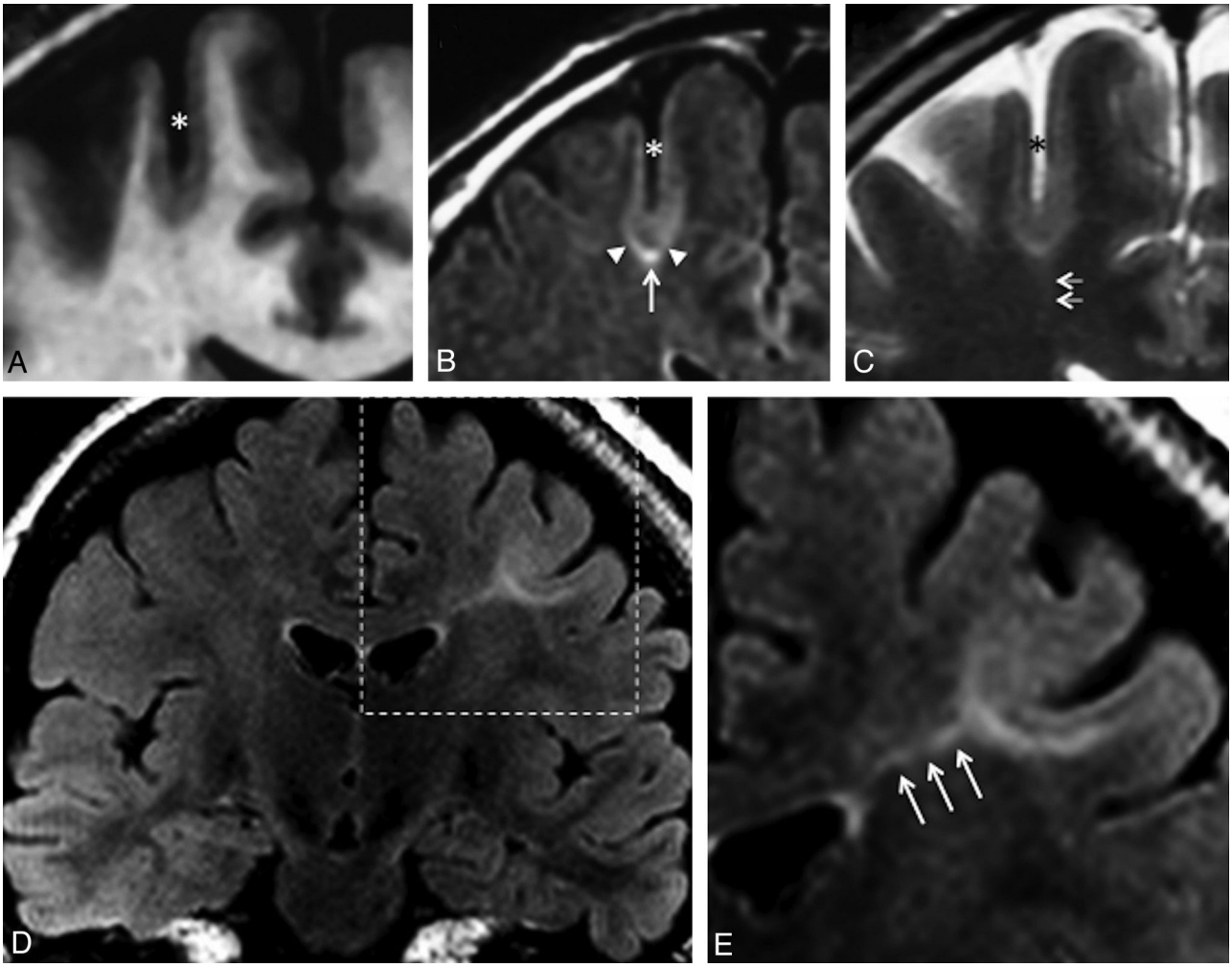

Fig 1. Typical MR imaging signs of type 2 FCD. Coronal 3D T1WI (*A*), coronal FLAIR (*B*), and coronal T2WI (*C*) in a 45-year-old man with left motor seizures, epilepsy onset at 6 years, and findings on several previous MR images considered normal. An unusually deep and straight sulcus in the precentral region (*asterisk*), with minimal cortical thickening at the bottom of the sulcus, and cortical signal increase in T2WI and FLAIR. Abnormal subcortical signal, marked at the bottom (*arrow*), surrounded by an area of subtle signal increase (*arrowheads*), responsible for a gradient of signal abnormalities from the periphery to the center of the dysplasia. Barely perceptible transmantle sign (*C*, *double arrows*). Coronal FLAIR (*D*) and magnification (*E*) of the left central region in a 19-year-old woman with right motor seizure, epilepsy onset at 16 years of age. These MR images show a marked increased signal, tapering gradually from the gray-white matter interface to the superolateral edge of the lateral ventricle (*triple arrows*), typical of a transmantle sign.

Positive Findings on MR Imaging

Forty-two patients (59%) had positive MR imaging findings. Twelve patients (29%) had all 6 criteria. All patients had at least 3 of the 6 criteria. All patients had either cortical thickening, blurring of GWM interface, or transmantle sign; 27 patients (64%) had all 3 of these signs.

Cortical thickening was present in 30 patients (71% of positive MR imaging findings), did not exceed twice the normal cortex, and was limited to a small cortical area. Seven other patients (17%) had "pseudothickening," visible on only 1 of the sequences. This "pseudothickening" was related to signal changes of the subcortical white matter (Fig 2).

Cortical signal changes were present in 21 patients (50% of MR imaging with positive findings). These consisted of hyperintensity on T2WI in 15 patients (best seen on FLAIR sequences), hyperintensity on T1WI in 2 patients, and increased signal on both sequences in the remaining 4 patients. These were located at the bottom of the dysplastic sulcus, variably spreading to the surrounding gyri.

Blurring of the GWM interface was present in 38 patients (90% those with positive MR imaging findings). It was colocated with cortical thickening, when present, in all patients except 1. As with cortical thickening, this sign could be obvious on 1 sequence and barely visible on others (Fig 2).

Abnormal signal intensity of subcortical white matter was seen in all patients with positive MR imaging findings. It was "marked" in 31 patients (73%). "Subtle" changes were not visible on T1WI. Most interesting, in 13 of the 31 patients with marked subcortical increased signal, this abnormality extended from the depth of the sulcus to the surrounding white matter, with a symmetric gradual centrifugal signal decrease (Fig 1).

The transmantle sign was present in 35 patients (83% of MR imaging with positive findings) and was typically mildly hyperintense on T2WI and FLAIR and hypointense in T1WI. It spread along the axis of the abnormal sulcus, running perpendicular toward the wall of the lateral ventricle (Fig 1). Its thickness was proportional to the width of the subcortical abnormalities.

Major sulcal abnormalities were present in 22 patients (52% of those with positive MR imaging findings). These con-

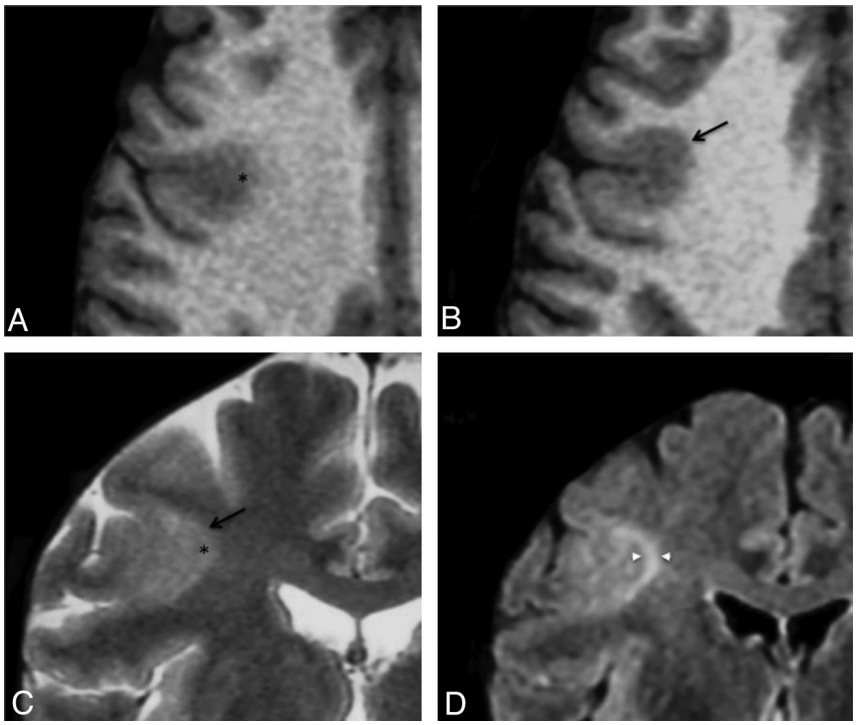

Fig 2. Cortical pseudothickening. Axial T1WI (*A* and *B*) and coronal T2WI (*C*) in a 29-year-old man with left motor seizures, onset at 3 years of age. These images show cortical thickening (*arrow*) and blurring (*asterisk*) of the gray-white matter interface of the right central sulcus. *D*, Coronal FLAIR image allowing cortical to be distinguished from subcortical signal increase (*arrowheads*).

sisted of sulci that were unusually deep ($n = 15$), wide ($n = 5$), and/or with unusual angulation ($n = 11$) (Fig 1). Such sulcal abnormalities were never isolated but were associated with other typical type 2 FCD features.

Microcalcifications were observed in the periventricular region in a patient with a large dysplasia in the temporal lobe. A developmental venous abnormality adjacent to a frontal dysplasia was seen in another patient. A small (<10 mm) cystic component was present in 3 patients. Parenchymal contrast enhancement, focal atrophy or mass effect, complete disappearance of the GWM interface, or marked thinning of the cortex was never observed.

Among the 42 patients with positive MR imaging findings, 16 had at least 1 brain MR imaging finding that had been considered normal during the course of epilepsy. In all 16 cases, the lesion was retrospectively visible. The delay from epilepsy onset to surgery was >5 years longer in patients with negative initial MR imaging (median, 17 years; range, 6–42 years) than in those whose first MR imaging findings were positive (11.5 years; range, 1–29 years), though not reaching significance due to the small number of patients ($P = .06$).

Negative Findings on MR Imaging

Twenty-nine patients (41%) had negative MR imaging findings (Fig 3), despite histologic confirmation of type 2 FCD (Table 2). For these patients, FDG-PET findings were positive in 25 (86%) cases, showing a focal or regional hypometabolism, contributing to the detection of the lesion. In addition, intracranial recording by using depth electrodes (stereo-EEG) was used to determine the epileptogenic zone and the extent of the cortical resection. In 4 patients, intracranial recording was deemed not necessary because PET demonstrated a focal hypometabolism corresponding to a single gyrus, highly suggestive of a focal lesion.

Moreover, in 13 cases of negative MR imaging findings, minor sulcal abnormalities were observed in the vicinity of type 2 FCD (Fig 4), sometimes not strictly co-localized with the dysplastic lesion. As with major sulcal abnormalities, minor features corresponded to the unusual depth, width, or shape of the sulcus but were not clear enough to be considered abnormal. In addition, none of the other criteria suggestive of type 2 FCD were found in these cases, in contrast to the major sulcal abnormalities described in cases with positive MR imaging findings, which were never isolated (Fig 1).

Balloon cells were present in 79% of the cases with negative MR imaging findings and with similar proportion in patients with minor sulcal abnormalities (10 of 13) than in those with strictly normal MR imaging findings (13 of 16).

The delay from epilepsy onset to surgery was shorter in the patients with negative MR imaging findings (median, 11.5 years; range, 1–31 years) than in the group with positive MR imaging findings (16 years; range, 1–42 years) ($P = .03$). This apparently surprising finding is related to a bias of recruitment, with a high proportion of children with negative MR imaging findings and short epilepsy duration due to special collaboration with pediatric teams and systematic use of FDG-PET in this population.

Discussion

The main findings of this systematic qualitative MR imaging analysis in a series of 71 consecutive patients with histologically confirmed type 2 FCD are as follows: 1) Only 59% had positive MR imaging findings despite optimal MR imaging techniques according to recommended guidelines;[23] 2) all pa-

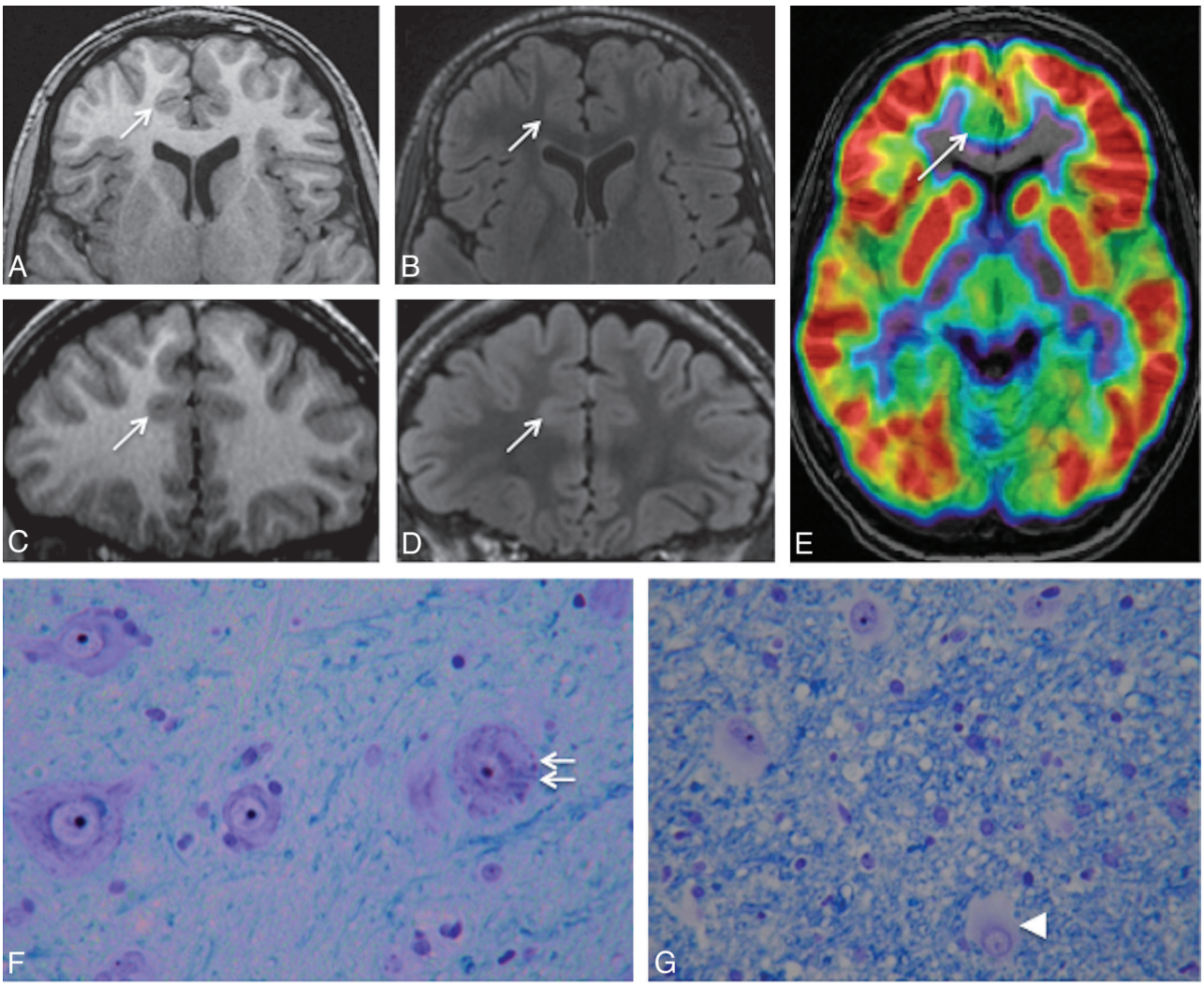

Fig 3. Negative MR imaging findings. Axial and coronal 3D T1WI (*A* and *C*) and axial and coronal 3D FLAIR (*B* and D) in a 15-year-old boy with right frontal lobe epilepsy, nocturnal seizure predominance, and onset at 12 years. Absence of the 6 criteria and no minor sulcal abnormality were found. *E*, ^{18}FDG-PET coregistered on MR imaging (axial section) allows recognition of a gyral hypometabolism corresponding to the anterior part of the right cingulate cortex (*arrow*). *F* and *G*, Histology slides show typical features of type 2b FCD with giant dysmorphic neurons in the cortex (*double arrow*) and balloon cells in the underlying white matter (*arrowhead*) (Klüver-Barrera, original magnification ×40).

Table 2: Clinical and histologic data of patients with positive and negative findings on MRI

	Negative MRI Findings	Positive MRI Findings	Total
No. of patients	29	42	71
Sex ratio (M/F)	0.8	1.8	1.3
Age at onset (yr) (median) (range)	6 (1–20)	5.8 (1–20)	6 (1–20)
Age at surgery (yr) (median) (range)	17 (8–41)	22.5 (8–52)	20 (8–52)
Location of FCD			
Left/right ratio	1.4	1.25	1.35
Frontal lobe	23	37	60
Parietal lobe	4	3	7
Temporal lobe	1	1	2
Occipital lobe	1	1	2
Type 2 FCD subtypes			
Type 2a (no balloon cells)	6	2	8
Type 2b (balloon cells)	23	40	63

tients with positive MR imaging findings presented with least 3 of the 6 recognized MR imaging criteria for type 2 FCD, with combined cortical thickening, blurring of the GWM interface, and the transmantle sign in 64% of patients; and 3) MR imaging features suggestive of type 2 FCD were overlooked on initial imaging in 40% of the cases, leading to late referral for surgical consideration.

Cortical thickening and blurring of the GWM demarcation are considered to be major signs, corresponding to the presence of dysmorphic neurons and balloon cells in the cortex and GWM junction, ectopic neurons, or axonal loss in white matter.[7,8,14,15] We additionally found subtle pseudothickening (ie, a subtle subcortical signal increase similar to that of the cortex) in a few patients, contrasting with the extensive thickening reported in previous studies.[3,7,11,15] The subtlety of this sign is in line with histologic data showing that cortical thickening is more focal and less obvious than previously described.[24,25] Cortical thickening has been the focus of an expert consensus, stipulating that it must be seen in 2 adjacent

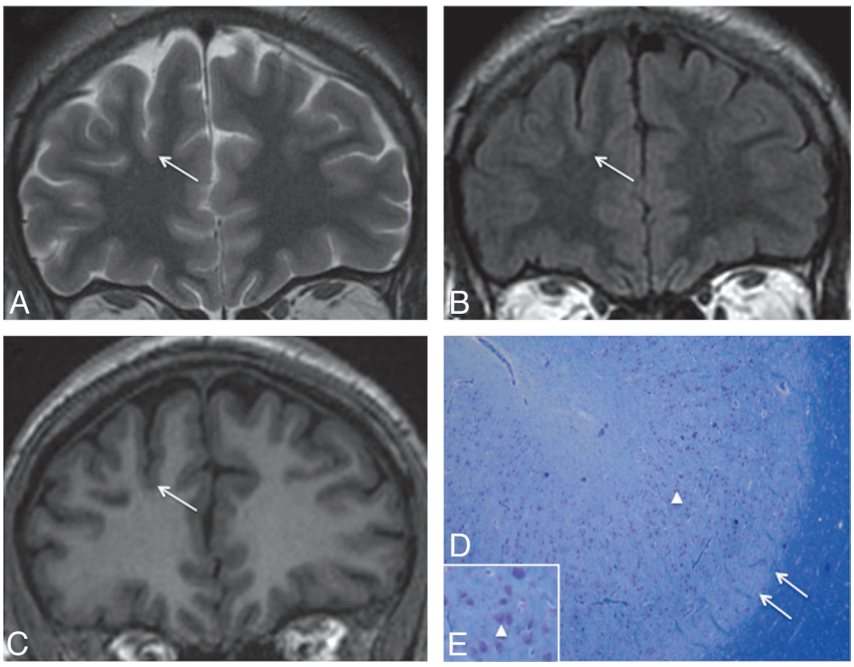

Fig 4. Negative MR imaging findings with minor sulcal abnormalities. Coronal T2WI (*A*), FLAIR (*B*), and T1WI (*C*) in a 36-year-old man with right nocturnal frontal lobe epilepsy, onset at 20 years of age. None of the 6 criteria were found. A minor sulcal abnormality is perceptible in the right superior frontal area, with an unusually large and deep sulcus (*arrow*). *D* and *E*, Cortical specimen. Deep part of the pathologic sulcus with typical type 2a FCD features: cortical disorganization and the presence of giant neurons (*arrowhead*) without balloon cells. Note that the good delineation of the gray-white matter interface (*double arrow*) is correlated with the absence of blurring on MR imaging (Klüver-Barrera, original magnification ×5 [*D*]; ×15 [*E*]).

sections and with 2 different pulse weightings, to avoid being confounded with pseudothickening.[25] We did not observe any sign of lobar, gyral, or focal cortical atrophy, in contrast to others who reported atrophy in 15%–44% of cases (Table 1). This subtle and subjective sign, more common in type 1 focal cortical dysplasia,[6] may have been underestimated in our analysis. It is also possible that what we considered a deep dysplastic sulcus was interpreted by others as pseudofocal atrophy.[26] We never observed any major cortical thinning as encountered in ischemic or traumatic sequelae.

The third major sign consisted of subcortical white matter abnormalities, which were found in all patients with positive MR imaging findings. This is likely due to the clear-cut signal changes on T2WI or FLAIR. Contrary to the authors of a previous report,[16] we found no correlation between the presence of balloon cells and subcortical signal abnormalities (Table 2).

The signal increase of the cortex is a well-known sign of type 2 FCD, though rarely emphasized.[3,14] It was found in 48% of patients with positive MR imaging findings, within the 15%–62% range of previous reports (Table 1).[3,6,13,15] It was often moderate and was more clearly seen on FLAIR sequences. This abnormality could be related to a high attenuation of balloon cells in the cortex.[14] With the increased use of 3D FLAIR and high-field MR imaging, this sign may, in the future, be easier to detect and become more reliable.

The transmantle sign is reported to be a specific feature for malformations of cortical development.[22] This typical pattern overlaps the path of migrating neuroblasts, consistent with a disruption of early corticogenesis. It has been related to the presence of balloon cells and hypomyelination in the white matter underlying the dysplastic lesion.[7,22] This sign may also occur in other developmental abnormalities, such as venous or arteriovenous malformations[27] and, when isolated, is not specific for type 2 FCD. However, its association with cortical thickening and GWM blurring provides the most reliable pattern for the diagnosis of type 2 FCD. We observed the transmantle sign in >80% of patients with positive MR imaging findings, which is a higher proportion than that reported in even the most recent studies. In 2 recent studies, the frequency of the transmantle sign reached 60%,[7,28] whereas its frequency did not exceed 30% in other studies, suggesting that it may have been underestimated in earlier reports.[6,7,13,15,26]

Abnormalities of sulcal morphology were present in nearly one-half of the cases with positive MR imaging findings. Such features are difficult to assess and are likely underestimated. Isolated minor sulcal abnormalities may also be retrospectively found in cortical areas containing a small type 2 FCD, as observed in nearly half of the cases with negative MR imaging findings (Fig 4). Sulcal abnormalities have already been described[29] but have received little attention, and their prevalence has never been evaluated. Only 1 study[26] confirmed by quantitative analysis that small type 2 FCDs were preferentially located at the bottom of an abnormally deep sulcus. Their physiologic mechanisms have not been elucidated to date. Nevertheless, most malformations of cortical development are associated with abnormal gyral/sulcal morphology, suggesting that the organization of sulci is intimately linked to the early stages of cortical development.[30]

Another striking finding in this study is that abnormalities were arranged symmetrically relative to an axis perpendicular to the cortex. Of note, the axis of symmetry overlapped the trajectory of the transmantle sign. In addition, in half of the cases, a gradient of decreasing abnormal signal intensity from the bottom of the dysplastic sulcus to the surrounding gyri was found (Fig 1). This finding confirms that irrespective of the size of the lesion, maximum cellular abnormalities are located deep in the sulcus.

The proportion of patients with type 2 FCD with negative MR imaging findings (41%) was higher than that in most reported series [3,6-8,13-15,26] but similar to the rate reported using stereo-EEG as a diagnostic tool.[31] This is likely explained by the fact that in our patients with negative MR imaging findings, surgery was based on a combination of FDG-PET and stereo-EEG. Balloon cells were found in the cortical specimens

of 79% of our patients with negative MR imaging findings (Table 2), in contrast to previous reports suggesting that balloon cell FCDs (type 2b) are generally characterized by signal changes in the white matter.[16]

Finally, the localization of type 2 FCD was overwhelmingly frontal and rarely temporal in our series, as in others,[8,14,15] whereas other epileptogenic lesions are predominantly located in the temporal lobe. This suggests that frontal drug-resistant partial epilepsy with normal MR imaging findings should raise the suspicion of type 2 FCD, and this is supported by surgical series of cryptogenic partial epilepsy, in which up to 40% of the resected cortical specimens (especially in the frontal lobe) corresponded to type 2 FCD at histology.[9,31,32] Moreover, a recent report of the International League against Epilepsy noted that none of the children with epilepsy diagnosed with tumor or ischemia had normal MR imaging findings.[11]

Our study has some limitations. It was retrospective and was based solely on patients who underwent surgery and thus does not represent the entire spectrum of type 2 FCD. Nevertheless, the study of unoperated patients would be limited by the lack of histologic confirmation. Furthermore, due to the lack of a control group, we cannot assess the specificity of the MR imaging abnormalities, especially the transmantle sign. In addition, positive MR imaging findings (59% of our patients) were based on conventional visual analysis. Voxel-based postprocessing methods proved a significant benefit in comparison with visual analysis alone[33,34] and would possibly decrease our rate of negative MR imaging findings. However, these techniques apply algorithms not applicable in routine practice. Furthermore, the feature maps direct the attention to suspicious regions, but the interpretation still requires an experienced reader to confirm, with conventional MR imaging, the presence of a type 2 FCD. Finally, the use of a 3T magnetic field could have increased the number of positive findings on MRI as reported in a recent study.[35]

Conclusions

We emphasize that nearly 60% of type 2 FCDs may be recognized on 1.5T MR imaging and propose that a combination of features (found in two-thirds of the cases), comprising focal cortical thickening, GWM blurring, and the transmantle sign, is highly suggestive of this FCD subtype. Early identification of this lesion is crucial to minimize the delay in referring patients for surgical consideration.

Disclosures: Baris Turak—*UNRELATED: Travel/Accommodations/Meeting Expenses Unrelated to Activities Listed*: Cyberonics, *Comments*: traveling expenses to epilepsy conferences in Rome and Bordeaux paid by Cyberonics.

References

1. Blumcke I, Thom M, Aronica E, et al. **The clinicopathologic spectrum of focal cortical dysplasias: a consensus classification proposed by an ad hoc Task Force of the ILAE Diagnostic Methods Commission.** *Epilepsia* 2011;52:158–74
2. Palmini A, Najm I, Avanzini G, et al. **Terminology and classification of the cortical dysplasias.** *Neurology* 2004;62(suppl 3):S2–8
3. Lerner JT, Salamon N, Hauptman JS, et al. **Assessment and surgical outcomes for mild type I and severe type II cortical dysplasia: a critical review and the UCLA experience.** *Epilepsia* 2009;50:1310–35
4. Kim DW, Lee SK, Chu K, et al. **Predictors of surgical outcome and pathologic considerations in focal cortical dysplasia.** *Neurology* 2009;72:211–16
5. Chassoux F, Devaux B, Landre E, et al. **Stereoelectroencephalography in focal cortical dysplasia: a 3D approach to delineating the dysplastic cortex.** *Brain* 2000;123:1733–51
6. Krsek P, Maton B, Jayakar P, et al. **Incomplete resection of focal cortical dysplasia is the main predictor of poor postsurgical outcome.** *Neurology* 2009;72:217–23
7. Urbach H, Scheffler B, Heinrichsmeier T, et al. **Focal cortical dysplasia of Taylor's balloon cell type: a clinicopathological entity with characteristic neuroimaging and histopathological features, and favorable postsurgical outcome.** *Epilepsia* 2002;43:33–40
8. Tassi L, Colombo N, Garbelli R, et al. **Focal cortical dysplasia: neuropathological subtypes, EEG, neuroimaging and surgical outcome.** *Brain* 2002;125(pt 8):1719–32
9. Jeha LE, Najm I, Bingaman W, et al. **Surgical outcome and prognostic factors of frontal lobe epilepsy surgery.** *Brain* 2007;130:574–84
10. Salamon N, Kung J, Shaw SJ, et al. **FDG-PET/MRI coregistration improves detection of cortical dysplasia in patients with epilepsy.** *Neurology* 2008;71:1594–601
11. Widdess-Walsh P, Diehl B, Najm I. **Neuroimaging of focal cortical dysplasia.** *J Neuroimaging* 2006;16:185–96
12. Chassoux F, Rodrigo S, Semah F, et al. **FDG-PET improves surgical outcome in negative MRI Taylor-type focal cortical dysplasias.** *Neurology* 2010;75:2168–75
13. Widjaja E, Nilsson D, Blaser S, et al. **White matter abnormalities in children with idiopathic developmental delay.** *Acta Radiol* 2008;49:589–95
14. Widdess-Walsh P, Kellinghaus C, Jeha L, et al. **Electro-clinical and imaging characteristics of focal cortical dysplasia: correlation with pathological subtypes.** *Epilepsy Res* 2005;67:25–33
15. Colombo N, Citterio A, Galli C, et al. **Neuroimaging of focal cortical dysplasia: neuropathological correlations.** *Epileptic Disord* 2003;5(suppl 2):S67–72
16. Chan S, Chin SS, Nordli DR, et al. **Prospective magnetic resonance imaging identification of focal cortical dysplasia, including the non-balloon cell subtype.** *Ann Neurol* 1998;44:749–57
17. Kuzniecky R, Morawetz R, Faught E, et al. **Frontal and central lobe focal dysplasia: clinical, EEG and imaging features.** *Dev Med Child Neurol* 1995;37:159–66
18. Lee SK, Choe G, Hong KS, et al. **Neuroimaging findings of cortical dyslamination with cytomegaly.** *Epilepsia* 2001;42:850–56
19. Mackay MT, Becker LE, Chuang SH, et al. **Malformations of cortical development with balloon cells: clinical and radiologic correlates.** *Neurology* 2003;60:580–87
20. Bernasconi A, Antel SB, Collins DL, et al. **Texture analysis and morphological processing of magnetic resonance imaging assist detection of focal cortical dysplasia in extra-temporal partial epilepsy.** *Ann Neurol* 2001;49:770–75
21. Colombo N, Tassi L, Galli C, et al. **Focal cortical dysplasias: MR imaging, histopathologic, and clinical correlations in surgically treated patients with epilepsy.** *AJNR Am J Neuroradiol* 2003;24:724–33
22. Barkovich AJ, Kuzniecky RI, Bollen AW, et al. **Focal transmantle dysplasia: a specific malformation of cortical development.** *Neurology* 1997;49:1148–52
23. Duncan JS. **Imaging in the surgical treatment of epilepsy.** *Nat Rev Neurol* 2010;6:537–50
24. Chamberlain WA, Cohen ML, Gyure KA, et al. **Interobserver and intraobserver reproducibility in focal cortical dysplasia (malformations of cortical development).** *Epilepsia* 2009;50:2593–98
25. Colombo N, Salamon N, Raybaud C, et al. **Imaging of malformations of cortical development.** *Epileptic Disord* 2009;11:194–205
26. Besson P, Andermann F, Dubeau F, et al. **Small focal cortical dysplasia lesions are located at the bottom of a deep sulcus.** *Brain* 2008;131:3246–55
27. Lasjaunias P, Manelfe C, Terbrugge K, et al. **Endovascular treatment of cerebral arteriovenous malformations.** *Neurosurg Rev* 1986;9:265–75
28. Widjaja E, Otsubo H, Raybaud C, et al. **Characteristics of MEG and MRI between Taylor's focal cortical dysplasia (type II) and other cortical dysplasia: surgical outcome after complete resection of MEG spike source and MR lesion in pediatric cortical dysplasia.** *Epilepsy Res* 2008;82:147–55
29. Bronen RA, Spencer DD, Fulbright RK. **Cerebrospinal fluid cleft with cortical dimple: MR imaging marker for focal cortical dysgenesis.** *Radiology* 2000;214:657–63
30. Regis J, Tamura M, Park MC, et al. **Subclinical abnormal gyration pattern, a potential anatomic marker of epileptogenic zone in patients with magnetic resonance imaging-negative frontal lobe epilepsy.** *Neurosurgery* 2011;69:80–93
31. McGonigal A, Bartolomei F, Regis J, et al. **Stereoelectroencephalography in presurgical assessment of MRI-negative epilepsy.** *Brain* 2007;130:3169–83
32. Chapman K, Wyllie E, Najm I, et al. **Seizure outcome after epilepsy surgery in patients with normal preoperative MRI.** *J Neurol Neurosurg Psychiatry* 2005;76:710–13
33. Bernasconi A, Bernasconi N, Bernhardt BC, et al. **Advances in MRI for 'cryptogenic' epilepsies.** *Nat Rev Neurol* 2011;7:99–108
34. Wagner J, Weber B, Urbach H, et al. **Morphometric MRI analysis improves detection of focal cortical dysplasia type II.** *Brain* 2011;134:2844–54
35. Knake S, Triantafyllou C, Wald LL, et al. **3T phased array MRI improves the presurgical evaluation in focal epilepsies: a prospective study.** *Neurology* 2005;65:1026–31

Annexe 2 : Article publié de l'étude n°2

FULL-LENGTH ORIGINAL RESEARCH

3T MRI improves the detection of transmantle sign in type 2 focal cortical dysplasia

***Charles Mellerio, *Marc-Antoine Labeyrie, †Francine Chassoux, *Pauline Roca, ‡Odile Alami, ‡Monique Plat, *Olivier Naggara, †Bertrand Devaux, *Jean-François Meder, and *Catherine Oppenheim**

Epilepsia, **(*):1–6, 2013
doi: 10.1111/epi.12464

Summary

Purpose: Type 2 focal cortical dysplasia (FCD2) is one of the main causes of refractory partial epilepsy, but often remains overlooked by MRI. This study aimed to elucidate whether 3T MRI offers better detection and characterization of FCD2 than 1.5T, using similar coils and acquisition time.

Methods: Two independent readers reviewed the 1.5T and 3T MR images of 25 patients with histologically proven FCD2. For both magnetic fields, the ability to detect a lesion was analyzed. We compared the identification of each of the five criteria typical of FCD2 (cortical thickening, blurring, cortical signal changes, subcortical signal changes, and "transmantle" sign) and artifacts, using a four-point scale (0–3). Interobserver reliability for lesion detection was calculated.

Key Findings: Seventeen lesions (68%) were detected at 3T, two of which were overlooked at 1.5T. Interobserver reliability was better at 3T ($\kappa = 1$) than at 1.5T ($\kappa = 0.83$). The transmantle sign was more clearly identified at 3T than 1.5T (mean visualization score: 1.72 vs. 0.56; $p = 0.002$).

Significance: The use of 3T MRI in patients suspected of type 2 FCD improves the detection rate and the lesion characterization owing to the transmantle sign being more clearly seen at 3T. This point is of interest, since this feature is considered as an MR signature of FCD2.

KEY WORDS: Intractable epilepsy, MR imaging, Focal cortical dysplasia, Transmantle sign.

Type 2 focal cortical dysplasia (FCD2) is one of the main causes of extratemporal drug-resistant partial epilepsy that is surgically curable. Magnetic resonance imaging (MRI) has contributed to the steady increase of candidates for surgery. According to large surgical series, the majority of patients with extratemporal cryptogenic epilepsy have FCD that cannot be detected on MRI.[1–6] Indeed, even with dedicated protocols, MR diagnosis remains difficult, with up to 40% of FCD2 cases either undetected or diagnosed late.[7–9] Consequently, detection and delineation of FCD2 with MRI in patients with medically refractory extratemporal epilepsy has become one of the most challenging goals for improving surgical outcome.[10,11]

Accepted October 2, 2013.

*Department of Neuroimaging, Sainte-Anne Hospital Center, Paris Descartes Sorbonne Paris Cité University, Paris, France; †Department of Neurosurgery, Sainte-Anne Hospital Center, Paris Descartes Sorbonne Paris Cité University, Paris, France; and ‡Department of Imaging, Le Mans Hospital Center, France

Address correspondence to Charles Mellerio, Service d'Imagerie Morphologique et Fonctionnelle, Centre Hospitalier Sainte-Anne, 1 rue Cabanis, 75014 Paris, France. E-mail: c.mellerio@ch-sainte-anne.fr

Owing to its higher signal-to-noise ratio and smaller voxel size for a given acquisition time, 3 Tesla (3T) may be better than 1.5 Tesla (1.5T) MRI for the detection of FCDs. Two studies have suggested that MRI at 3T using phased array coils performed better than 1.5T MRI using a standard quadrature head coil for the detection and characterization of epileptogenic lesions.[12,13] Yet, this improvement might not solely be due to the increase in field strength but rather to the use of phased array coils.[13–15] The benefit of 3T MRI, if any, is likely not identical for all types of epileptic lesions. Hippocampal sclerosis and tissue loss are reported to be best seen at 1.5T,[14,16] whereas cortical development lesions, including FCDs, would be best seen at 3T.[12–14,17] However, these studies relied on heterogeneous series of epileptogenic lesions with only a few cases of histologically proven FCD2. The most recent studies dealing with epilepsy and FCD imaging used 3T MR.[18–23] One would not therefore expect its superiority over 1.5T for detecting subtle lesions such as FCD to be in doubt, although a comparison of these two magnetic fields focusing on FCD has never been carried out.

Based on a population of proven FCD2, we compared the yield of 1.5T and 3T MRI both using an eight-channel

phased-array head coil and similar acquisition time for the detection and characterization of FCD2. To further elucidate the expected superiority of 3T over 1.5T MRI, we also analyzed separately each MR sign of FCD2 at both magnetic fields.

Methods

Patients

We retrospectively identified all consecutive epileptic patients who underwent both 1.5 and 3T MRI between January 2010 and May 2013 and who had a final diagnosis of FCD2.

Twenty-five patients fulfilled these criteria. The reasons for rescanning patients at 3T MRI (3T MR unit installed at the start of the study period) included previously normal or equivocal 1.5T MRI findings or referral for functional MRI (fMRI) tasks or neuronavigation in the case of visible 1.5T lesion. In such cases, additional morphologic sequences were obtained during the same imaging session. Presurgical evaluation included ictal video-EEG, and 18F-fluorodeoxyglucose positron emission tomography (FDG-PET) scans for all patients, and stereo-EEG for 10 of them. The diagnosis of FCD2 was based on histologic confirmation (focal disorganization of the cortical cytoarchitecture and presence of giant dysmorphic neurons) in all patients. Balloon cells were found in all specimens (FCD type IIb), except in three (FCD type IIa). The study was approved by the ethics committee of Ile de France III and was found to conform to generally accept scientific principles and ethical standards.

Data acquisition

Patients were scanned using a 1.5T (Signa Excite; General Electric Healthcare, Milwaukee, WI, U.S.A.) and a 3T (Discovery MR750; General Electric Healthcare) clinical MRI with similar eight-channel phased-array head coils. The epilepsy imaging protocol included volumetric gradient-echo T_1-weighted inversion recovery acquisition, coronal and/or axial two-dimensional (2D) fast spin echo T_2-weighted acquisition fluid-attenuated inversion recovery (FLAIR) using 2D contiguous slices and/or 3D acquisition (Table 1).

Data analysis

Both 1.5T and 3T MR images were reviewed on a dedicated workstation (Advantage Windows Workstation; General Electric Medical Systems, Buc, France) for each patient, first independently and then in consensus, by two neuroradiologists (7 and 9 years of experience), one of whom was specialized in epilepsy imaging. Readers were aware of electroclinical data and that all patients had one histology confirmed FCD2. Each MR examination (3T or 1.5T) was analyzed in a random order, with availability of the complete MR image set at a given magnetic field. Each reader was asked to state if the lesion was visible, based on five imaging criteria: (1) cortical thickness, (2) cortical signal intensity, (3) blurring of the gray–white matter junction, (4) signal intensity of subcortical white matter, and (5) transmantle sign, defined as a subcortical white matter signal intensity change, tapering toward the ventricle. Each feature was rated on a four-point visualization scale from 0 (normal) to 3 (marked). Imaging artifacts (susceptibility, motion, or aliasing artifacts) were also quoted using a similar scale from 0 (none) to 3 (marked).

We compared the findings (number of lesions detected, visualization scores) between readers at a given magnetic field, and the consensus reading at 1.5 and 3T using a Wilcoxon test. Interobserver agreements were measured at 1.5T and 3T, using Cohen's kappa test. All data were analyzed using the SAS v9.1 statistical package (SAS Institute Inc., Cary, NC, U.S.A.).

Results

The 25 patients (15 male) had a median age of 21 years (range 13–50) at surgery. The median (interquartile range)

Table 1. MRI protocol at 1.5T and at 3T

	Slice thickness (mm)	FOV (mm)	Acquisition matrix	TE (msec)/TR (msec)/TI (msec)/Flip angle (degrees)	Scan time (min:s)	No. of patients
1.5T						
Axial and/or coronal FLAIR	5	240 × 240	256 × 192	140/9,202/90	3:41	25
3D FLAIR	1.2	240 × 240	256 × 226	162/6,000/90	5:39	4
Axial and/or coronal T_2 FSE	4	240 × 240	512 × 256	102/4,200/90	5:11	25
3D T_1 SPGR IR	1.4	240 × 240	256 × 192	2.1/10/15	5:57	25
3T						
Axial FLAIR	3.5	220 × 220	356 × 256	143/8000/90	3:13	5
3D FLAIR	1	256 × 230	256 × 224	127/5000/90	5:23	25
Axial and/or coronal T_2 FSE	3.5	220 × 165	512 × 320	102/9757/90	3:25	25
3D T_1 SPGR IR	1.2	250 × 175	512 × 256	4.3/10/15	5:29	25

FLAIR, fluid attenuated inversion recovery; SPGR IR, spoiled gradient-echo inversion recovery; FSE, fast spin echo; FOV, field of view; TE, echo time; TR, repetition time; TI, inversion time.

delay from 1.5T to 3T MRI was 13.1 (1–20) months. FCD2 was located in the frontal lobe in 22 cases (including nine in the central region and one in the insula), 2 lesions were parietal, and one was in the temporal lobe, with 12 lesions in the right hemisphere and 13 in the left hemisphere. Interobserver reliability for the detection of the lesion (detected vs. not detected) was perfect at 3T ($\kappa = 1$) and almost perfect at 1.5T ($\kappa = 0.83$). No lesion was detected other than in the area corresponding to the site of FCD2, as determined by histology. After consensus, 15 of the 25 FCD2s (60%) were detected at both magnetic field strengths and two lesions were detected at only 3T (Figs. 1 and 2) reaching thus 68% of detected lesions. Visualization scores for each individual sign of FCD2 were higher at 3T than at 1.5T (Fig. 3) and reached significance for the transmantle sign ($p = 0.002$) (Fig. 4). Of note, in our study, four patients had 3D FLAIR at both magnetic field strengths; two of these were negative. For the two other patients, transmantle sign was not or barely visible at 1.5T due to a low signal-to-noise ratio, while being conspicuous at 3T (Fig. 4, Case 1). Artifacts were less frequent at 1.5T than at 3T, with slight to moderate artifacts in both cases involving five patients at 3T (motion, n = 2; aliasing, n = 2; susceptibility artifact, n = 1) and two patients at 1.5T (motion). No marked artifacts were recorded.

Discussion

We report here the first study comparing the diagnostic performance of 1.5T and 3T MRI in a homogenous series of 25 patients with FCD2. In this series, 3T MRI improved FCD2 characterization owing to the transmantle sign being more clearly seen at 3T. This point is of interest, since this feature is considered an MR signature of FCD2.[7,24–26]

One of the strengths of our study is that the same patients were scanned at both magnetic fields on a magnet from the same manufacturer, using similar head coils and similar acquisition time. 3T MRI allows a high spatial resolution in a given acquisition time with isotropic millimetric voxels. This small voxel size helps in delineating and characterizing a cortical lesion, particularly for subtle signs, such as blurring of the gray–white matter interface, a cardinal feature of FCD2.[7,21,25] Reformatting images is particularly helpful to search for cortical thickening, thereby avoiding partial volume effect by observing the cortical surface in a plane orthogonal to the sulcus. Nevertheless, 3D T_1 sequences are

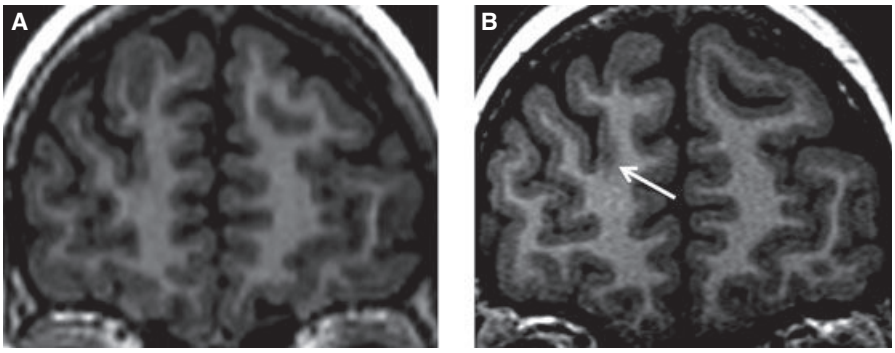

Figure 1.
FCD2 detected at 3T but not at 1.5T. Coronal reformats of 3D T_1-weighted MRI at 1.5T (**A**) and 3T (**B**). Blurred thickening of the cortex in the right anterior frontal region (arrow) is visible at 3T but not at 1.5T.
Epilepsia © ILAE

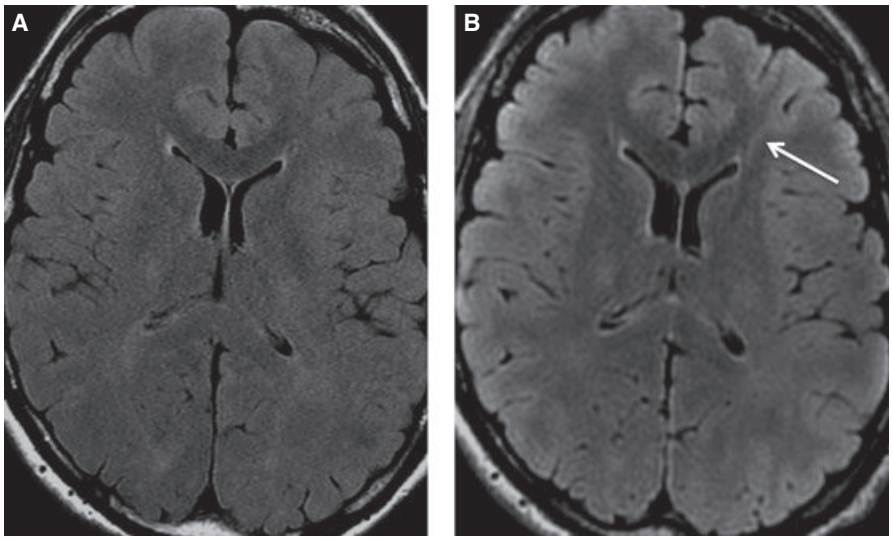

Figure 2.
Other patient with FCD2 visible at 3T and overlooked at 1.5T: axial FLAIR images at 1.5T (**A**) and at 3T (**B**). Subcortical hyperintensity with a transmantle sign (arrow) is seen at 3T but not at 1.5T.
Epilepsia © ILAE

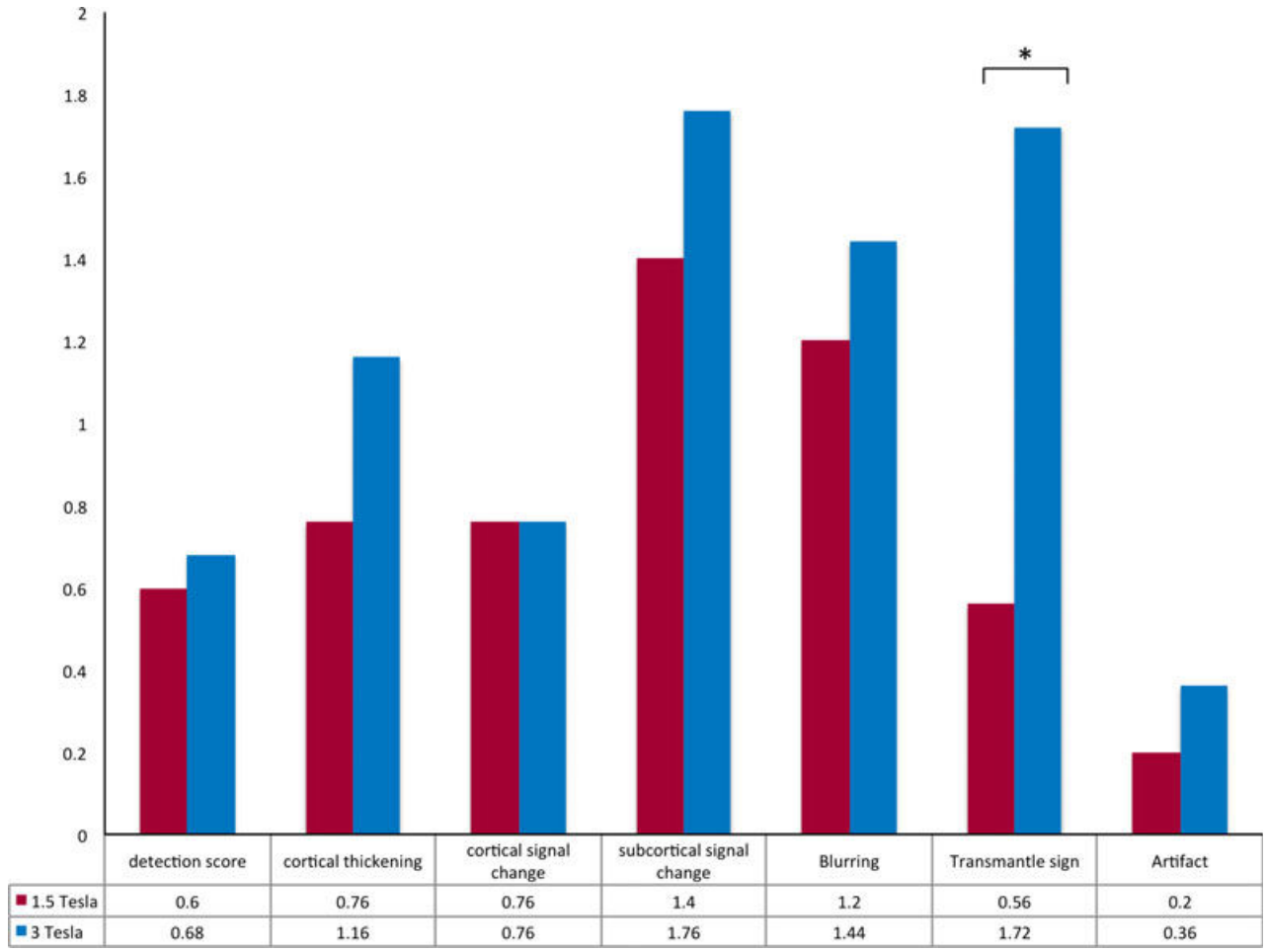

	detection score	cortical thickening	cortical signal change	subcortical signal change	Blurring	Transmantle sign	Artifact
1.5 Tesla	0.6	0.76	0.76	1.4	1.2	0.56	0.2
3 Tesla	0.68	1.16	0.76	1.76	1.44	1.72	0.36

Figure 3.
Comparison of visualization scores for each criterion between 3T and 1.5T. Numbers correspond to the mean of the scores calculated for each of the 25 patients, based on consensual reading. Visualization score of the five imaging criteria and artifacts are calculated using a four-point scale as detailed in the method section. *0.002.

also available at 1.5T with an excellent spatial resolution. This likely explains the limited difference between the two magnetic fields for detection of cortical features (thickness, blurring), which relies almost exclusively on T_1 contrast.

The most striking finding in our study is the contribution of 3T MRI for detection of the transmantle sign. This improvement has direct consequences for the MRI report, since it allows not only the detection of FCD2 but also its characterization,[7,21,24–26] given that the transmantle sign has not been described in other developmental or acquired cortical lesions. Moreover, the detection of the transmantle sign has been recently associated with a positive prognosis, with highly favorable seizure-free outcome after surgical treatment.[27] The systematic use of 3D FLAIR largely explains the increased detection of the transmantle sign at 3T. Multiplanar reformatting mainly benefits the detection of this linear T_2 signal abnormality, which does not systematically taper in the acquisition plane and can thus be overlooked with 2D FLAIR/T_2 images. Better visualization of the transmantle sign might have resulted simply from a transition from 2D FLAIR on 1.5T to 3D FLAIR on 3T. A study indeed illustrated the benefit of 3D FLAIR over conventional sequences for detection and delineation of FCD in nine patients.[28] In our study, only four patients had 3D FLAIR at both magnetic field strengths, among which two were negative, preventing from drawing a firm conclusion. However, in the two other patients, 3D FLAIR at 3T best detected the transmantle sign. From a practical point of view, 3D FLAIR at 1.5T suffers from a limited signal-to-noise ratio, for fixed acquisition duration compatible with routine clinical practice (5–6 min). To equal the signal to noise ratio at 3T, one should theoretically double the acquisition time at 1.5T,[29] resulting in a long acquisition time (>10 min) at 1.5T increasing the risk of motion artifacts.

When all signs of FCD2 were considered together, the proportion of positive MRI findings at 3T was only slightly

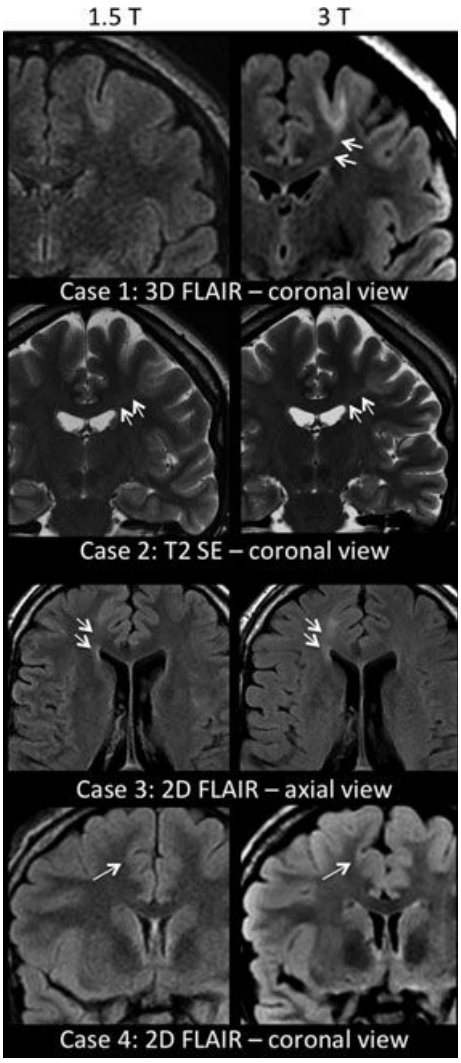

Figure 4.
Comparison of 1.5T and 3T in four different patients. Cases 1–3 illustrate a transmantle sign better visible at 3T than at 1.5T. Coronal reformats of 3D FLAIR sequences (case 1), coronal T_2-weighted images (case 2), and axial 2D FLAIR (case 3) show a well-delineated transmantle sign at 3T that is not or barely visible at 1.5T (double arrows). Of note, cortical and subcortical signal changes are visible at both magnetic fields, although more obvious at 3T. Case 4 illustrates a negative MRI on 3D FLAIR images at each magnetic field of a histologically confirmed FCD2 in the cingular gyrus (arrow).

better than at 1.5T, with two cases being visible only at 3T in our series of patients. Accordingly, a recent study on 91 patients with FCD who underwent either 1.5T or 3T MRI, found similar visual detection rates at both magnetic fields.[30] However, we also found a benefit of 3T MRI for improved FCD characterization. 3T MRI was able to clarify equivocal features generated by the 1.5T magnet, including abnormal signal from the bottom of the gyri to the ventricle surface without clearly showing the "transmantle line." Therefore, ambiguous pattern at 1.5T became typical and convincing at 3T. This could partly explain the increased sensitivity for the detection of FCD reported at a higher magnetic field in previous studies, although these studies analyzed patients with focal intractable epilepsy regardless of the causal lesion, with only a few suspected FCD cases (respectively, nine, eight, and seven cases),[12–14] half of which lacked histologic confirmation.

Taken together, our results and those of previous studies may help to estimate the sample size for a larger prospective study comparing 1.5T to 3T with similar acquisition time for FCD2 detection. We found a difference between proportion of lesion detected at 3T and at 1.5T of approximately 10% (2 of 25 patients). Based on a power analysis using a McNemar test to achieve 80% power at 0.05 significance with 10% of FCD2 switching from undetected to detected, the sample size required would be equal to 77 patients.

The limitations of high–field-strength imaging include a propensity to certain types of imaging artifacts, such as susceptibility and a perceived sensitivity to motion, as shown in our study. Disadvantages of imaging at 3T also include longer T_1, increased acoustic noise, greater power deposition, and device incompatibility.[31,32] Aliasing artifact, seen only at 3T in our study, may mimic the transmantle sign on 3D FLAIR images, as observed here in one case. This reinforces the need to integrate all MRI features when searching for FCD.

Finally, our findings illustrate that even with an appropriate magnetic field and imaging protocol, with precise information regarding electroclinical data and a thorough analyze, about 30% of FCD2 remain overlooked. This outcome strengthens the need for new sequences, such as double inversion recovery imaging,[33] arterial spin labeling,[34] and refinement of morphometric postprocessing tool,[6,30] which may also benefit from imaging at high field.

Our study has some limitations. First, it is retrospective, based on a small sample of patients, and lacks a control group that would allow determination of specificity. This lack also likely introduces a bias in interpretations, given that readers searched thoroughly for signs of FCD with no risk of overdiagnosis. Yet, we did not find any false-positive cases (i.e., in erroneous location). The fact that reading was guided by clinical and electroclinical data, according to guidelines,[35] might in part explain that no lesion was detected elsewhere than in the area corresponding to the site of the FCD2. Second, the acquisition times were short and similar at both field strengths. By using longer times, the image quality could have been improved at 1.5 or at 3T. Third, readers could not be completely blind for magnetic field strengths, given that images are visually distinguishable. This limitation is inherent to all studies comparing 3T and 1.5T images.

In conclusion, we have shown that the detection and characterization of FCD2 is better at 3T than at 1.5T with similar head coils and acquisition time, owing to greater ability to

detect the transmantle sign. The use of 3T MRI may help to improve the selection of candidates for epilepsy surgery.

Disclosure

None of the authors has any conflict of interest to disclose. We confirm that we have read the Journal's position on issues involved in ethical publication and affirm that this report is consistent with those guidelines.

References

1. Chassoux F, Rodrigo S, Semah F, et al. FDG-PET improves surgical outcome in negative MRI Taylor-type focal cortical dysplasias. *Neurology* 2010;75:2168–2175.
2. Chassoux F, Landre E, Mellerio C, et al. Type II focal cortical dysplasia: electroclinical phenotype and surgical outcome related to imaging. *Epilepsia* 2012;53:349–358.
3. Jeha LE, Najm I, Bingaman W, et al. Surgical outcome and prognostic factors of frontal lobe epilepsy surgery. *Brain* 2007;130:574–584.
4. McGonigal A, Bartolomei F, Regis J, et al. Stereoelectroencephalography in presurgical assessment of MRI-negative epilepsy. *Brain* 2007;130:3169–3183.
5. Chapman K, Wyllie E, Najm I, et al. Seizure outcome after epilepsy surgery in patients with normal preoperative MRI. *J Neurol Neurosurg Psychiatry* 2005;76:710–713.
6. Bernasconi A, Bernasconi N, Bernhardt BC, et al. Advances in MRI for 'cryptogenic' epilepsies. *Nat Rev Neurol* 2011;7:99–108.
7. Mellerio C, Labeyrie MA, Chassoux F, et al. Optimizing MR imaging detection of type 2 focal cortical dysplasia: best criteria for clinical practice. *AJNR Am J Neuroradiol* 2012;33:1932–1938.
8. Lerner JT, Salamon N, Hauptman JS, et al. Assessment and surgical outcomes for mild type I and severe type II cortical dysplasia: a critical review and the UCLA experience. *Epilepsia* 2009;50:1310–1335.
9. Hauptman JS, Mathern GW. Surgical treatment of epilepsy associated with cortical dysplasia: 2012 update. *Epilepsia* 2012;53(Suppl. 4):98–104.
10. Krsek P, Maton B, Jayakar P, et al. Incomplete resection of focal cortical dysplasia is the main predictor of poor postsurgical outcome. *Neurology* 2009;72:217–223.
11. Madan N, Grant PE. New directions in clinical imaging of cortical dysplasias. *Epilepsia* 2009;50(Suppl. 9):9–18.
12. Knake S, Triantafyllou C, Wald LL, et al. 3T phased array MRI improves the presurgical evaluation in focal epilepsies: a prospective study. *Neurology* 2005;65:1026–1031.
13. Phal PM, Usmanov A, Nesbit GM, et al. Qualitative comparison of 3-T and 1.5-T MRI in the evaluation of epilepsy. *AJR Am J Roentgenol* 2008;191:890–895.
14. Zijlmans M, de Kort GA, Witkamp TD, et al. 3T versus 1.5T phased-array MRI in the presurgical work-up of patients with partial epilepsy of uncertain focus. *J Magn Reson Imaging* 2009;30:256–262.
15. Orbach DB, Wu C, Law M, et al. Comparing real-world advantages for the clinical neuroradiologist between a high field (3 T), a phased array (1.5 T) vs. a single-channel 1.5-T MR system. *J Magn Reson Imaging* 2006;24:16–24.
16. Hashiguchi K, Morioka T, Murakami N, et al. Utility of 3-T FLAIR and 3D short tau inversion recovery MR imaging in the preoperative diagnosis of hippocampal sclerosis: direct comparison with 1.5-T FLAIR MR imaging. *Epilepsia* 2010;51:1820–1828.
17. Strandberg M, Larsson EM, Backman S, et al. Pre-surgical epilepsy evaluation using 3T MRI. Do surface coils provide additional information? *Epileptic Disord* 2008;10:83–92.
18. Craven IJ, Griffiths PD, Hoggard N. Magnetic resonance imaging of epilepsy at 3 Tesla. *Clin Radiol* 2011;66:278–286.
19. Doelken MT, Mennecke A, Huppertz HJ, et al. Multimodality approach in cryptogenic epilepsy with focus on morphometric 3T MRI. *J Neuroradiol* 2012;39:87–96.
20. Craven IJ, Griffiths PD, Bhattacharyya D, et al. 3.0-Tesla MRI of 2000 consecutive patients with localisation-related epilepsy. *Br J Radiol* 2012;85:1236–1242.
21. Kim DW, Kim S, Park SH, et al. Comparison of MRI features and surgical outcome among the subtypes of focal cortical dysplasia. *Seizure* 2012;21:789–794.
22. Focke NK, Symms MR, Burdett JL, et al. Voxel-based analysis of whole brain FLAIR at 3T detects focal cortical dysplasia. *Epilepsia* 2008;49:786–793.
23. Fonseca Vde C, Yasuda CL, Tedeschi GG, et al. White matter abnormalities in patients with focal cortical dysplasia revealed by diffusion tensor imaging analysis in a voxelwise approach. *Front Neurol* 2012;3:121.
24. Barkovich AJ, Kuzniecky RI, Bollen AW, et al. Focal transmantle dysplasia: a specific malformation of cortical development. *Neurology* 1997;49:1148–1152.
25. Colombo N, Citterio A, Galli C, et al. Neuroimaging of focal cortical dysplasia: neuropathological correlations. *Epileptic Disord* 2003;5 (Suppl. 2):S67–S72.
26. Colombo N, Tassi L, Deleo F, et al. Focal cortical dysplasia type IIa and IIb: MRI aspects in 118 cases proven by histopathology. *Neuroradiology* 2012;54:1065–1077.
27. Wang DD, Deans AE, Barkovich AJ, et al. Transmantle sign in focal cortical dysplasia: a unique radiological entity with excellent prognosis for seizure control. *J Neurosurg* 2013;118:337–344.
28. Saini J, Singh A, Kesavadas C, et al. Role of three-dimensional fluid-attenuated inversion recovery (3D FLAIR) and proton density magnetic resonance imaging for the detection and evaluation of lesion extent of focal cortical dysplasia in patients with refractory epilepsy. *Acta Radiol* 2010;51:218–225.
29. Lu H, Nagae-Poetscher LM, Golay X, et al. Routine clinical brain MRI sequences for use at 3.0 Tesla. *J Magn Reson Imaging* 2005;22:13–22.
30. Wagner J, Weber B, Urbach H, et al. Morphometric MRI analysis improves detection of focal cortical dysplasia type II. *Brain* 2011;134:2844–2854.
31. Pattany PM. 3T MR imaging: the pros and cons. *AJNR Am J Neuroradiol* 2004;25:1455–1456.
32. Schmitz BL, Aschoff AJ, Hoffmann MH, et al. Advantages and pitfalls in 3T MR brain imaging: a pictorial review. *AJNR Am J Neuroradiol* 2005;26:2229–2237.
33. Rugg-Gunn FJ, Boulby PA, Symms MR, et al. Imaging the neocortex in epilepsy with double inversion recovery imaging. *Neuroimage* 2006;31:39–50.
34. Pendse N, Wissmeyer M, Altrichter S, et al. Interictal arterial spin-labeling MRI perfusion in intractable epilepsy. *J Neuroradiol* 2010;37:60–63.
35. Guidelines for neuroimaging evaluation of patients with uncontrolled epilepsy considered for surgery. Commission on Neuroimaging of the International League Against Epilepsy. *Epilepsia* 1998;39:1375–1376.

Annexe 3 : Caractérisation des motifs sulcaux normaux de la région centrale en IRM

(étude non publiée)

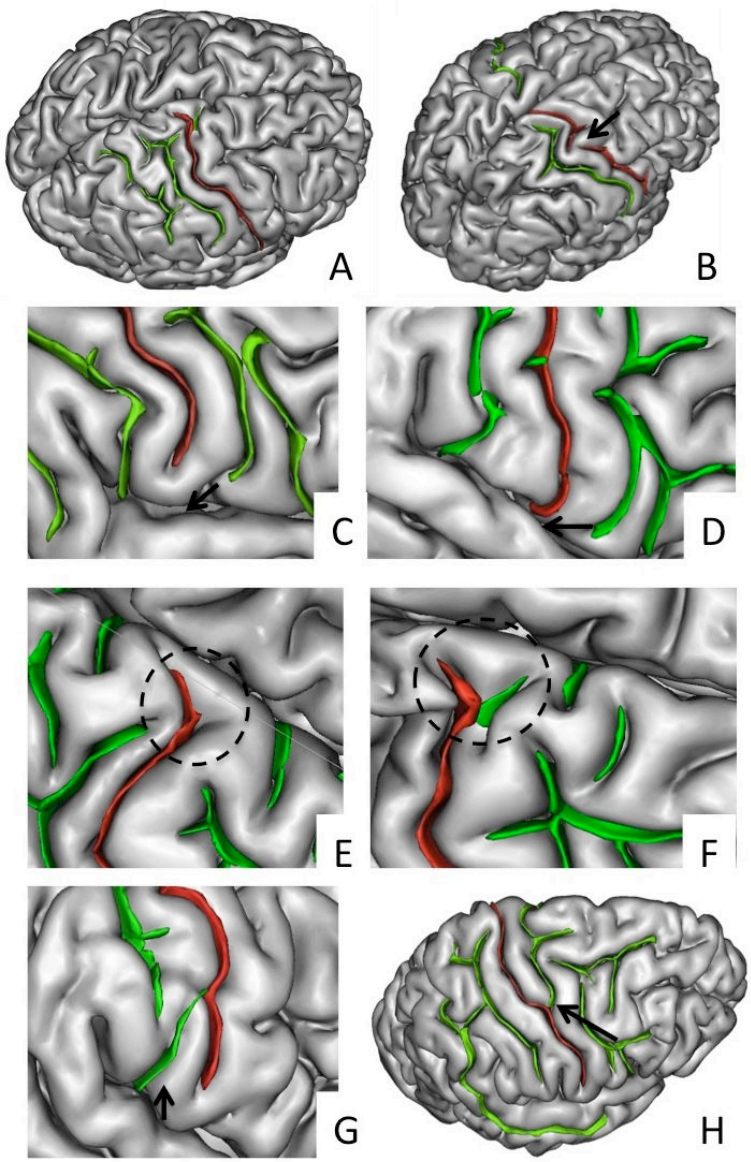

Morphological features of the central sulcus (CS) with an excellent inter-rater concordance (kappa >0.80) and which did not significantly differ with Ono's post-mortem values (p>0.05). The central sulcus (in red) is represented on a three dimensional mesh-based reconstruction of the cortex surface. Continuous (A) or interrupted (B, arrow) CS. CS inferior end without (C) or with extension to the sylvian fissure (arrow). CS superior end shape: "T" (E) or "Y" shape (F). CS inferior end shape: "Y" shape (G). CS connection with precentral sulcus (H, arrow).

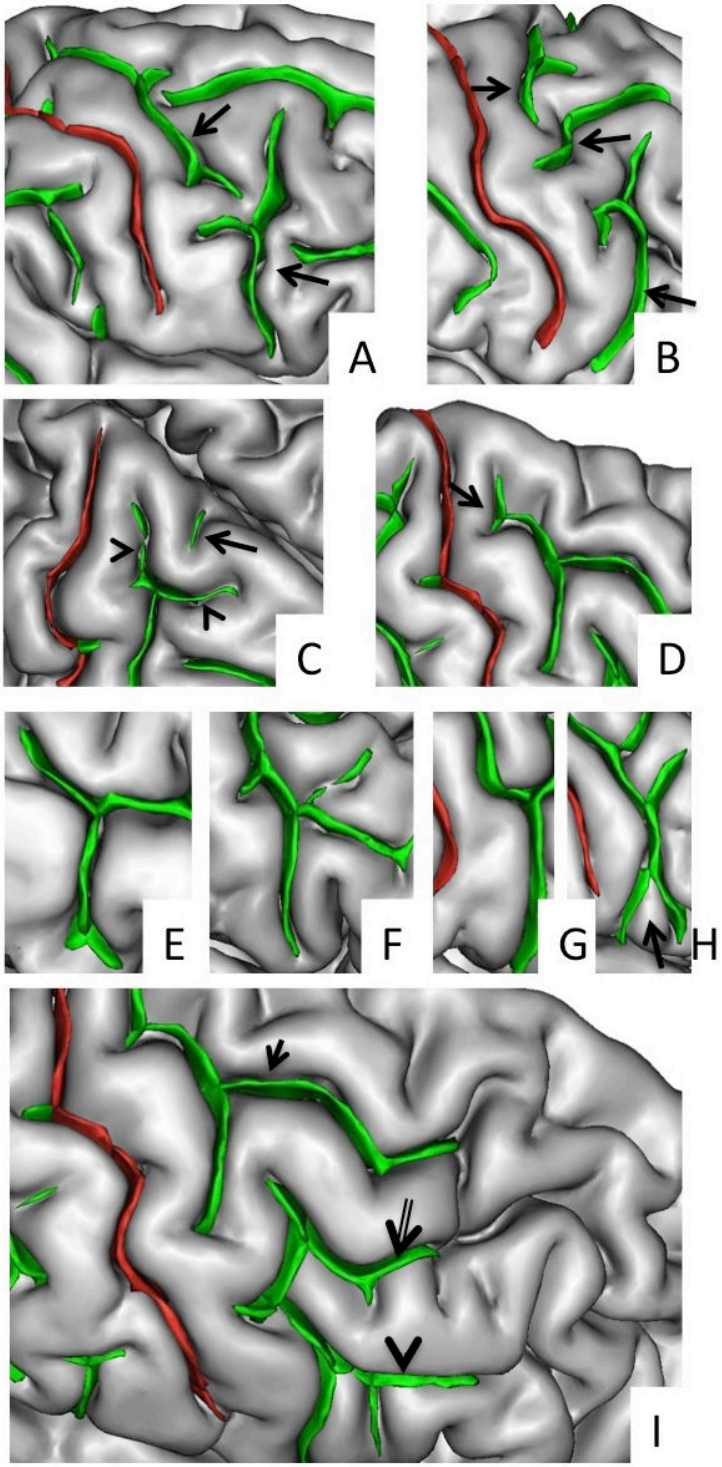

Morphological features of the pre-central sulcus (PreCS) with an excellent inter-rater concordance (kappa >0.80) and which did not significantly differ with Ono's post-mortem values (p>0.05). The pre-central sulcus (in red) is represented on a three dimensional mesh-based reconstruction of the cortex surface. PreCS with two (A) or three (B) segments (arrows). CS superior end patterns (C) with marginal precentral sulcus (arrow heads) and medial precentral sulcus (arrow). Pre-CS superior segment shape with arcuate termination with Y-shaped end (arrow). Pre-CS inferior segment patterns with arcuate form (E), ramified form (F), bayonet form(G) and Y-shaped end (H, arrow). Pre-CS connections with superior frontal sulcus (arrow), intermediate frontal sulcus (double arrow) or inferior frontal sulcus (arrow head).

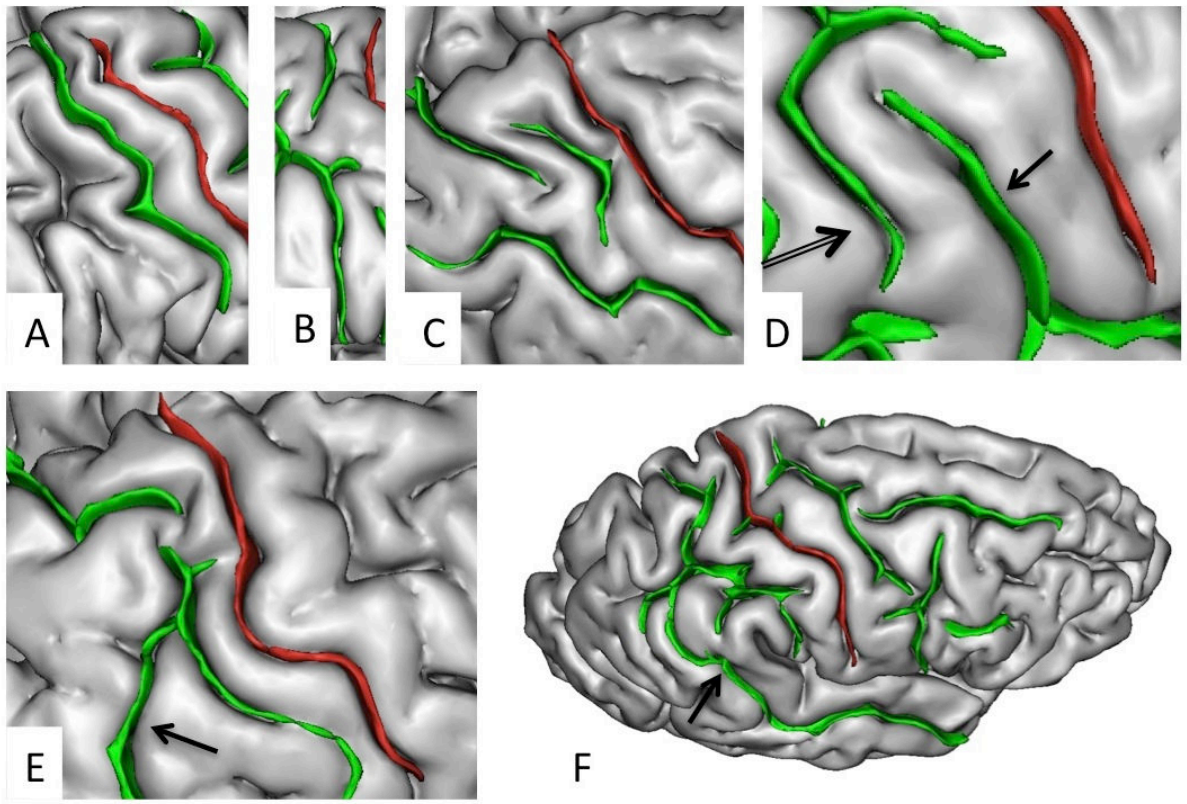

Morphological features of the post-central sulcus (PostCS) with an excellent inter-rater concordance (kappa >0.80) and which did not significantly differ with Ono's post-mortem values (p>0.05). The post-central sulcus (in red) is represented on a three dimensional mesh-based reconstruction of the cortex surface. Post-CS with one (A), two (B) or three (C) segments (arrows). Post-CS with double parallel pattern (D): sylvian fissure posterior end (posterior subcentral sulcus, arrow) and Post-CS inferior end (double arrow). Post-CS connection with intraparietal sulcus (E, arrow) and with superior temporal sulcus (F, arrow).

Résumé (français) :

Les dysplasies corticales focales de type 2 (DCF2) sont une cause fréquente d'épilepsie partielle pharmacorésistante pouvant bénéficier d'un traitement chirurgical. Leur détection en IRM est un facteur indépendant de bon pronostic. Leur diagnostic reste difficile avec jusqu'à 40% d'IRM négatives.

Le travail de cette thèse a pour principal objectif d'améliorer la détection des DCF2 à partir des séquences conventionnelles, d'évaluer la pertinence d'une augmentation de champ magnétique, et de valider de nouveaux outils de détection, en particulier par l'identification d'anomalies des sillons associées aux DCF2 de manière automatique puis visuelles. Cette étude a été réalisée à partir d'une des plus importante cohorte de patients (>80 patients) porteurs de DCF2 prouvée histologiquement.

L'évaluation de la fréquence de chacun des signes en IRM nous a permis de démontrer que, bien qu'aucune anomalie ne soit visible dans 41% des cas, les différents signes chez les patients avec une IRM positive n'étaient jamais isolés et que la combinaison des 3 signes les plus évocateurs de DCF2 (épaississement cortical, flou de l'interface blanc-gris et « transmantle sign »), était retrouvée chez 27 patients (64%) suggérant que l'IRM puisse être un examen très caractéristique.

En augmentant le champ magnétique de 1,5 à 3T en IRM le taux de détection n'est que peu modifié mais la caractérisation des DCF2 est améliorée en raison d'une meilleure visualisation du « transmantle sign », considéré comme une signature en IRM des DCF2.

L'analyse automatisée des sillons basés sur le calcul d'un nouveau paramètre appelé « énergie sulcale » permet d'identifier des motifs sulcaux anormaux chez les patients porteurs de DCF2 dans la région centrale en comparaison aux sujets sains. Ce résultat souligne l'importance d'une étude des sillons et pourrait fournir un critère supplémentaire pour détecter et localiser la lésion chez des patients à IRM négative.

Enfin, l'analyse visuelle des sillons par un reformatage 3D du cortex nous a permis de décrire un nouveau marqueur des DCF2 de la région centrale : un motif sulcal dénommé le "Power Button Sign". Compte tenu de son excellente reproductibilité et de sa spécificité, il pourrait être utilisé comme un nouveau critère diagnostic majeur de DCF2 de la région centrale.

L'ensemble de ces résultat participe à la meilleure compréhension des phénomènes développementaux impliqués dans la physiopathologie des DCF2 et offre de nombreuses perspectives pour l'amélioration de leur détection en imagerie.

Title : Optimization of advanced MRI tools in the detection and characterization of epileptogenic developmental lesions

Abstract :
Focal cortical dysplasia type 2 (FCD2) is a common cause of intractable partial epilepsy surgically treatable. Their detection by MRI is an independent factor of good prognosis. The MR imaging diagnosis remains difficult with up to 40% negative MRI.

Our main objective is to improve the detection of FCD2from conventional sequences, to assess the relevance of increased magnetic field and validate new tools for detection, in particular by identifying sulcal abnormalities associated with FCD2 automatically and visually. This study was carried out from one of the largest cohort of patients (> 80 patients) with histologically proven FCD2.

The evaluation of the frequency of each MR signs showed that, although no abnormality is seen in 41% of cases, the different signs in patients with a positive MRI were never isolated and the combination of the 3 most suggestive signs of FCD2 (cortical thickening, bluring of the gray-white matter interface and "transmantle sign") was found in 27 patients (64%), indicating that MRI can be very suggestive.

By increasing the magnetic field from 1.5 to 3T MRI detection rate is only slightly changed but characterization of FCD2 is improved thanks to a better visualization of the " transmantle sign " considered as a MR signature of FCD2.

The automated sulcus analysis based on the calculation of a new parameter called "sulcal energy" identifies abnormal sulcal patterns in patients with FCD2 in the central region in comparison to healthy subjects. This result underlines the importance of the identification of sulci and could provide an additional criterion for detecting and locating the lesion in patients with negative MRI.

Finally, the visual analysis of sulci by 3D reformatting of the cortex allowed us to describe a new MR sign of FCD2 in the central region: a sulcal pattern called the "Power Button Sign". Given its excellent reproducibility and specificity, it could be used as a new major diagnostic criterion of FCD2 in the central region.

All these results contribute to the better understanding of the developmental processes involved in the pathophysiology of FCD2 and offers many opportunities for improving their MR detection.

Mots clés (français) :
Epilepsie partielle pharmacorésistante, IRM, dysplasie corticale focale, transmantle sign, anatomie sulcale, sillon central

Keywords :
Intractable epilepsy, MR imaging, focal cortical dysplasia, transmantle sign, sulcal anatomy, central Sulcus